DRYING OF GRANULAR MATERIALS IN ROTATING FLUIDIZED BED IN A STATIC GEOMETRY (RFB-SG)

A Thesis

Submitted in Partial Fulfillment of the Requirements for the Award of the Degree of

DOCTOR OF PHILOSOPHY

By

JNYANA RANJAN PATI

CENTRE FOR ENERGY
INDIAN INSTITUTE OF TECHNOLOGY GUWAHATI
GUWAHATI – 781039, INDIA

SEPTEMBER 2016

This thesis is dedicated to my father

Late Dinabandhu Pati

DECLARATION

I hereby certify that the information presented in this thesis is entirely my own account of my research and contains at its main content work except where otherwise stated, which has not previously been submitted for a degree or diploma at this institute or any tertiary educational institution.

Jnyana Ranjan Pati
Regd. No. - 126151007
Centre for Energy
Indian Institute of Technology Guwahati
Guwahati - 781039, India
September 2016.

CERTIFICATE

It is certified that the work contained in the thesis entitled **Drying of Granular Materials in Rotating Fluidized Bed in a Static Geometry (RFB-SG)** by **Jnyana Ranjan Pati (Regd.No. 126151007)**, a research scholar in the Centre for Energy, Indian Institute of Technology Guwahati, India, for the award of the degree of the **Doctor of Philosophy** has been carried out under my supervision and this work has not been submitted elsewhere for a degree.

Prof. PinakeswarMahanta
Professor
Department of Mechanical Engineering,
Indian Institute of Technology Guwahati.
Guwahati – 781039, India.

Date:

ABSTRACT

Scarcity of food and imbalance in production and consumption of the same are major problems in the world. This problem can be solved to a large extent by reducing the food loss which occurs due to the lack of suitable and economic technology in developing countries. Food preservation is the only way to reduce food loss. Drying is identified to be one of the postharvest technologies to reduce losses of food and improvement of quality as well. Drying is one of the most energy intensive unit operations in post-harvest processing. The purpose of reducing the moisture content is to prolong the shelf-life of the products of bio-origin by reducing the moisture activity to a level low enough where growth of microorganisms, enzymatic reactions, and other deteriorative reactions are inhibited. Some products of bio-origin such as herbs have to be dried before the active ingredients can be extracted. Furthermore, the products in the dry form losses weight and volume are reducing transportation costs. Most of the available dryers do not perform well and have low efficiency as reported in literature. One of the modern technologies emerging out to the market is the Fluidized bed dryer which is energy intensive. In conventional fluidized bed is found to have trouble due to mechanical vibration and sealing (need for rotating seal) in critical components. Further, particle feeding and removal from this type of dryer is difficult. Hence there is a need for development of an efficient dryer for quality drying.

Present work is focused towards development and performance analysis of a rotary fluidized bed with static geometry (RFB-SG). This dryer is developed based on the concept of injecting the fluidization gas tangentially into the fluidization chamber with the help of multi gas inlet slots. Upon contact with particles, the gas- phase motion quickly shifts from tangential to radial direction and gas leaves the vortex chamber through a chimney. Due to inertia, the particles follow a different gas flow path and form a rotating particles bed. The fluidizations of the particles are depending on the radial gas-solid drag force and the countering centrifugal force. Thus a very high acceleration in order of 7-8 times that of acceleration due to gravity is achieved which helps in quick removal of moisture even from the core of the particles to be dried.

In the present work drying characteristics of different agricultural products, such as paddy and wheat grains were considered. Effects of air flow rate, relative humidity, air

temperature and inventory on drying characteristics are established. Performance of RFB-SG was compared with a bubbling fluidized bed. A set of correlations for moisture removal are also developed. Finally comparison of thermo-economic aspects of both the dryer are presented. It was observed from this work that RFB-SG is one of the most promising dryers for cereal crop drying. Moreover, present study will be helpful in improving RFB-SG for scale up.

ACKNOWLEDGEMENT

I express my deepest gratitude to my supervisor, Prof. Pinakeswar Mahanta and Prof. Juray De Wilde (UCL, Belgium) for their inestimable guidance and support for the constant inspiration. I drew from his critical thinking, approach and for providing an excellent working atmosphere. Their thoughtful suggestions, ideas were vital for the framework and outcome of this research. It has been a rewarding experience for me in working with them all these years and has inspired me enough in different aspects of research and life, for the years to come. I would like to thank my doctoral committee members, Prof. G. Pugazhenthi, Dr. Vinayak Kulkarni and Dr. V.V. Goud for their valuable suggestions and encouragement during my research work.

I would like to acknowledge Indian Institute of Technology Guwahati (Centre for energy) and IMAP, UCL (Belgium) for providing the funds and facilities for carrying out my research. I would like to show my sincere gratitude to Prof. P. Goswami (H.O.C, Centre for Energy) for providing the facilities needed during my research work and also thank the Marie-Curie project FP7-PEOPLE-2012-IRSES, project no. 312261, project name, IComFluid (Belgium, UCL, IMAP) for financial support.

I am thankful to many friends at UCL, Belgium and IIT Guwahati. Special mention to acknowledge, Subhajit Dutta, Philippe Eliaers, Luc Wautier for their suggestion, technical support is helped during my experiment time. Dr. Pankaj Kalita, Dr. L. Barbora (Scientific Officer) Centre for Energy, IIT Guwahati. Mr. Ashish J. Chaudhari, Mr. Ramesh Ch. Mishra, Mr Santosh Ku. Hotta, Miss. Dipti Yadav, Mr Abinash Mahaparto and Soumya Ranjan Nanda here are being with me in good and difficult times through these years. Special thanks to Mrs. Anita Mahanta for her kind support and encouragement in my social life, which is unforgettable forever.

I am very much grateful to my beloved parents, family members, my wife Mrs. Madhsmita Tripathy, son, Krishna and daughter Urrbi and all other relatives for their immeasurable love, understanding and unwavering support, which has made this feat possible.

Author

CONTENTS

NOMENCLATURE

A	:	Cross sectional area (cm^2)
a_c	:	Centripetal acceleration (m/s^2)
β	:	Drag Coefficient
C_p	:	Specific heat (kJ/kg °C)
C_{pda}	:	Specific heat of dry air(kJ/kg °C)
C_D	:	Drag coefficient
C_{Dr}	:	Total drying Cost (Rs)
C_{Fix}	:	Fixed Cost (Rs)
C_V	:	Variable Cost (Rs)
d_p	:	Mean Particle diameter (mm)
D	:	Diameter of the vortex chamber (cm)
D_j	:	Diameter of the jacket (cm)
E_x	:	Exergy of the system (j)
F_D	:	Drag force (N)
g	:	Acceleration due to gravity (m/s^2)
h_g	:	Enthalpy of gas (J/kg)
h	:	Enthalpy (J/kg)
I	:	Solid inventory (g)
K_1, K_2	:	Drying constant (min^{-1})
K	:	Thermal conductivity (W/m °C)
L	:	Length of the vortex chamber (cm)
L_r	:	Bed height (cm)
dM/dT	:	Moisture gradient
ΔMCp	:	Moisture content difference of product
m_i	:	Initial weight of sample (kg)
m_f	:	Final weight of sample at the end of drying (kg)
$\dot{m}_w$	:	Mass flow rate of water (kg/s)
m_{wp}	:	Mass of the wet paddy (kg)
$\dot{m}_a$	:	Mass flow rate of air (Nm^3/h)

$\dot{m}_p$: Mass flow rate of product (g/s)

$\dot{m}_w$: Mass flow rate of water (g/s)

N : Drying parameters

n_{rot} : Number of rotation

n : Number of slots

ΔP : Pressure Difference (m bar)

Q_g : Volumetric gas flow rate (Nm^3/h)

Re : Reynolds number

s : Width of the slots (mm)

T_o : Ambient Temperature (°C)

T_1 : Drying air Temperature (°C)

T_2 : Dry product temperature (°C)

T_3 : Outlet temperature in (°C)

t Drying Time (min)

Ta : Temperature of Fluidization air (^oC)

$u_{g,t}$: Gas tangential velocity (m/s)

$u_{s,t}$: Solid tangential velocity (m/s)

U_{mf} : Minimum fluidization velocity (m/s)

U_t : Terminal velocity (m/s)

U_{sf} : Superficial Velocity (m/s)

U_g^* : Non dimensional fluidizing velocity

U_h : Overall uncertainty in calculating heat transfer coefficient (W/m^2 k)

u_{mf} : Minimum fluidization velocity (m/s)

U_{sup} : Superficial velocity (m/s)

u_t : Terminal velocity of particle (m/s)

V : velocity of the fluidizing air (m/s)

X : Moisture Content ratio

Y Scaling parameter

λ : Force Ratio

ε_s : Solid Volume fraction

ϕ_{am} : Moisture of the ambient air

ρ_{da} : Density of dry air (kg/m^3)

ρ_{dp} : Density of dry paddy grain ((kg/m^3)

ϕ_{wp} : Moisture of the wet paddy (g water/kg air)

ϑ_{fc} : Volume of the fluidization chamber (m^3)

ρ_{ma} : Density of moist air ((kg/m^3)

ϕ : Relative humidity

ε : Bed voidage

ε_{mf} : Bed voidage at minimum fluidization

ρ_f : Gas density (kg/m^3)

ρ_p : Solid density (kg/m^3)

μ_f : Viscosity of gas (kg/ms)

ABBREVIATION

AFR	:	Air flow Rate
BFB	:	Bubbling Fluidized Bed
CMC	:	Critical Moisture Content
CFB	:	Conventional Fluidized Bed
CFD	:	Computational fluid dynamics
db	:	Dry Basis
EUR	:	Energy Utilization Ratio
EMC	:	Equilibrium Moisture Content
FMC	:	Final Moisture Content
HRY	:	High Rice Yield
IMC	:	Initial Moisture Content
IMAP	:	Institute of Materials and Process Engineering
kWe	:	Kilo watt electrical
MC	:	Moisture Content
MFC	:	Mass Flow Controller
MER	:	Moisture Extraction Ratio
NCD	:	Natural Convection Dryer
NIR	:	Near Infrared Reflectance
PCM	:	Phase Change Material
PID	:	Proportional–integral–derivative
PI	:	Process Intensification
RH	:	Relative Humidity
RTD	:	Resistance Temperature Detectors
RFB-SG	:	Rotating fluidized bed in static geometry
SHSM	:	Sensible Heat Storage Materials
UCL	:	Universite of Catholique de Louvain
wb	:	Weight Basis

LIST OF FIGURES

LIST OF TABLES

CHAPTER-1

INTRODUCTION

1.1 MOTIVATION

Rice, obtained after processing of paddy is the primary source of staple food for more than half of the world's population followed by wheat.About 250 million tons of food grains produced in India annually including 104 million tons of paddies, 93 million tons of wheat and 18 million tons of pulses. (Annual reports 13-14 ministry of agriculture Government of India (www.agricrop.nic.in)). Unfortunately, 10% of the food grain produced is lost during post-harvest operations of drying from fields to the consumers. This 10% loss accounts for 25 million tons of food grain equivalent to 4000 million Indian rupees. Figure 1.1 shows various post-harvest losses of paddy and wheat per year.

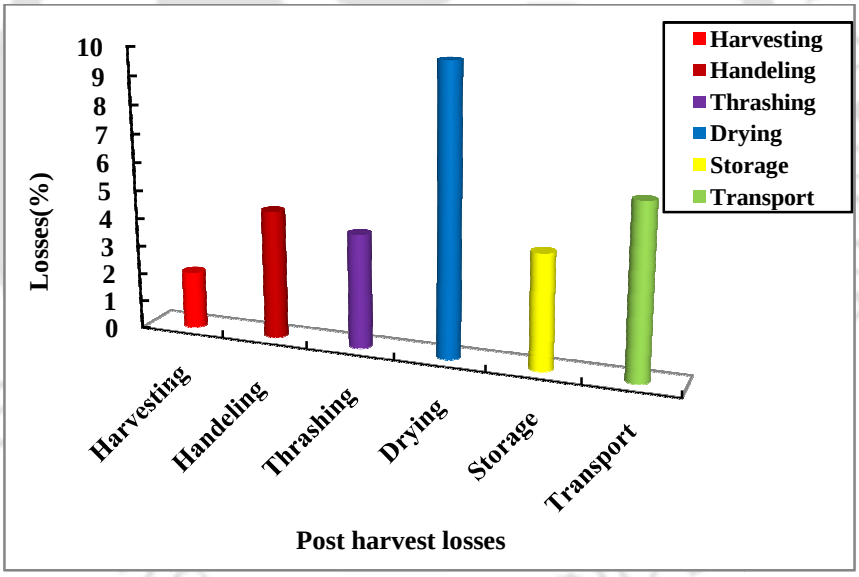

Fig.1. 1Different post harvesting losses of paddy (www.agricrop.nic.in).

It is observed from the figure that major loss of food grain is due to improper drying after harvesting. It is reported that improper drying leads to uneven drying of food grain leading to cracking of the same during milling. Moreover, nutritional value or quality of the grain deteriorates. Traditional sun drying being weather dependent leads to pilferage losses by rodents and birds and formation or growth of mould becomes common Prasad et al., (2006). To mitigate these problems, researchers have been developing improved dryers worldwide. However, most of the developed

dryers are having demerits such as high cost, complexity in operation as well as long pay-back period leading to non-acceptability by small and marginal farmers in the developing countries.

Present work is an attempt towards the development of an efficient grain dryer suitable to dry both the paddy and wheat in an efficient manner.

1.2 DRYING CONCEPT

There are many routes for drying agricultural products such as vacuum, steam or freeze drying, chemical methods, microwave drying, infrared drying, etc. Drying with the application of hot air is popular as the same can be achieved with inexpensive means Jangam, (2011). Even waste heat of any engine or a thermal plant may be utilized to produce hot air Akhter et al., (2007). Hot air passing over the product to be dried forms a thermal boundary layer with a steep thermal gradient with the product surface rendering evaporation of moisture from the surface of the product. Thus the drying with hot air involves the simultaneous action of heat and mass transfer.

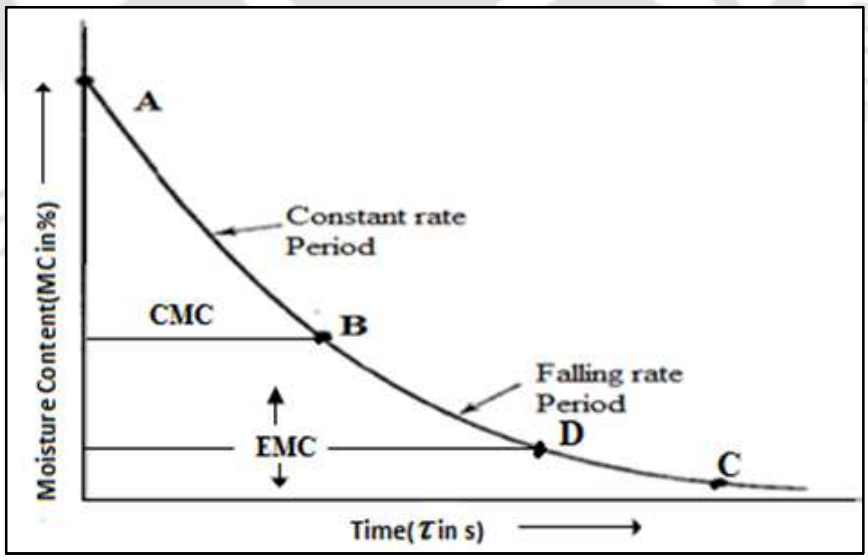

Fig.1. 2Drying Process, (A.S. Mujumdar, (2007))

Usual practice is to consider the product to be in a thin layer (less than 20 cm thickness) to maintain uniformity in drying Chakraverty, (1981). A standard drying curve representing variation of moisture content (MC) of the product with time of drying may be presented as shown in Fig. 1.2. Mujumdar, (2007). It is observed

from the figure that the drying process can be divided in two distinct regimes, namely, (1) Constant-rate period A-B and (2) Falling-rate period B-C.

1.2.1 CONSTANT RATE PERIOD

As the name suggest the gradient of moisture removal rate $\left(\frac{dM}{d\tau}\right)$ remains constant during the constant rate period. The phenomena involve equalization of the vapour pressure at the particle surface with the statured vapour pressure at the surface temperature of the product. The moisture removal continues at constant surface temperature and constant evaporation rate. The drying rate is strongly dependent on the interfacial heat and mass transfer rates. Convective heat transfer is predominating mode in this regime.

The rate of moisture transfer from the surface of the product may be expressed as Zaman and Bala, (2001),

$$\frac{dM}{d\tau} = -kA(M - M_e) \qquad (1.1)$$

where $\frac{dM}{d\tau}$ is the moisture gradient, M, M_e, k and τ are the MC of the grain, equilibrium moisture content (EMC), drying constant (h^{-1}) and drying time, respectively. It is interesting to note that point (namely, Point B in Fig. 1.2) at which the drying rate ceases to be constant is termed as critical moisture content (CMC) of the product.

1.2.2 FALLING RATE PERIOD

The second stage of the drying starts once the vapour pressure at the particle surface decreases below the saturated vapour pressure. Alternatively, falling rate period begins after crossing of CMC. Temperature of the product surface no longer remains constant rather there will be increase in temperatures both at the surface and the core of the product. During this period the drying rate may be determined by intra particle diffusion limitation. At this stage, the rate of migration of water from the interior to the product surface becomes less than the rate of evaporation of water from the surface. The transition between the two regimes and their relative

importance depends on the structure of the drying materials. However, properties of product does not affect the constant rate period.

At a particular condition of MC of the product (say point D in Fig. 1.2) comes to an equilibrium state with the surroundings. This is termed as equilibrium moisture content (EMC). Some of the recommended EMC value for different duration of storage of paddy is given in Table 1.1 (www.irri.org).

Table 1.1 Recommended value of EMC of paddy for safe storage (www.irri.org)

Storage period	EMC	Potential problems if EMC is disturbed
2 to 3 weeks	14 - 18%	Molds, discoloration, respiration loss
8 to 12 months	13% or less	Insect damage
More than 1 year	9 % or less	Loss of viability

1.3 DRYING METHODS AND DRYER

There are different type of drying processes and devices used for drying. Interestingly, none of them meet the drying requirement which leads to the development of dryers based on products to be dried. Microwave, vacuum, freeze and steam drying are getting importance for drying of pharmaceutical, chemical, biological and other highly valued products. These dryers are expensive and not affordable by small and medium category of farmers for the drying of cereal crops like paddy and wheat.

1.4 HOT AIR DRYING

As the name suggest, hot air drying involves utilization of hot air for drying. Thus this class of dryers basically operates based on simultaneous transfer of heat and mass. Figure1.3 is presents the classification of different hot air dryers. From the schematic diagram it is clear that the entire domain of hot air drying is divided in two classes, viz., (1) Sun drying and (2) Mechanical drying. Flash drying and low temperature drying are hardly used. Hence major focus on mechanical drying is given on (1) Heated air drying, and (2) Fluidized bed dying.

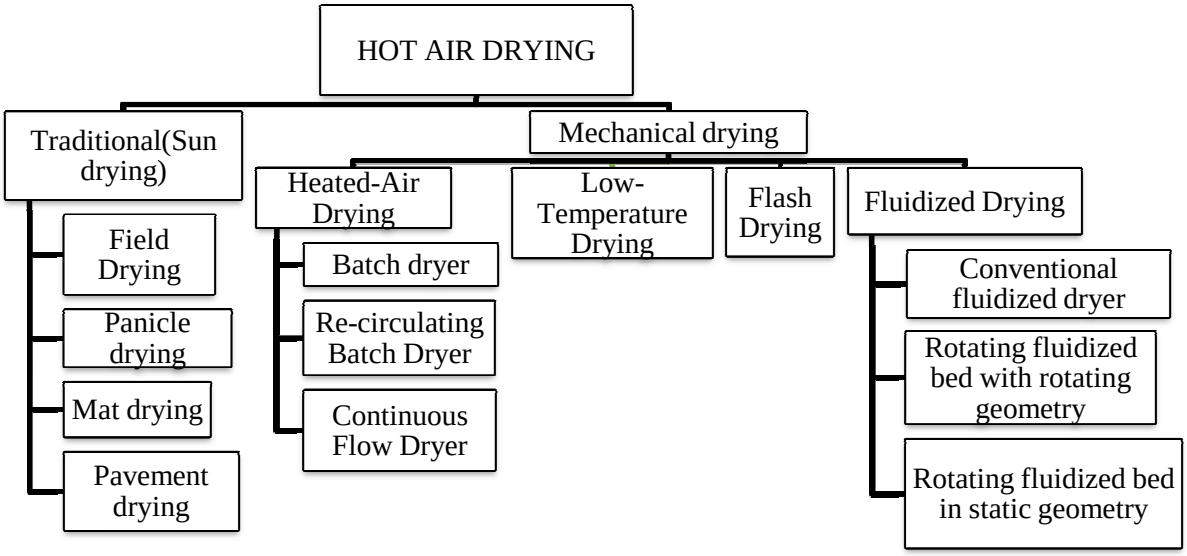

Fig.1. 3Flow diagram of different dryer

1.4.1 TRADITIONAL SUN DRYING

Traditional sun drying is a process in which agricultural products drying under the direct sunlight. Traditional sun drying are field drying, panicle drying, mat drying and pavement drying. Figures.1.4((a) – (d)) describes in different open sun drying methods of field, panicle, mat and pavement drying in rural area of developing country in India. In case of field drying the paddy/wheat are cut into a bundle and kept in field for drying. Sometimes grains are spread on the mat, pavement or the road for drying.This type of open sun drying practice is a lot of demerit. These types of drying are depend on sunlight (weather depended), ambient temperature and relative humidity.

Fig.1.4(a)Field drying[Kamrup, Assam]

Fig.1.4(b) Panicle drying

Fig.1.4(c) Mat drying

Fig.1.4(d) Pavement drying (IRRI, (2005))

Fig.1. 4(a)-(d) various type of sun drying.

Due to low ambient temperature, dying process is very slow. Thus, the EMC takes very long time as a result mould, discolour of grain, non-uniform drying, losses by rodents, birds and breakage due to movement of traffic are occurred IRRI, (2005). It is also contaminated with dust, sand particles, soil. So there is heavy loss after milling. It has limited capacity and labour intensive.

1.4.2 SOLAR HOT AIR DRYERS

In case of solar hot air dryer, sun's radiation passes through the transparent roof, usually glazed with plastic sheet. These sheets are painted with black for absorbing maximum amount of heat. Solar hot air dryers are generally classified in two types namely, direct and indirect type.Figure 1.5 and 1.6 describe direct and indirect solar dryer. In direct solar dryer, air is heated and passed through drying products inside the drying chamber by sun light. So, there are different type of products can be dried such as chillies, coconut and fish etc. Ayensu, (1997).It has advantages of comparatively low cost and provides faster and more hygienic conditions than open sun drying but it has low capacity and no control on drying temperatures. Indirect solar dryer, solar collector receives the sun's radiation and heated the air. Due to density variation, hot air circulated inside the drying chamber containing drying products Pangavhane et al., (2002). Inside the drying chamber, temperature is very low, so complete drying takes more than one day. Due to long drying process, there are no uniform drying and mould growth occurred.

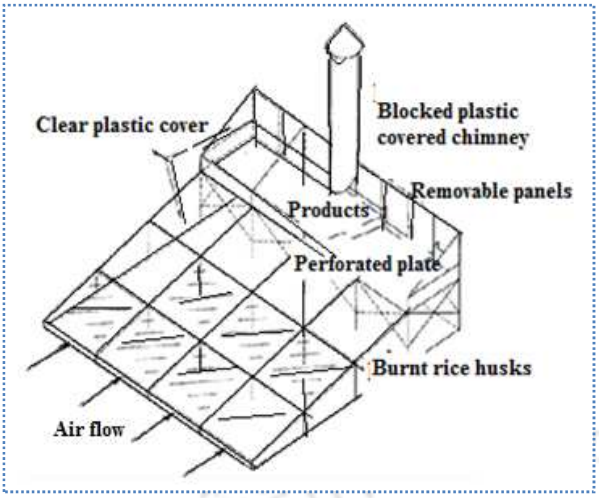

Fig.1. 5Direct solar dryer (Ayensu,(1997))

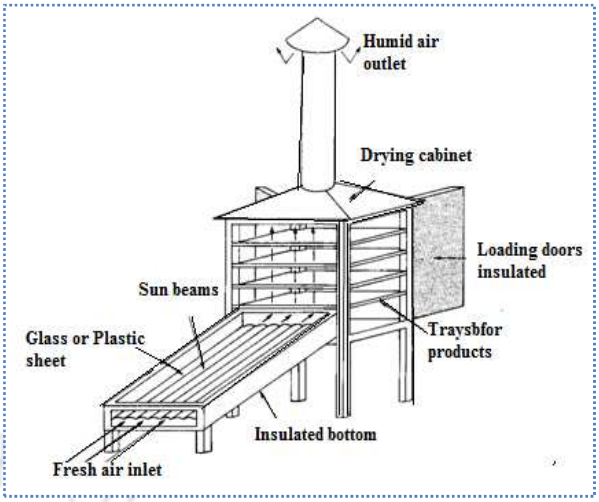

Fig.1. 6Indirect solar dryer (Pangavhane et al., (2002))

1.5 MECHANICAL DRYER

Mechanical dryers are gaining importance from the view of controlled drying. Close control of drying temperature, moisture, etc. can be maintained in this type of dryers. Based on the capacity and methods of drying, these dryers are classified into the following categories

1.5.1 BATCH DRYER

Batch dryer capacity is order of 1-3 tons per day with drying times 6-12 hours. Air temperature is maintained depend upon type of material to be used. Kerosene or rice husk has been used as fuel in batch dryer. These dryers are simple and affordable. This type of dryers is costly and labour intensive. Further, there is wide variation of moisture gradient along the vertical direction of the drying tray illustrated in Fig. 1.7.Wimberly, (1983).

1.5.2 RE-CIRCULATING BATCH DRYERS

This dryer has 4 – 12 tons per batch capacity and 8 hours is required for moisture removal. Kerosene is used as the fuel. The recirculation batch dryers have has automatic operation, requires less floor space, and produces grains with excellent quality. Re-circulating batch dryer is shown in Fig. 1.8.

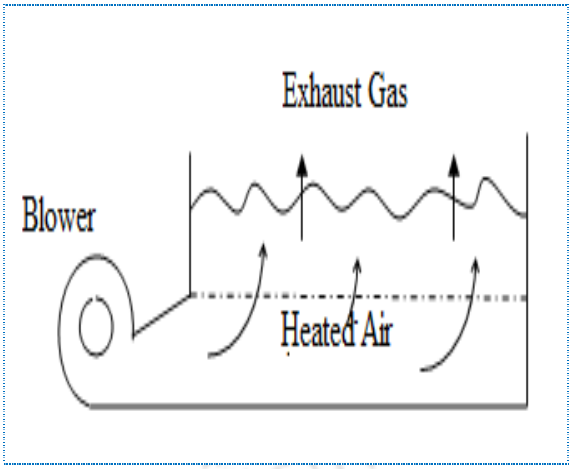

Fig.1. 7Batch bin type dryer (Wimberly, (1983))

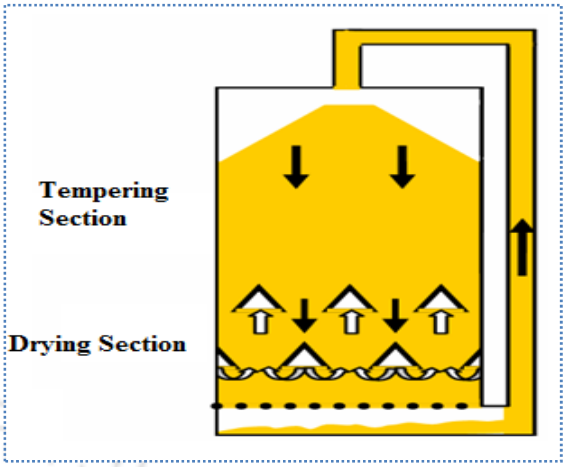

Fig.1.8Re-circulating batch dryer (www.irri.org)

1.5.3 CONTINUOUS-FLOW DRYER

In a continuous-flow dryer as shown in Fig. 1.9, wet paddy enters at the top and flows continuously through the dryer during the drying process. Hot air is blown through the paddy, which moves down the dryer. The dryer is designed such that it takes the paddy 15 to 30 minutes to move through the dryer.

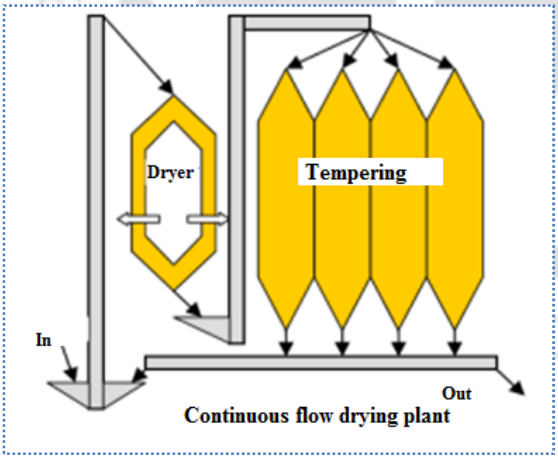

Fig.1.9Continuous flow dryer (www.IRRI.org)

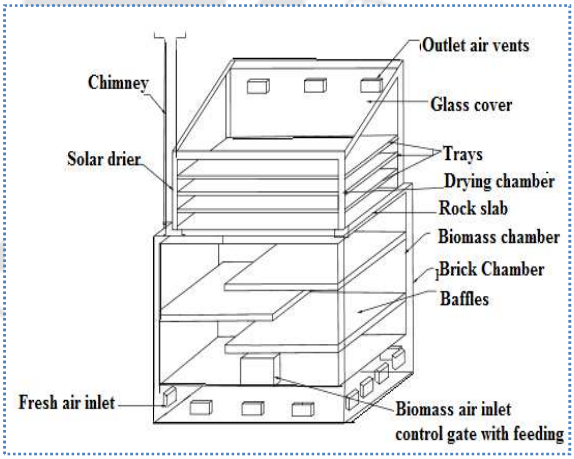

Fig.1. 10Schematic diagram of solar biomass drier (Prasad et al., (2006))

During the period, there is a reduction of 1 to 3% moisture of the product. It can operate continuously during harvest season, drying large volumes of paddy before storage. The dryers can only be used with conveying equipment, usually associated

with a bulk handling and storage system. Investment cost is high, but they can dry large volumes quickly, their operating cost per ton can often be lower than that for the larger size batch dryers and re-circulating dryers. Apart from convection solar dryer, mix/hybrid dryer (Fig.1.10) is operated with solar combination with biomass or coal. It is operated in dual mode.

1.6FLUIDISED BED DRYER

In fluidised bed drying, heat is supplied by the fluidisation gas. The gas flow need not be the only source. Heat may be introduced by the heating surfaces immersed in the fluidised state. Fluidised bed processing involves drying, agglomeration, granulation and coating of particulate materials as shown in Fig. 1.11. It is worked for a wide range of both heat sensitive and non-sensitive products.

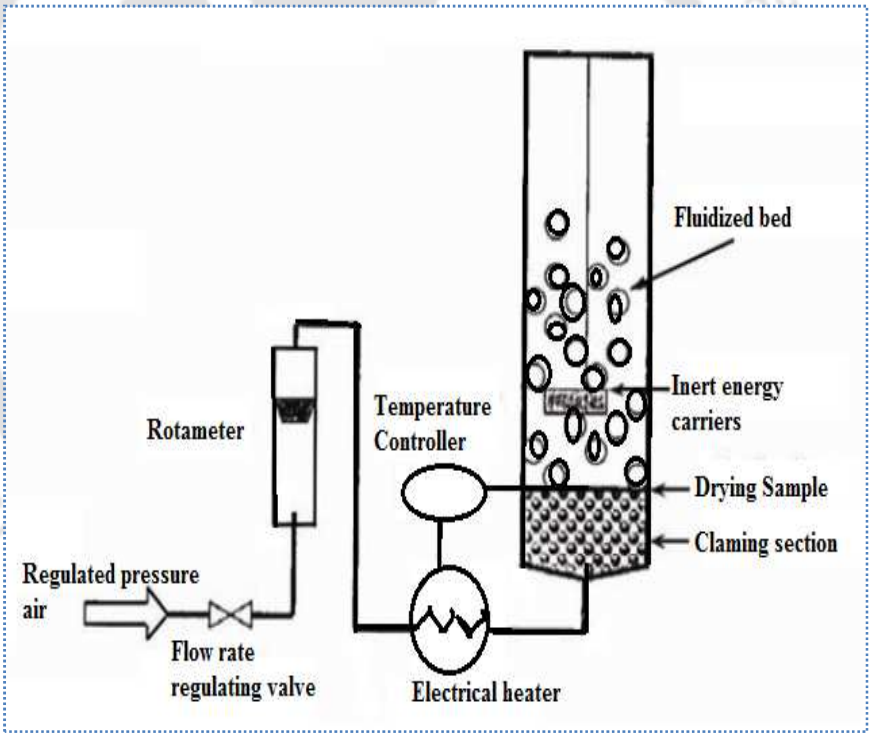

Fig.1. 11 Schematic diagram of batch fluidized bed dryer

(A. Karbasis et al., (2008))

The gas (usually air) is passing through a product layer under controlled velocity to create a fluidise state. It is of two types i.e. continuous and batch dryer. Fluidised bed drying has important advantage over other methods of drying particulate

materials. Particle fluidisation gives easy materials transport, high rate of heat exchange at high thermal efficiency while preventing overheating of individual particles

1.6.1 ROTATING FLUIDIZED BED DRYER

Rotating fluidised bed (RFB) is a fluidised bed technique but air distributor can be rotated about its axis of symmetry. The air flow is introduced in the inward direction of the radius to fluidise the bed. In a conventional fluidised bed having fixed gravity (single 'g') field but in RFB the body force in a centrifugal bed is adjusted by the rotating speed and air distributor radius. The strong centrifugal field is much higher than gravity. The large amount of air flow can able to withstand the particle bed without formation of bubbles. The gas and solid contact at high air flow is improved Triratanasirichai et al., (2011).

1.6.2 ROTATING FLUIDIZED BED IN A STATIC GEOMETRY (RFB-SG)

Rotating fluidised bed in a static geometry (RFB-SG) is based on new concept of drying. The fluidization gas is injected tangentially in the fluidization chamber, via multiple gas inlet slots in its cylindrical outer wall. The fluidization gas is injected tangentially so it fluidizes the particles tangentially and also generating centrifugal field to induce a rotating motion. The radial fluidisation of the particle bed is created by radially inwards motion of the fluidisation gas, towards a centrally positioned chimney. The radial gas solid drag force and centrifugal force are correctly balancing as it requires for design of fluidisation chamber. Feeding and removal of solids can be continuous via one end plates of the chamber. If solid feeding is sufficiently high, rotating fluidised bed in static geometry is obtained to be stable. The loading of solid in the chamber is the major factor for stable and uniform RFB-SG. The gas flow rate has minor effect for channelling and slugging but for low solids loading effect channelling and slugging de Wilde et al. (2008).

1.7 AIM AND OBJECTIVES

Since a large amount of losses and degradation of quality of agricultural products take place due to improper drying, it is necessary to explore for a right technology

for the reduction of losses so as to produce good quality products. The technology should be simple, affordable, efficient and easy from the user point of view.

The objectives of present study are as follows:

- To modify and develop an efficient rotating fluidized bed dryer in a static geometry (RFB-SG).
- Performance evaluation of the RFB-SG dryer in terms of drying air temperature, relative humidity, inventory and drying time for removal of moisture frompaddy and wheat grains.
- Comparison of performance of RFB-SG with conventional bubbling fluidized bed (BFB).
- Comparison of RFB-SG and BFB in terms of thermo economic study.

1.8 ORGANISATION OF THE THESIS

An extensive literature pertaining to drying is presented in Chapter 2. Based on the available literature research gap and need for the present research is highlighted in the chapter and also described about research on drying at IIT Guwahati. Chapter 3 deals with the theoretical background of rotating fluidized bed in a static geometry (RFB-SG) and conventional fluidized bed (BFB). Principles of operation of each type of the dryers along with relevant mathematical formulations are discussed. Experimental set-ups and procedure are described in Chapter 4. Results and discussion on parametric studies for RFB-SG and BFB are presented in Chapter 5. Thermo-economic studies along with comparisons of the two types of dryers, their relative merits and demerits are elaborated in Chapter 6. Conclusions and scope for future work are discussed in Chapter 7.

CHAPTER-2

LITERATURE REVIEW

2.1 INTRODUCTION

This chapter presents the review of the literatures available on the different types of dryers such as solar dryer (passive and active mode), hybrid dryer, conventional bubbling fluidized bed (BFB), rotating fluidised bed with rotating geometry and rotating fluidised bed in static geometry (RFB-SG). Performance analysis of these dryers along with energy and exergy analysis are reported in various literatures. A thorough discussion in this regard is presented in the following sub-sections. Summary of the literature review and the scope of the present research are presented at the end of the chapter.

2.2 DRYING CHARACTERISTICS OF DIFFERENT DRYER

Traditional open sun drying depends on various external factors such as solar intensity, ambient air temperature, relative humidity, wind velocity apart from initial moisture content and depth of the grain bed etc. Moreover, this type of drying is time consuming and difficult to maintain the quality of final products. This has motivated the researchers to develop new type of mechanical dryers throughout the world.

2.2.1 NATURAL CONVECTION SOLAR DRYER

Sun drying is the most widely traditional method of drying grain. In this method, the grains are spread on flat surface and solar energy is directly absorbed. Bala and Woods, (1994) had investigated the indirect natural convection solar dryer for moisture removal of rough rice using deep bed drying. Due to low air flow rate produced by natural convection, the drying rate was observed to be slow with non-uniformity in drying across the bed. The grain bed required regular stirring so as to obtain uniform moisture removal. Moreover, they had reported that the drying process was very sensitive to chimney height, grain bed thickness and collector length.

A low-temperature, low-cost, and simple to operate solar dryer was constructed with locally available materials by Ayensu, (1997) and Gbaha et al., (2007). Ayensu, (1997) had observed reduction of MC to 14% with ambient air at 32^0C and 80% relative humidity (RH). Similarly, Gbaha et al., (2007) had observed reduction in MC of cassava and bananas from 80% to 13%. Forsona et al., (2007) reported significant reduction in MC in drying of cassava using a mixed mode natural convection solar dryer.

A mixed mode type natural convection solar rice dryer was studied by Basunia and Abe, (2001) for thin layer drying of rough rice. They had reported the drying air temperature and RH of ambient in the range of 22.3 - 34.9^{0}C and 34.5% - 57.9%, respectively. The drying data were fitted with Page model based Diamante and Munro, (1993)on the ratios of the differences between the IMC and the EMC. They had reported error in moisture content to the extent of ± 0.38 % db.

Pangavhane et al.,(2002) developed a new natural convection solar dryer consisting of a drying chamber and a solar air heater and reported that the drying process to be energy intensive. They reported reduction in drying time (4 days) in the set-up compared to open sun drying (7 days) and shade drying (15 days).Moreover, quality of the dried product was observed to be superior to other two methods for the drying air temperature between 50^0C and 55^0C.

An indirect type natural convection flat plate solar air heater was designed, constructed and investigated by EI-Sebaiiet al., (2002).Sand was used as a thermal storage medium in order to improve the drying process. They observed significant decrease in drying time with drying air temperature in the range of 45.5 to 55.5^{o}C for agricultural products like seedless grape, apples, tomatoes, green peas and onions.

Mohaparta and Mahanta, (2012) designed and developed a natural convection dryer (NCD) with biomass as fuel. Sensible heat storage materials (pebbles) were used as thermal storage medium and phase change materials (paraffin wax) also used for constant temperature to improve the drying process. Performance evaluation of a natural convection grain dryer was observed by different drying parameters. The drying time was high to reach the desired storage moisture content of paddy.

2.2.2 FORCED CONVECTION SOLAR DRYER

As observed in section 2.2.1, time of drying in natural convection dryer was significantly high Forsona et al., (2007), Bala and Woods, (1994), Pangavhane et al., (2002). Some researchers had attempted to improve the drying process using forced convection drying Majumder, (2006), Chakraborty, (1994).

Experimental investigation was conducted by Anwar and Tiwari, (2001)for drying of 6 (six) different products, such as, green chilli, green peas, white grams, onion, potato and cauliflower and MC with time was compared with simulation. The data was analysed in terms of percent uncertainty. They reported experimental error for natural and forced convection mode operation in the ranges of 7-24% and 6-20%, respectively. Role of convective heat transfer coefficients in forced convective dryer was reported to be significant.Similar comparative studies on free and forced convection drying were conducted by Kudal et al., (2009).

Jain and Tiwari, (2004)compared forced convection drying with open sun drying and green house drying. They observed that the convective mass transfer coefficient influences the drying process significantly. Decrease in drying time was reported to be half that of open sun drying. Sreekumar et al., (2008) reported drying of bitter gourds using a double chambered forced convection solar dryer. They achieved maximum drying air temperature of 78.1 ^{0}C with the prototype and could reduce moisture content from 95% to 5% in 6 hours maintaining the quality of the product.

2.2.3 HYBRID DRYER

Bena and Fuller, (2002) has reported the performance of a hybrid natural convection dryer utilizing solar energy as well as biomass. They had reported drying of 20-22 kg of products with drying efficiency 9% with biomass as fuel. However, the drying efficiency was observed to be 22% with standalone solar drying without load. Combining the solar and biomass gave overall 27% drying efficiency. The combine solar and biomass drying technology is suitable for non-electrified areas of developing countries of the world.

A solar cum biomass fuelled dryer was developed by Prasad et al., (2006). They had reported that the system was capable of generating an adequate and continuous flow

of hot air temperature between 55-60^{0}C to dry turmeric. The traditional drying, i.e., open sun drying took 11 days to dry the turmeric while solar biomass drier took only 1.5 days and produced better quality products. The efficiency of the whole unit was reported to be 28.57%.

Madhlopa and Ngwalo, (2007) developed an indirect type natural convection solar dryer with biomass backup heaters for the drying of fresh pineapples. The dryer consists of solar collector, drying cabinet and a backup biomass heater. The collector of the dryer has a horizontal concrete absorber painted matt black on its top part and integrated to a pile of rock to store sensible heat. They reported average values of drying efficiency to be 15%, 11% and 13% for the solar, biomass and solar–biomass modes of operation, respectively.

The hybrid solar dryer with heat exchanger cum heat storage unit and drying chamber was investigated by Amer et al., (2010). The dryer was operated as a hybrid solar dryer during cloudy days and as a solar dryer during normal sunny days. Drying was also carried out at night with heat energy stored in water which was collected during the time of sun-shine hours.

2.3 PARAMETRIC STUDY ON DRYING

2.3.1 EFFECT OF DRYING AIR TEMPERATURE

Ojha and Chakraverty, (1975) studied the effect of the drying air temperature on moisture removal from paddy grain. Experiments were conducted by exposing paddy grains to air temperature in the range of 45-85^{0}C for various duration of 5 - 20 minutes in steps of 5 minutes. They had observed the moisture content 13.5, 12.5, 11.5 and 10.5% for the duration of study(each step of 5 minutes starting from exposure time of 5 min). High rice yield (HRY) as well as MC is decreased with increase of drying air temperature. Tabassum and Jindal, (1992) had reported insignificant moisture removal rate at 40^{0}C. However, Yadollahinia et al., (2008) had observed the increase in the drying rate for the drying air temperature from30to 70^{0}C. Similar observations are reported by Doungporn, (2012).

Chungu, (1985) had compared the drying of paddy under a shade as well as in a natural convection and reported there is no significant difference in HRY of paddy

for both the systems up to drying air temperature of 60°C. However, HRY percentage is decreasing with drying air temperature above 60°C resulting in increase in broken rice in subsequent milling operation.

Luangmalawat et al., (2007) reported the sensitiveness of quality of grain with drying air temperature. Higher temperature caused the degradation of the food quality such as colour, shrinkage and nutritional value of the grain.

2.3.2 EFFECT OF DRYING AIR FLOW RATE

Effect of air flow rate on moisture removal rate in NCD is reported to be insignificant in literature Henderson and Pabis, (1961), Tabassum and Jindal, (1992). Results of moisture removal rate with drying time for the air flow rate between 0.2 to 0.52 m/s for drying of paddy grain (Fig. 2.1) is reported by Tabassum and Jindal, (1992)and observed the effect of air flow rate to be insignificant on moisture removal rate.

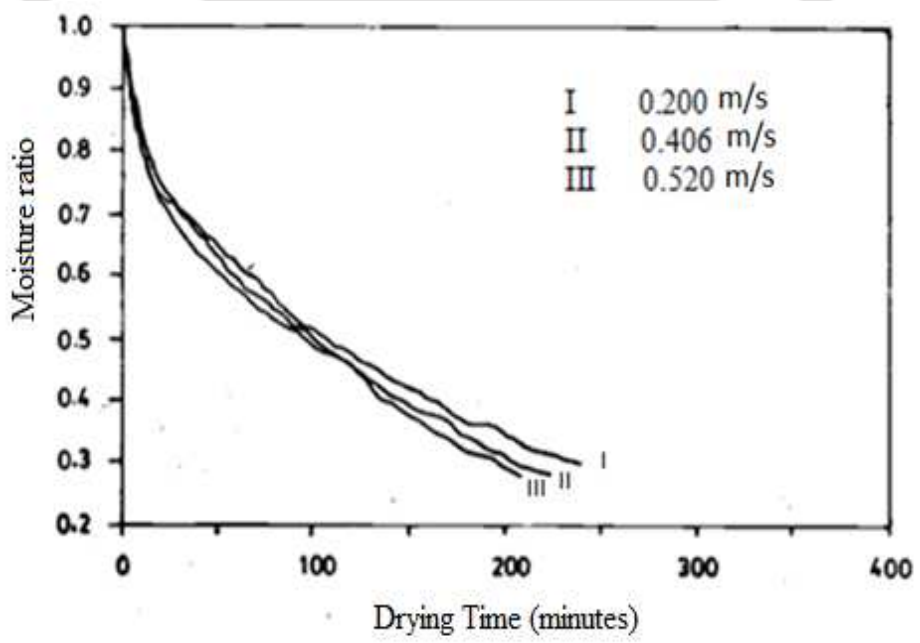

Fig.2. 1 Effect of air flow rate on moisture removal rate (Tabassum and Jindal, (1992))

Similar observations are reported by Henderson and Pabis, (1961)for the drying of wheat grain in the air flow rate between 10-68 cm^3/s.Akpiner et al., (2003) and Yadollahina et al., (2004) had studied the effect of air velocity on drying period and moisture removal rate and reported little effect of air velocity on the drying rate.

However, it was observed that air flow rate plays an important role in moisture removal rate in case of forced convection drying described by Chinenye, (2009), and Chakraverty, (1994).

Drying of cocoa bean was studied by Chinenye, (2009). He reported the increase in drying rate with increase in air inlet velocity from 1.3 m/s to 2.51 m/s. similar observation was reported by Hustrulid, (1962) and Hustrulid, (1963)for the constant rate period of drying.

Ertekin and Yaldiz, (2004) had observed the decrease in drying time by 2 hours with increase in air velocity from 0.5 to 2.0 m/s while drying the eggplant at air temperature of 70^0C as shown in Fig. 2.2.

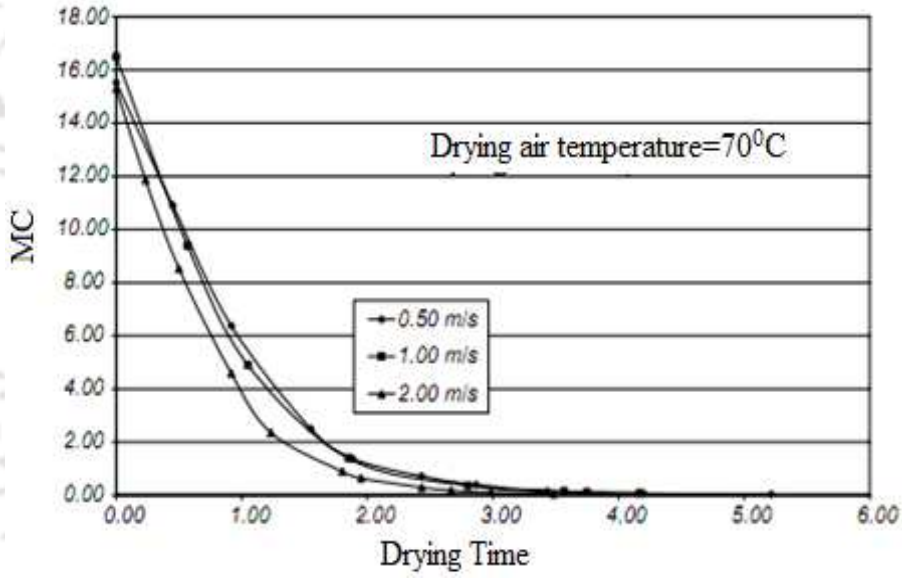

Fig.2. 2Effect of drying air velocity on MC (kg water/kg dry matter) and drying time (Ertekin and Yaldiz, (2004)).

Sarsavadia et al., (1999) performed thin layer drying of onion with air inlet temperature and air flow velocity range of 50^0C - 80^0C and 0.25-1.00m/s,respectively. They had reported that drying rate increase with increase of air flow velocity and decrease in drying time.

Ozbey and Soylemez , (2005) had reported batch drying of wheat grainin a fluidized bed dryer with air inlet temperature and air flow mass flow rate of 40-70^0C and 0.1- 0.264kg/s, respectively and observed increase in drying rate with increase in mass flow rate of air.

2.3.3 EFFECT OF RELATIVE HUMIDITY (RH)

Henderson, 1957 has studied the effect of RH changed from 8 to 65%. He observed that, HRY of total yield decreased with decreasing RH and is increased with increasing air temperature. Similarly Tabassum and Jindal, (1992) has reported, the moisture removal rate was faster at low RH as compare to higher RH.

Increase of air RH, the moisture removal rate decreases slightly described by Chakraverty, (1994). The effect is very small as compare to the effect of increases of drying air temperature.

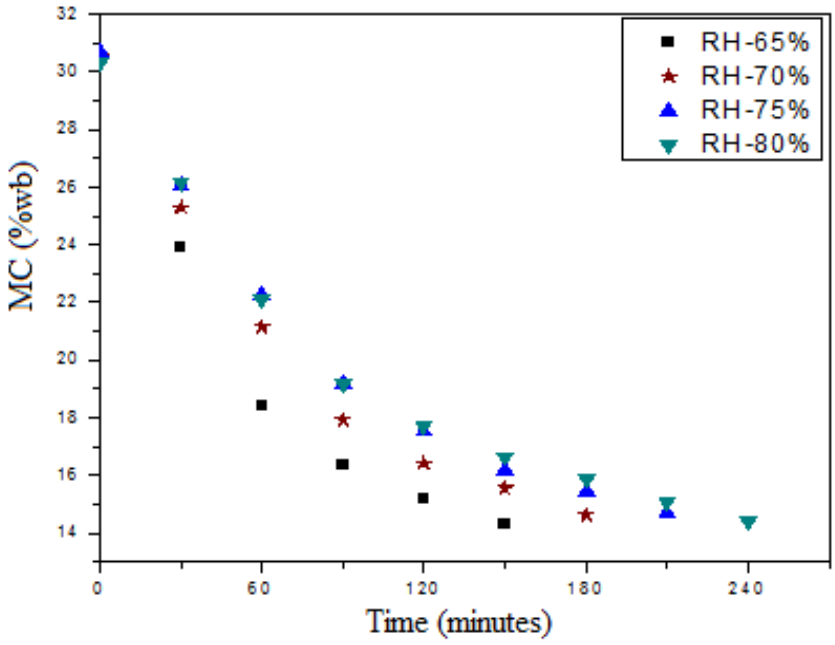

Fig.2. 3 Variation of average moisture content with time at different RH (Mohapatra and Mahanta, (2012)).

The low RH and high temperature surrounding the kernel caused rapid evaporating capacity and increased the moisture gradient has reported by Nag et al. (2005). Mohapatra and Mahanta, (2012) has reported that the moisture removal rate is decreasing with increase of RH from 65% to 80% and drying time increased from 150 minutes to 240 minutes described in Fig.2.3.

2.4 MODELLING AND SIMULATION OF DRYING PROCESS

Laohavanich and Wongpichet, (2008) had compared paddy drying for five different existing mathematical models and reported that the modified Page model is the best

with highest value of $R^2 = 0.9952$. Hacıhafızoglu et al., (2008) reported that both the Page Model and Diffusion Approach Model give the best results for thin layer drying for rough rice (long) with drying air temperature and air velocity in the range of 40-60^{O}C and 1.5 - 3.0 m/s, respectively as shown in Fig. 2.4.

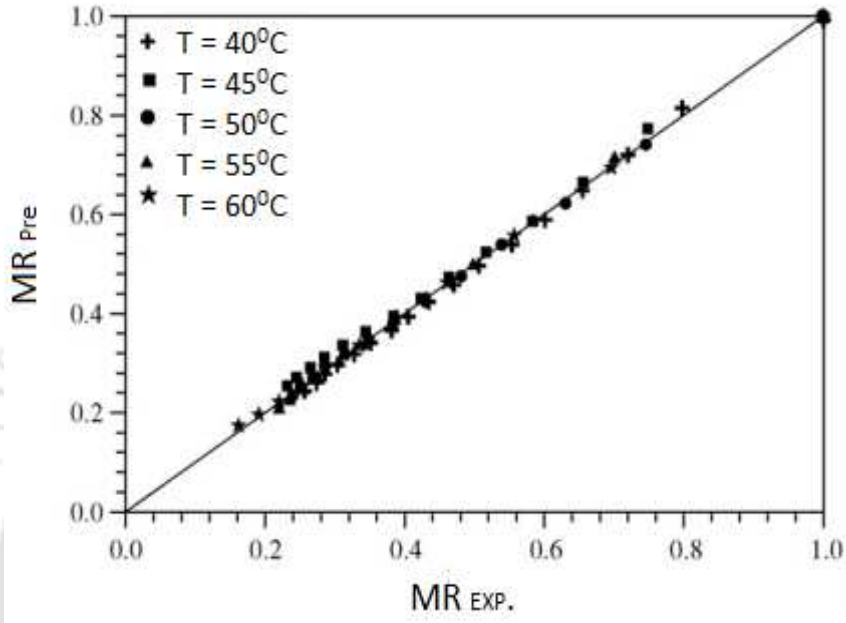

Fig.2. 4Comparison of experimental and predicted moisture ratios for V=3.0 m/s (Hacıhafızoglu et al., (2008))

However, deep bed drying behaviour is complex due to shrinkage leading to the changes in diameter of the product, bed porosity, specific heat, conductivity and air velocity Bennamoun and Belhamri, (2008).

Golmohammadi et al., (2015) has studied the model of Fick's second law of diffusion for both the drying and tempering stage of paddy. They observed that the effect of air velocity plays insignificant role in the drying process. But drying time reduces withincrease in drying air temperature. They suggested that the model may be used for optimization ofthe total energy consumption.

2.5 REVIEW ON THE PERFORMANCE OF THE FLUIDIZED BED DRYER

Fluidized bed dryer have successfully been used for drying of various products such as coal, maize, paddy, coconut, chilli and black tea, etc. Daud, (2008) had reported that fluidized bed drying has the advantages of large contact surface area between

solids and gas, high thermal inertia of solids, good degree of solids mixing. Karbassi and Mechdizadeh, (2008) investigated the quality of paddy drying using a traditional method and a bubbling fluidized bed. They reported that paddy drying in a fluidized bed dryer reduces HRY. But colour of the dried paddy gets faded.

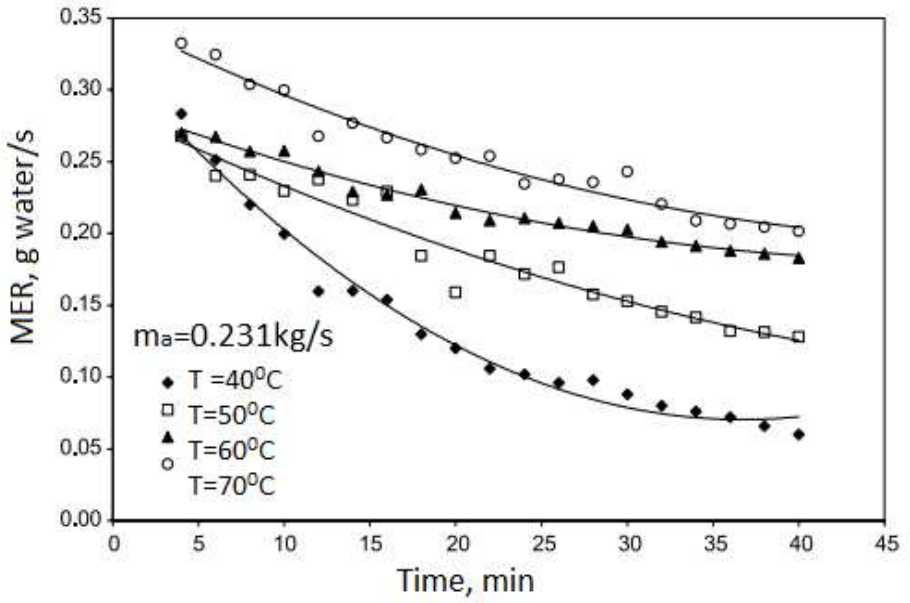

Fig.2. 5Variation of Drying time and MER (moisture extraction rate) with air inlet temperature (Ozbey and Soylemez , (2005))

Ozbey and Soylemez , (2005) had reported the drying of wheat grain in a fluidized bed dryer with air inlet temperature and velocity of 40-70^{0}C and 0.1- 0.264kg/s, respectively. They had observed an increase of drying rate with the increase of air inlet temperature. Subsequently, drying time was reported to be decreased as shown in Fig. 2.5.

Soponronnarit et al. (2001) described the drying of soybeans at inlet air temperature in the range of 110-140^0C. They had reported increase in cracking and breakage of soybean with increase in air temperature. They recommended reduction in final MC to be23.5% db for safe drying. Further, they had concluded that rapid transfer of heat and moisture between solids and gas had shortened drying time considerably without damaging heat sensitive materials. Similar results are reported by Shi et al., (1998) for the drying of potato slices.

A vibro fluidised bed paddy dryer with capacity of 2.5 to 5.0 tons/h was developed by Watchacama et al., (2000). It was reported that the moisture content of paddy reduced from 28 to 23% d.b. The average percentage of HRY was 5% higher than that of the traditional sun drying.

Silva-Moris and Rocha, (2003) had investigated the drying of adipic acid with particle size and density of 75-600 µm and 1340 kg/m^3, respectively in a vibro-fluidized bed dryer and observed strong dependence of frequency and intensity of vibration on the drying rate.

The mathematical modelling and simulated the drying of a cross flow continuous fluidised bed dryer was studied by Izadifar and Mowal, (2003). The RH, temperature of air, IMC, feed rate and FMC were considered to be the parameter for simulation. They reported a good agreement of experimental results with the modified Euler's model for the drying air temperature of 60^0C.

Prachayawarakorn et al., (2005) studied the performance of pulsed and conventional fluidised paddy dryer. They had recommended that inlet temperature should be lower than 145^0C. They had reported decrease in energy consumed by 30% in the pulsed fluidised bed compared with the conventional fluidized bed dryer (CFB).

Numerical simulation of two phase theory of a continuous fluidised bed dryer was reported byGarnaviet al.,(2006)and observed the superficial air velocity and to be a strong function of drying rate. They had observed decrease in mass of inventory and heat transfer rate with the increase in bubble size in the bed resulting in decrease in bed temperature leading to the increase in MC.

Nitz and Taranto, (2007) had reported the drying characteristics of beans in a pulsed and conventional fluidised bed. In a pulsed fluidised bed, the drying rate of beans was well predicted by the Page equation and energy saving without affecting the quality of beans.

In conventional fluidized bed, the heat, mass and moment transfer rates are limited due to the fact that the gas-solid slip velocity cannot exceed the terminal velocity of the particles in the gravitational field of the earth Eliaers and de Wilde, (2013). They

also observed that the increase of the gas flux enhances both the mass and heat transfer rates leading the dramatic decrease in volume fraction in conventional fluidized beds.

The fluidization behaviour of Geldart B silica particles with mean diameter of 300µm and density of 2600kg/m^{3}was studied by Sobrino et al.,(2008)using a rotating distributor fluidized bed. They observed that the fluidisation could be controlled by controlling the rotational speed. The distributer plate rotation had promoted an increase in the radial dispersion of the particle reducing the high concentration zones present at the fluidised beds. Nakamura et al., (2013) studied fluidization behaviour of micro particles with Geldart-C type in similar way. However, it was reported by Moon et al., (2006)that fluidization of fine or light particle is extremely difficult in a conventional fluidized bed.

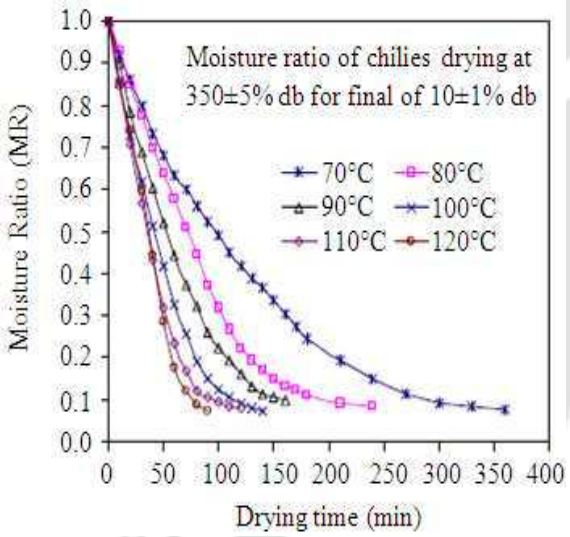

Fig.2. 6Variation of drying time withMR for drying air inlet temperature

Fig.2. 7 Quality of dried chillies (Dongbang et al., (2010))

Dongbang et al., (2010) investigated experimentally the drying of chillies in a rotating fluidised bed. Experiments were conducted by them with drying temperature in the range of 70-120^{0}C and drying air velocity of 1.8m/s.Chillies with IMC of 350% db were dried till 10±1%db (Fig. 2.6). They had compared the results with traditional sun drying. However, quality of final product appeared deep dark red due to the application of high temperature as shown in Fig. 2.7.

The drying characteristics of cohesive particulate materials of 2-hydroxybenzoic acid (Geldrat's group 'A') were reported by Ambrosio-Ugri and Taranto, (2007). They reported the difficulty in fluidization of this type of particles due to the strong cohesive force under wet condition in the conventional fluidized bed. They had investigated the fluidization of the same in arotating pulsed fluidised bed and reported high quality drying of finished products with the decrease in drying time.

However, rotating fluidized bed with rotary geometry is prone to vibration and leakage and difficult to maintain de Wilde and de Broqueville, (2008). They had also reported difficulties in feeding and removal of particles from the drying chamber. This lead to the development of rotating fluidized bed with static geometry (RFB-SG) de Wilde and de Broqueville, (2007).

2.6 RFB IN STATIC GEOMETRY (RFB-SG)

RFB-SG was conceptualized based on the work of Ye-Mon Chen, (1987) in which he had reported effect of centrifugal force in an inward direction to a rotating cylindrical drying chamber. He had observed layer wise motion of gas-solid in radial direction of the bed improving the drying rate. RFB-SG was reported by de Wilde and de Broqueville, (2007). In this bed a radially outwards centrifugal force exerted on the solids is balanced by a radially inwards gas-solid drag force. The centrifugal force is determined by the rotational speed of the particles in the bed and is a multiple of acceleration due to gravity ('g') Axel de Broqueville, (2004), Quevedo et al., (2005) and Ahmadzadeh et al., (2005).

The hydrodynamic behaviour of a RFB-SG was studied by Dutta et al., (2010) by using CFD simulation. An Eulerian two fluid model was used and also K-$\boldsymbol{\varepsilon}$ model was adopted for rotational flows. This simulation is an attempt to design the RFB-SG with high efficiency gas –solid momentum transfer. Geldart A and B of particles were used to evaluate the pressure, centrifugal force, redial and tangential slip velocity inside the RFB-SG. It was reported that the motion of the particles in the bed was mostly tangential due to tangential direction of gas injection. However, fluidization in the radial direction was also reported to be significant.

Abdollahi et al., (2010) has performed experiments both CFB and RFB-SG dryer for gasification and reported improvement in syngas quality. They observed an improvement of the heat, mass transfer and gas-solid contact for the same equivalence ratio. De Wilde and de Broqueville, (2010) introduced a rotating chimney for reducing the phenomenon of bubbling in RFB resulting in increase in bed density. They had reported that this improvement can easily fluidize Geldart-B particles.

Eliaers and de Wilde, (2013) experimentally studied the performance of RFB-SG for the drying of woody biomass and compared their results with CFB simulation. They observed that high acceleration due to gravity inside the bed facilitates the operation of RFB-SG with more inventories (dense bed) at higher gas-solid slip velocities. They further emphasised that RFB-SG to be compact and economical for drying of biomass. Performance in terms of specific drying rate of biomass in RFB-SG and CFB dryer were reported by them as shown in Figs. 2.8-2.9.

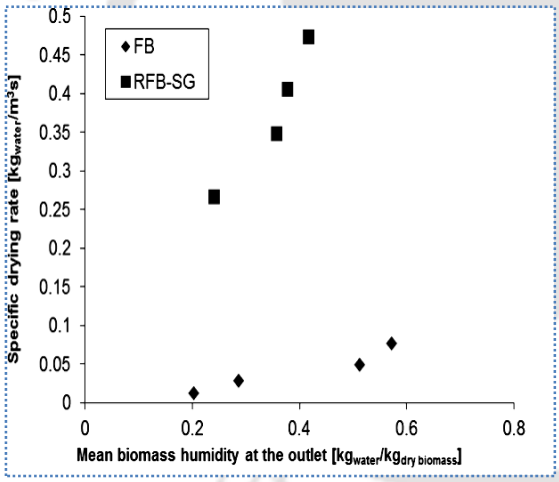

Fig.2. 8Biomass humidity vs. Specific Drying rate

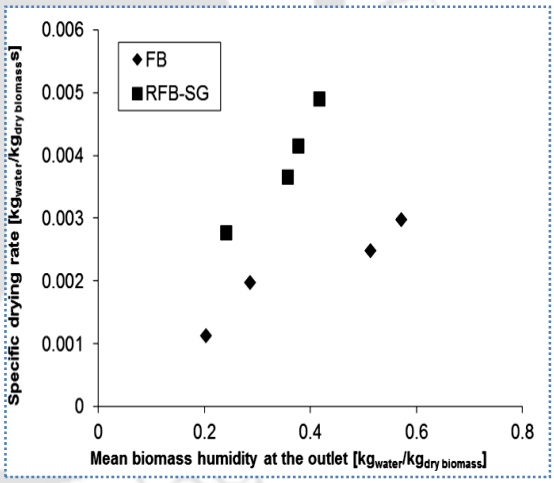

Fig.2. 9Biomass humidity vs. Specific Drying rate

(Eliaers and de Wilde , (2013))

2.7 QUALITY OF DRIED PRODUCTS

Quality of grain is determined by two ways i.e. subjective and objective methods described IRRI, (2002). Subjective method is based on individual preferences such as taste, smell and appearance of the products. Similarly objective method involves characterization of physical and chemical properties. Determination of MC,

Maturity and HRY involves physical characterization whereas chemical characteristics refer to the nutritional value of the products. Broker et al., (1974) described the shrinkage of grain due to rapid drying known as case-hardening. It can prevent further drying producing dormant seeds.

The qualities of grain are deteriorated by water, insects and heat expose. Biochemical changes occur in the grain resulting in the development of odour and colour change Bakker-Atkema and Salleh, (1985), IRRI, (2002).

Due to fluctuating temperature, mechanical impact leads to development of crakes and it leads to growth of mould, insects and bad smell. Over expose of the mature grain to variable temperature and moisture content in the field results in adsorption and desorption of moisture creating fissuring of rice kernel Dong and Zhihuai, (2003).

Wongpornchai et al., (2004) reported the effect of drying rate on moisture removal from the grain at high temperature. They reported, reduction in the concentration of the key aroma constituent (2- acetyl-1- pyrroline) of the paddy at high temperature drying is incurring loss in quality.

2.8 THERMODYNAMIC ANALYSIS

Thermodynamic analysis of drying system is important for understanding and improving the energy utilization Nag, (2005), Chengal, (2006). Most of the dryers reported in literature are of low thermal efficiency attributing to significant losses of thermal energy. Thus energy and exergy analysis can help in overall improvement of the dryers Akpiner et al., (2005), Bolaji(2011), Saidur et al.,(2012).

Midilli and Kucuk, (2003) had carried out energy and exergy analysis of a solar cabinet dryer for the drying of unshelled pistachios. They had estimated both the energy and exergy in various locations of the dryer for drying air temperature, relative humidity of surroundings and drying air velocity of 40-60 ^{0}Cand 37-62%, 1.23m/s, respectively. It was observed that the energy utilization decrease from bottom to the top of the dryer.

Akpinar et al., (2005) reported energy and exergy analysis of the single layer drying process of potato slices. The potato slices were dried in the range of 60-80^{0}C with 20-10 % RHof surroundings for the air velocity of 1 and 1.5m/s. It was observed that that exergy losses are increasing from the bottom to the top of the dryer in the same direction of air flow.

Mohapatra and Mahanta, (2012) had designed a natural convection dryer (NCD) and reported energy and exergy of paddy drying with air inlet temperature ranges between 50 to 65^{0}C and RH 65%. They reported EUR and exergetic efficiencyto be in the range of 17.19-52.1% and 38.94%, respectively to reach the desired moisture level.

The thermodynamics analysis of cyclone type dryer using single layer drying process of pumpkin slices was investigated by Akpinar et al., (2006). They had experimented on the drying ranges between 60-80^{0}C, RH 10%-20%, and drying air velocity 1-1.5 m/s. It was reported utilized exergy to be 2.198kJ/s and same was obtained at the bottom of the dryer.

Aghbashlo et al., (2008) had estimated EUR, energy and exergy efficiency for a continuous bed dryer for the drying of potato chips whereas Promas et al., (2010) has investigated energy and exergy analysis using hot air in drying process for a porous media. They reported that EUR and efficiency were dependent on the particle size as well as hydrodynamics properties. The drying rate was slightly higher in fine particles than course particles. Energy and exergy balance of a forced convective solar dryer with thin layer drying for mulberry was investigated Akbulut and Durmus, (2010).They reported decrease in EUR and exergy loss with increase in mass flow rate of air. Similar studies were conducted by Aviara et al., (2014)for the drying of cassava starch drying. They had reported increase in energy efficiency from 16 to 30% (approx). However, there was only nominal variation in EUR.

Sarker et al., (2015) has investigated energy and exergy analysis of industrial fluidized bed paddy dryer with capacity of 2t/h. They reported variation of EUR (in percentage) from 5.24 and 13.92% with exergy efficiency from 31.18 to 37.0%.

Energy and exergy analyses were conducted for the drying of wheat grain in fluidized bed by Syahrul et al., (2002). They reported that exergy efficiency were less than energy efficiency and both energy, exergy efficiencies decreases with increase in drying time. Moreover, same was reported to decrease sharply with decrease in as well as sharply with the MC of the grain. Similar observation was reported by Husain et al., (2007).

2.9 RESEARCH ON DRYING AT IIT GUWAHATI

Mahapatra and Mahanta (2012) designed and developed a natural convection dryer (NCD) with sensible and latent heat storage for quality drying as shown in Fig. 2.10. It consists of (1) biomass burner, (2) biomass feeding pipe (BFP), (3) tray containing phase change material (PCM), (4) flue gas pipe, (5) perforated drying tray, (6) air inlet vents, (7) sensible heat storage materials (SHSM) and (8) rectangular brick chamber.At the core of the dryer a conical furnace fabricated with MS sheet was placed centrally 22 cm above the bottom of the dryer. The furnace was placed over a base plate made of GI sheet with 1700 holes each of 5 mm diameter to facilitate the supply of air for combustion. The top of the biomass furnace is connected to the exhaust pipe .Wood chips were fed to the furnace through an inclined inlet connected to the body of the furnace.

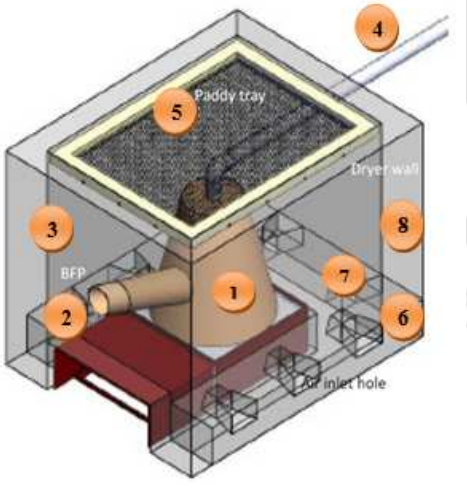

Fig.2. 10 Schematic diagram of NCD dryer

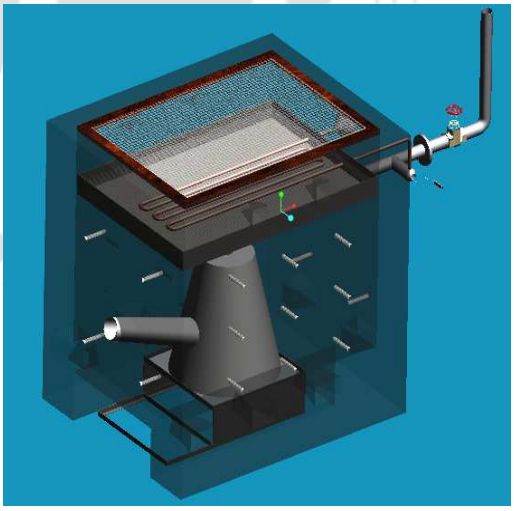

Fig.2. 11Schematic diagram of NCD dryer with heat exchanger

Eight rectangular venturi holes (3 nos. each on the left and right walls and 2 nos. each on the rear and front wall) are constructed in equal spacing at the bottom of the

dryer walls to facilitate air supply to the wax tray. In addition, a paraffin wax tray was fabricated for storage of PCM to facilitate constant temperature drying. Pebbles of 5-7 cm diameter are used in the lower section of the dryer around the biomass furnace as sensible heat storage material (SHSM) to supply the heat for a longer period of time by storing it as internal energy.

2.9.1 MODIFICATION OF THE NCD

As the flue gas coming out from the furnace in the NCD carries lots of heat and rejects it to atmosphere, a preliminary work was done to capture the waste heat and increase the drying efficiency at the initial stage of present thesis. In the present modification, the high temperature flue gas coming out from the biomass furnace through the main exhaust pipe was recirculated inside the paraffin wax tray by using a recuperative heat exchanger as shown in Fig. 2.11.

Figures 2.12 (a)-(b) present the variation of moisture with drying time. Effect of relative humidity (RH) of laboratory is shown in Fig. 2.13(b). It is observed that for drying of 10 kg of paddy grains at an average controlled temperature of 62.9^{0}C, drying time is quite high (240 minutes) to reach the desired moisture content of 13-14%(db). It is also observed that the drying time increases significantly with increase in RH.

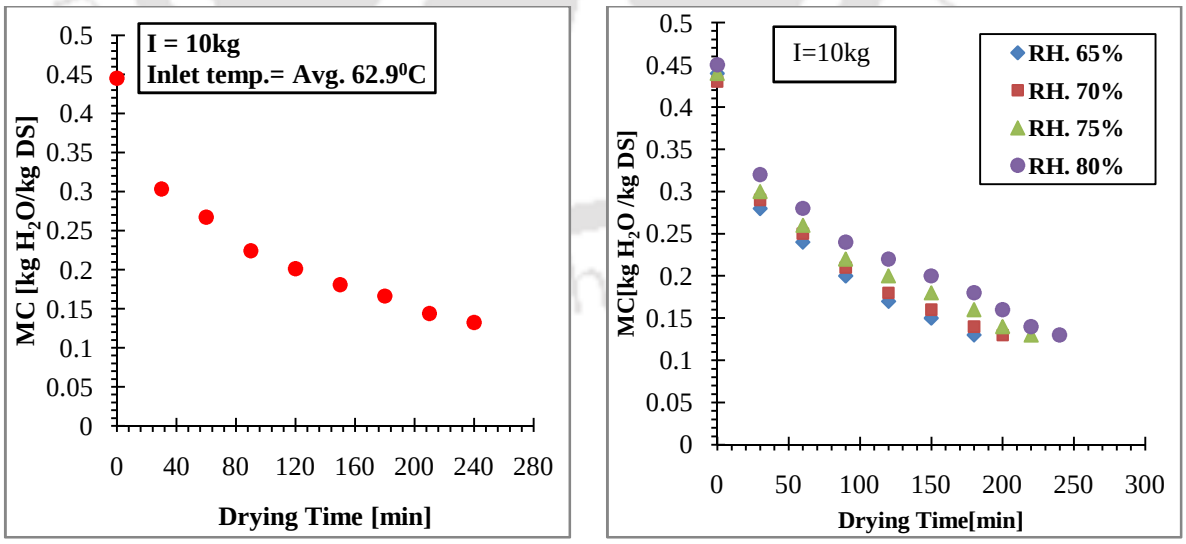

(a) (b)

Fig.2. 12(a) Moisture content varies with drying time (b) Effect of relative humidity on the variation of MC with drying time

2.10 RESEARCH GAP

An extensive literature review was conducted involving drying of various products in natural convective, forced convective as well as hybrid dryers. Excellent studies are reported regarding performance of various types of dryers for wide range of input parameters and environmental conditions. Preliminary experiments conducted at IIT Guwahati with natural convection dryer indicate significantly large drying time even for the drying of 10 kg of paddy grains. As such dryers work with the phenomena of natural convection, large output is hardly achievable. Conventional fluidized bed drying was reported to be fast but energy intensive. A new version of dryer with rotary matrix evolved to overcome the drawbacks of conventional fluidized bed. It was reported to be prone to leakage at the bearings. Moreover, rotary fluidized bed is subjected to wear and tear causing mechanical failure after several cycles of operation. Loading and unloading of product to be dried is also reported to be difficult in continuous mode of operation as the whole dryer rotates about its axis. RFB-SG eliminates the problems encountered in the rotary fluidized bed. While in operation, RFB-SG structure remains statically balanced over its axis but the drying air and product to be dried are in fluidized condition. Moreover, experiments and analytical studies on RFB-SG reveal that a high value of acceleration due to gravity in the order of 10g is realized inside the drying chamber causing tremendous centrifugal force towards the axis of the dryer which is balanced by formed drag as reported by Ye-Mon Chen, (1987), Eliaers and de Wilde, (2013). They further reported the bed to be dense and compact with high rate of heat and mass transfer. A few studies are only conducted in RFB-SG to dry sample of biomass. Moreover, detail thermo-economic studies are hardly reported. Hence, there is a need to explore the feasibility of RFB-SG for the drying of cereal crops. Present works is an attempt towards drying of paddy and wheat grains in RFB-SG and evaluate the effect of influencing parameters on drying time and drying rate taking into considerations of thermo-economic analysis.

2.11 SCOPE OF THE RESEARCH

As discussed in the previous sub-section, an attempt has been made to investigate the drying characteristics of paddy and wheat grain in RFB-SG with different operating parameters. The scope of the study includes:

- To modify and develop an efficient rotating fluidized bed dryer in a static geometry (RFB-SG).
- Performance evaluation of the RFB-SG dryer in terms of drying air temperature, relative humidity, inventory and drying time for removal of moisture from paddy and wheat grains.
- Comparison of performance of RFB-SG with bubbling fluidized bed (BFB).
- Comparison of RFB-SG and BFB in terms of thermo economic study.

Overall, above study will help in design and improvement of the RFB-SG.

2.12 SUMMARY

A thorough literature review was conducted and discussed in the present Chapter. Drawbacks of different dryers and their performances are presented. Based on the same, problem for the present work is identified. Experimental set-up and procedure are discussed in the next Chapter.

CHAPTER-3

THEORETICAL BACKGROUND OF RFB-SG AND BFB DRYERS

3.1 INTRODUCTION

Drying is a continuous process to reduce the moisture content of the feed materials bearing a simultaneous functional relationship with the conditions of the inlet air, grain temperature and the humidity of the environment, etc. In this chapter, theories related to heat and moisture transfer in rotary fluidized bed with static geometry (RFB-SG)and conventional bubbling fluidized bed (BFB) is discussed.

3.2 ROTATING FLUIDIZED BED IN A STATIC GEOMETRY (RFB-SG)

In conventional fluidized bed the gas-solid slip velocity cannot exceed the terminal velocity of the drying materials under the influence of the gravitational field of the earth. Therefore, the mass, momentum and heat transfer rates are limited. Moreover, it is difficult to fluidize fine or light cohesive particles in fluidized bed because of the prevailing van derWaals force. To deal with these issues, concept of rotating fluidized bed with static geometry (RFB-SG) has been developed. A vortex chamber is used in the context of the RFB-SG to achieve tangential and radial fluidization of particles against a very high acceleration due to gravity ('g'). This helps in enhancing heat and mass transfer process in RFB-SG in comparison to the other available dryers.

3.2.1 CONCEPT OF RFB-SG DRYER

The conditioned air is injected tangentially through the multiple air inlet slots of the outer cylindrical wall of the vortex chamber in RFB-SG as shown in Figs. 3.1(a)-(b). The drying particles are entrained by the air supplied resulting in a rotational motion of the air-particle motion in the vortex chamber. The air-particle mixture at any location in the vortex chamber will be subjected to the following forces (1) inertia forces: both the centrifugal as well as coriolis forces and (2) drag forces. The drag forces counter balances the outwardly directed centrifugal force while coriolis force aligns the air-solid mixture to undergo in circular motion. Resultants of the

combination of these three forces determine the rate of the air-solid mixture at the outlet of the vortex chamber (at chimney outlet).

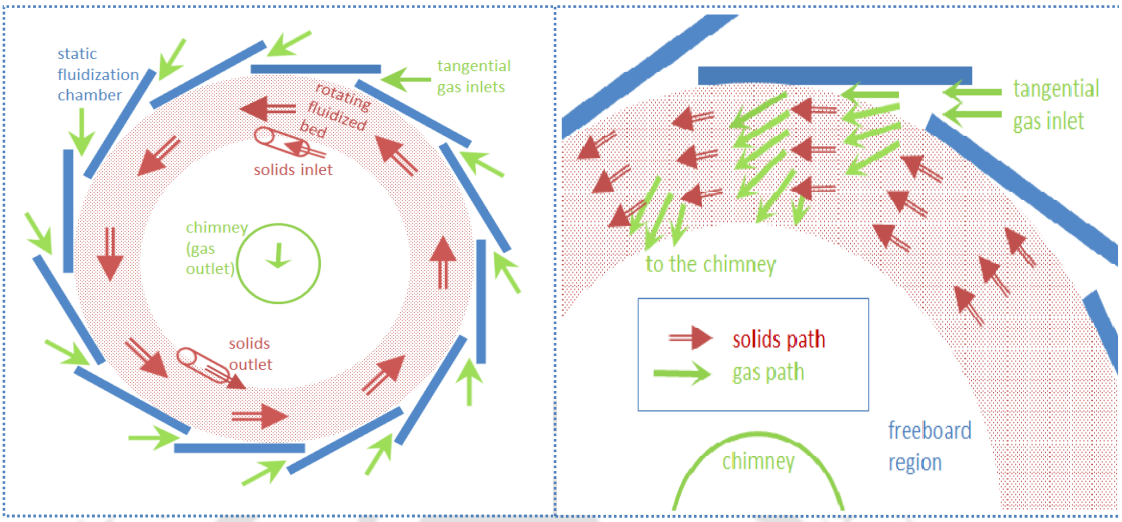

Fig.3. 1(a) Rotating fluidized bed with a static geometry (vortex chamber) (b) Gas and solids paths in a vortex chamber

3.2.2 DESIGN AND HYDRODYNAMIC OF RFG-SG

For proper fluidization, the vortex chamber design allows balancing the centrifugal force with the drag force. So the theoretical expressions of the centrifugal force, gas-solid drag force, the minimum fluidization velocity and the terminal velocities in the vortex chamber are the function of the total volumetric gas flow rate Q_g de Broqueville and de Wilde, (2009). The centrifugal force, expressed per unit volume fluidization chamber is given by

$$f_c = \varepsilon_s \rho_s a_c \tag{3.1}$$

The centripetal force a_c can be expressed as

$$a_c = \frac{u^2_{s,t}}{r} = \frac{(s_{gs} u_{g,t})^2}{r} \tag{3.2}$$

Where $u_{g,t}$ and $u_{s,t}$ are the tangential velocity of the gas and solid phase respectively. S_{gs} is the tangential gas –solid slip factor, which is assumed to be constant.

The tangential velocity of the gas is related to the total volumetric gas flow rate Q_g.

$$u_{g,t} = \frac{Q_{g,t}}{S_t} = \frac{Qg.n_{rot}}{S_t} = \frac{Q_g.n_{rot}}{\varepsilon\,((D/2) - R_f)\,L} \tag{3.3}$$

where $Q_{g,t}$ is the tangential volumetric gas flow rate, n_{rot} is the number of rotation of the gas phase in the particle bed, S_t is the surface area of gas phase in the particle bed, D is the diameter of the vortex chamber, R_f is the radial position of the freeboard and L is the vortex chamber length.

Combining equations (3.2) and (3.3)

$$\bar{a}_c = \left(\frac{2\pi\, Q\, \bar{n}_{rot} S_{gs}}{\bar{\varepsilon}_g V_{bed}} \right)^2 \bar{r} \tag{3.4}$$

The centrifugal force is consequently given by

$$\bar{f}_c = \bar{\varepsilon}_s \rho_s \left(\frac{2\pi\, Q_g \bar{n}_{rot} s_{gs}}{\varepsilon_g V_{bed}}\right)^2 \bar{r} \tag{3.5}$$

The radial drag force per unit volume fluidization chamber can be expressed as

$$f_{d,r} = \beta\,(u_{g,r} - u_{s,r}) \tag{3.6}$$

where the drag coefficient β in fluidization bed is given by Gidaspow, (1994).The drag and pressure drop in a denser bed fluidized bed is explained by Ergun's equation (Ergun, (1952)).

$$\beta = \frac{3}{4} C_D \frac{\varepsilon_g \varepsilon_s}{d_p} \rho_g |u_g - u_s| \varepsilon_g^{-2.65} \text{ for } \varepsilon_s \le 0.2 \tag{3.7}$$

$$\beta = 150 \frac{\varepsilon_s^2 \mu_g}{\varepsilon_g d_p^2} + 1.75 \frac{\varepsilon_s \rho_g}{d_p} |u_g - u_s| \text{ for } \varepsilon_s > 0.2 \tag{3.8}$$

The drag coefficient can be correlated with the particles Reynolds number as shown in Eq.(3.9).The radial velocity of the gas phase is related to the gas flow rate by the surface area available for the radial motion of the gas phase.

$$Re_p = \frac{|u_g - u_s| \varepsilon_g \rho_g d_p}{\mu_g} \tag{3.9}$$

$$C_D = \frac{24}{Re_p}\left(1 + 0.15 Re_p^{0.687}\right) \text{ for } Re_p \leq 1000 \quad (3.10)$$

$C_D = 0.44$ for $Re_p > 1000$

The terminal and minimum fluidization velocities can be calculated from de Wilde and deBroqueville, (2007) and Froment and Bischoff, (1990).

$$u_t = \sqrt{\frac{4\bar{a}_c d_p (\rho_s - \rho_g)}{3\rho_g C_D}} \quad (3.11)$$

The minimum fluidization velocity U_{mf} can be calculated from Wen and Yu, (1966).

$$u_t = \sqrt{\frac{4\bar{a}_c d_p (\rho_s - \rho_g)}{3\rho_g C_D}} \quad (3.12)$$

$$u_{mf} = \frac{\mu_g}{d_p \rho_g}\left(33.7\left[\left(1 + 3.6.10^{-5} Ar\right)^{0.5}\right]\right) \quad (3.13)$$

3.2.3 GAS INLET SLOTS DESIGN

The force ratio is considered to be an important factor for the design of the gas inlet slots. It is defined as Kochetov et al., (1969).

$$\lambda = \frac{\text{Centrifugal force}}{\text{Drag force}} \quad (3.14)$$

For a vortex chamber of RFB-SG, the force ratio, λ is given by

$$\lambda = \frac{n \,.\, s}{\pi \,.\, D} \quad (3.15)$$

where n, s and D is the number of gas slots, width and vortex chamber diameter, respectively. The number of slots has to be high enough for ensuring the tangential uniform gas flow along with the solid distribution and the vortex chamber circumference. Design value of the force ratio has been considered to be 0.025 - 0.038 for all the subsequent design calculations.

3.3 CONVENTIONAL BUBBLING FLUIDIZED BED (BFB)

3.3.1 CONCEPT OF FLUIDIZATION BED

Fluidization is the operation by which solids particles are transformed into the fluid like state through suspension in a gas or liquid. In a fixed bed, the fluid particles passed upward through a bed of fine particles at a low flow rate, the fluid merely percolates through the void spaces between the stationary particles.

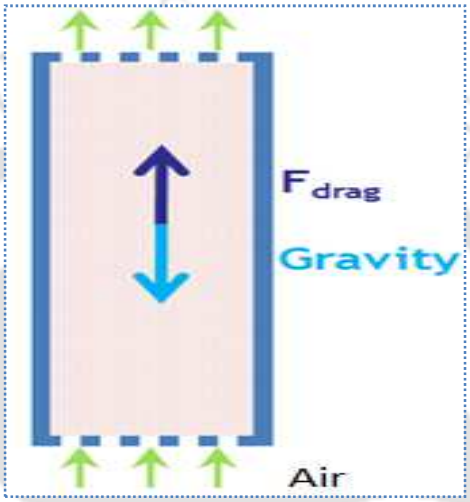

Fig.3. 2Schematic diagram of BFB

But in a expand bed, with an increase in flow rate, particles move apart and few vibrate and move in restricted region. At a still higher velocity, a point is reached where all particles are just suspended by upward flowing fluid. At this point, the frictional force between particle and fluid just counter balances the weight of the particles. The vertical component of the compressive force between adjacent particles disappears and pressure drop though any section of the bed about equal the weight of the fluid and particle in that section. At this condition the bed is just considered to be fluidized. On the other hand, if the minimum fluidization velocity is higher than the terminal velocity, the particles are entrained by the fluid and out of the reactor. The drag force is balanced by gravitational force shown in Fig.3.2

3.3.2 FLUIDIZATION FEASIBILITY AND CHARACTERISTICS

In case of proper fluidization, the particle bed density is approximately same everywhere. So bed is considered to be uniform.

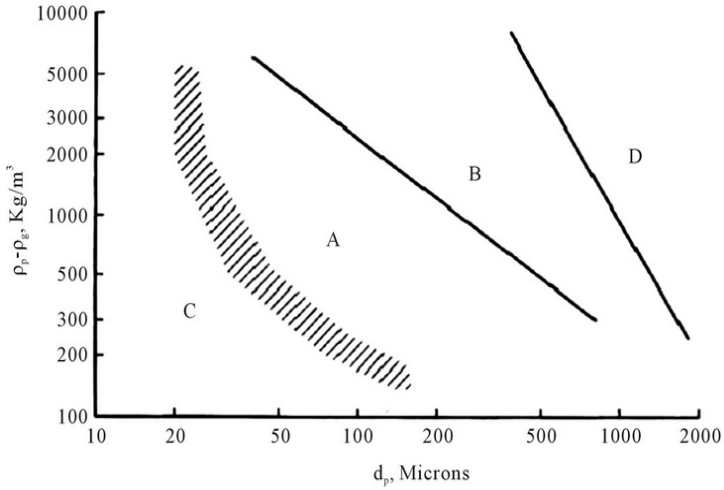

Fig.3. 3 Geldart's classification, (1973)

Geldart (1973), Geldart and Abrahamsen (1978) classified solid particles in to four categories according to their fluidization behaviour described in Fig.3.3. The classification depends on the apparent density $(\rho_s - \rho_f)$ and equivalent mean diameter d_p of the particles Kunni and levenspiel, (1992).

Table 3.1 Geldart classification of particles according size.

Class	Particle size	Regimes of the fluidization
C	0 - 30 µm	The particles are extremely fine and most cohesive powder. Interparticle forces greatly affect the fluidization behaviour of these powders.
A	20 – 100 µm	The bed expands before bubbles appeared particulate fluidization.
B	100 - 500 µm	The particle size lies in between, aggregative fluidization. Bubbles appeared from the beginning of the fluidization.
D	>600 µm	The particles size is greater than 600 µm, fluidization is possible but the particles bed is not stable. Fluidization can even impossible for too large particles (> 50 mm)

3.3.3 REGIMES OF FLUIDIZATION

As discussed in the previous subsection, different regimes of fluidization are shown in Fig. 3.4. A brief description of each of the regime is presented in this subsection.

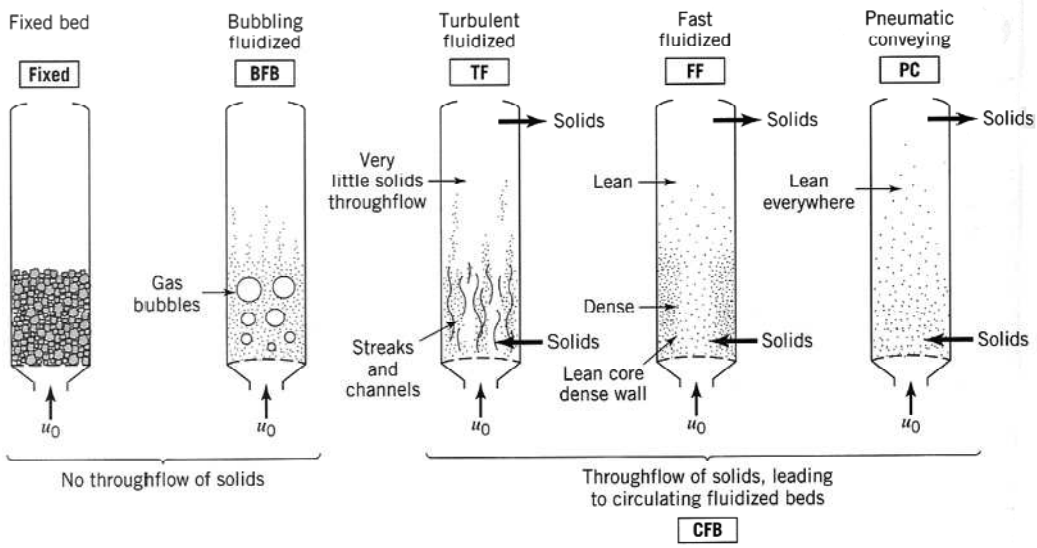

Fig.3. 4Schematic view of the different fluidization behaviors O Levenspiel, (1999)

Fixed bed regime

If a fluid particle is passed upward through a bed of fine particles at a low flow rate, the fluid merely percolates through the void spaces between the stationary particles. This is a fixed bed. With increase in superficial air velocity the solid particles suspends in the gas causing minimum fluidization. The weight of the particle and gas in any of the sections perpendicular to the axial flow direction balances the buoyancy force under this situation.

Bubbling fluidization regime

As the superficial air velocity is increased beyond the minimum fluidization condition, the bubble starts forming, expands and the mixing of gas and solids becomes more intense. The size and population of bubbles in the bed is increase. The walls of the bubbles start thinning till a particular superficial velocity they collapse into dense strands moving randomly in a continuum of dilute phase. There is large increase in voidage under bubbling regime.

Turbulent bed regime

It is the regime beyond the bubbling fluidization where excessive bed expansion causes bubble walls too collapse giving rise to vigorous mixing between the solid agglomerates or clusters and the dilute phase of low solid concentration. As the air velocity is increased further, the particles are entrained in the air stream, from

agglomerates or cluster and flow with the stream. There is considerable back mixing near the walls.

Fast fluidization regime

At high velocity (U_0>20 U_t) the fast fluidization occurs. It is often described by the core-annulus models. There is up flowing dilute gas stream in the core and down flowing dense phase in the annulus with clusters or streamers, the long slender solid agglomerates continuously forming , dissolving and reforming.

Pneumatic transport regime

If the superficial velocity is high enough and the feed rate of solids is small enough, then all the solids will be carried up the tube as separate particles widely dispersed in gas. The relative velocity between the gas and solid is called slip velocity. Up to a certain point, flow rate of solid or gas may be changed to get a lean dispersed up flowing gas-solid mixture. This regime is called pneumatic transport regime. When the gas velocity is reduced or flow rate is increased, a condition is reached where the character of the mixture changes drastically, with clumping, slugging and solid falling below the solid feed port. This transition is called the choking condition and it represents the limit of pneumatic transport regime.

3.3.4 STUDIES ON HYDRODYNAMICS OF FLUIDIZED BED

Hydrodynamic parameters are important while investigating the fluidization behaviour of the fluidized bed. Minimum superficial fluidization velocity is U_{mf}. The terminal velocity is Ut, which is the fluid superficial velocity above which particles entrained. The fluid volume fraction at the fluidization threshold is ε_{mf}. The bed expansion with the fluid superficial velocity is Usf.

The minimum fluidization velocity can be determined from a pressure drop measurement. Figure 3.5 shows the evolution of the pressure drop over the particle bed with the superficial velocity of the gas for a bed composed of sand particles with uniform size. As shown on the graph, the pressure drop over the bed increases with the superficial velocity i.e. at low superficial velocity (from point 1 to point 3).

The pressure drop in this range of superficial velocity is due to the resistance to a fluid flow through a fixed bed granular medium and can be calculated using the Ergun equation Kunii and Levenspiel, (1969).

$$\frac{\Delta p}{L} = 150\frac{\varepsilon_s^{\,2}}{(1-\varepsilon_s)^3}\frac{\mu_f u_{sf}}{\bar{d}_p^{\,2}} + 1.75\frac{\varepsilon_s}{(1-\varepsilon_s)^3}\frac{\rho_f \cdot u_{sf}^{\,2}}{\bar{d}p} \qquad (3.16)$$

whereε_s [m^3 s /m^3r] is the solids volume fraction(ε_s = 1-ε_f where ε_f [m^3_f /m^3_r] is the fluid volume fraction), μ_f [Pa.s] [kg/m.s] fluid viscosity, $\bar{d}p$ [m] mean equivalent diameter of the particles and ρ_f [kg_f/m^3_f] is the fluid density.

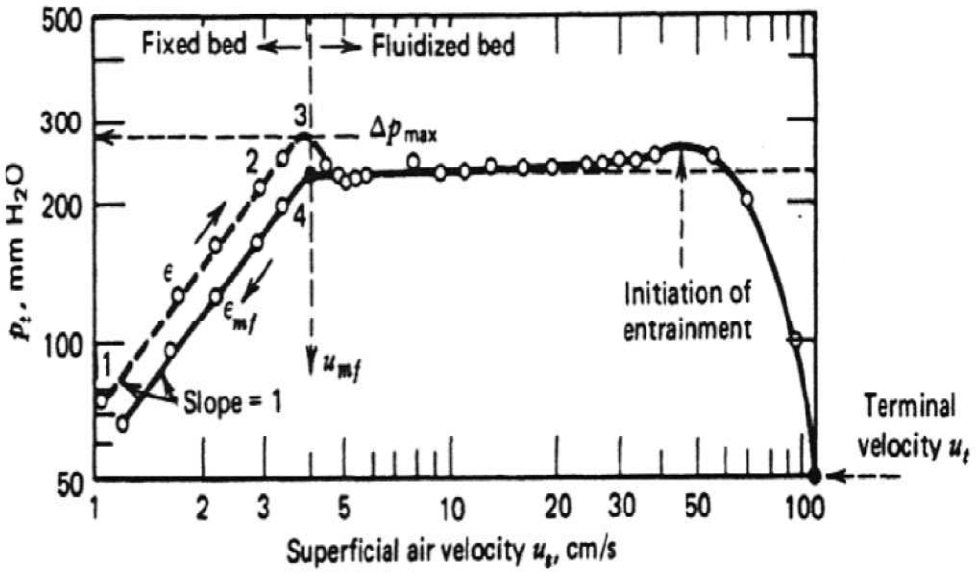

Fig.3. 5Pressure drop ΔP over the particle bed as a function of the superficial velocity of the gas u_{sg} for a bed composed of sand particles with uniform size, Shirai, (1958) and Kunii and Levenspiel, (1969).

The force applied on the bed by the friction of the fluid and turbulence generated by the pressure drop. This force increases the fluid flow rate until reaching the apparent weight of the bed when Usg = Umf. At this point, the particles start to be suspended and the bed loses its consistency. The small decreases of the pressure drop after point 3 in figure 3.5 is due to the re-arrangement of the particles. Beyond the fluidization threshold, the particles move relative to each other and the bed is fluidized.

The fluid volume fraction at the minimum fluidization point can be determined from the pressure drop compensates for the weight of the bed.

$$\frac{\Delta P}{L_{mf}} = (1-\varepsilon_{mf})\cdot(\rho_s - \rho_f)\cdot g \qquad (3.17)$$

where L_{mf} [m] is the bed height of the minimum fluidization point. ρ_s [kg_s/m^3_s] is the density of the particles.

3.3.5 TERMINAL VELOCITY OR FREE FALL VELOCITY

When the fluid velocity increases, the pressure drop decreases, and the particles start entrained by the fluid out of the reactor until the bed disappear. When $U_{sf} = U_t$, the particles entrainment is generally undesired in industrials operation although it is useful for some processes. The terminal velocity is reached when the drag force F_D exerted on the particles by the fluid becomes higher than the apparent weight of these particles. The drag force is defined as:

$$F_D = \frac{1}{2} C_D \cdot \rho_f \cdot A \cdot u_{sg}^{\ 2} \qquad (3.18)$$

WhereC_D is the drag coefficient, A [m^2] is the cross sectional area.

$$\text{For spherical particle, } A = \frac{\pi \cdot d_p^{\ 2}}{4}$$

Consequently, when $u_{sg} = u_t$ the following equation can be written as

$$\frac{1}{2} C_D \cdot \rho_f \cdot \frac{\pi \cdot dp^2}{4} u_t 2 = \frac{\pi \cdot dp^3}{6}(\rho_s - \rho_f)\cdot g \qquad (3.19)$$

$$u_t = \sqrt{\frac{4 \cdot g \cdot dp \cdot (\rho_s - \rho_f)}{3 \cdot \rho_f \cdot C_D}} \qquad (3.20)$$

The drag coefficient C_D depends on the Reynolds number, $Re_p = \frac{\bar{d}_p \cdot \rho_f \cdot u_t}{\mu_f}$.

For spherical particles and laminar flows ($Re_p \langle 0.4$), $C_D = \frac{24}{Re_p}$

According to Stoke's law

$$u_t = \frac{(\rho_s - \rho_f)\cdot g.\bar{d}_p^{\ 2}}{18 \cdot \mu_f} \qquad (3.21)$$

For intermediate Reynolds number ($1<Re_p< 10^3$), the following expression can be used

$$C_D = -5.50 + \frac{69.43}{\ln Re_p + 7.99} \tag{3.22}$$

For high Reynolds number ($Re_p > 10^3$), $C_D = 0.44$

The terminal velocity is given by the Newton's law:

$$u_t = \sqrt{\frac{3.1 \cdot \bar{d}_p \cdot (\rho_s - \rho_f) \cdot g}{\rho_f}} \tag{3.23}$$

An alternative for $Re_p< 10^3$ is given by

$$C_D = \frac{24}{Re_p}(1 + 0.15 \cdot Re_p^{0.687}) \tag{3.24}$$

The terminal velocity increases with the particle mean diameter. That means fine particles are more easily entrained

3.4 SUMMARY

The theoretical background of RFB-SG and BFB are described in the present Chapter. The concept design and mathematical formula related heat and mass transfer are elaborated. Experimental set-ups and procedure are described in the next Chapter.

CHAPTER - 4

EXPERIMENTAL SET-UPS AND PROCEDURE

4.1 INTRODUCTION

Rotating fluidized bed in a static geometry (RFB-SG) and conventional bubbling fluidized bed (BFB) setup were extensively used in the present investigation. Studies were conducted at UCL, Belgium with instrumentation and modification of existing set-ups. Experimental set-ups of both RFB-SG and BFB are described in the following sub-sections followed by experimental procedure.

4.2 EXPERIMENTAL SETUP ON RFB-SG

Figure 4.1 presents the schematic diagram of the RFB-SG experimental set-up used for drying of cereal grains.

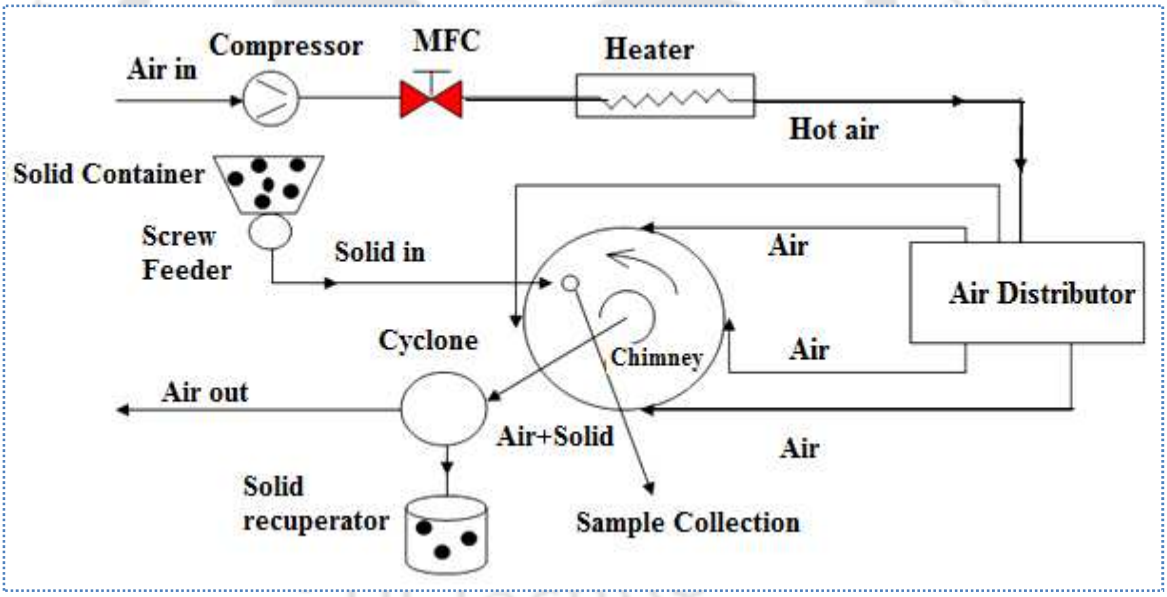

Fig.4. 1A schematic of RFB-SG experimental set-up at IMAP-UCL, Belgium.

It consists of a (a) rotary air compressor, (b) Micro-flow controller, (c) electric heater, (d) air distributor, (e) vortex chamber/reactor, (f) Feed material hopper with screw feeder, (g) cyclone separator and (h) solid recuperator.

The core of the set-up, made of cast iron, consists of a vortex chamber (also called reactor) with 0.26 m outer jacket diameter (Fig. 4.2).

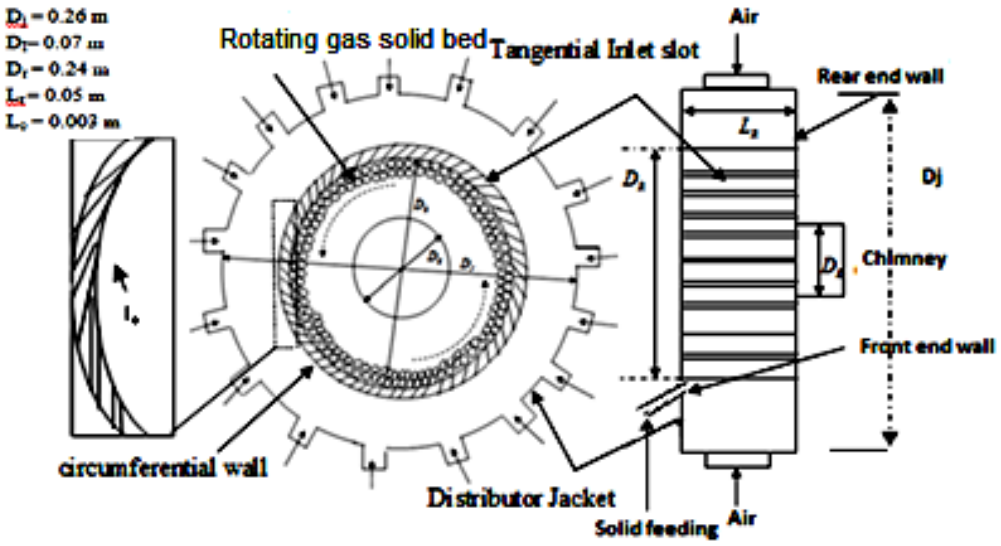

Fig.4. 2 Schematic diagram of reactor/vortex chamber.

The inner diameter of the drying chamber is 0.24 m made of a stainless steel structure. The width of the reactor is 0.05 m. Stainless steel slots shrouded at both the ends were fixed in the rectangular holes of the drying chamber structure uniformly. Each slot is sized to 5mm breadth and 0.05 m width having shrouding at both the ends like steam turbine blades. The gap between each pair slots was maintained at 3 mm with an inclination of 30^0 in inward direction with respect to the tangential direction as shown in Fig. 4.3.

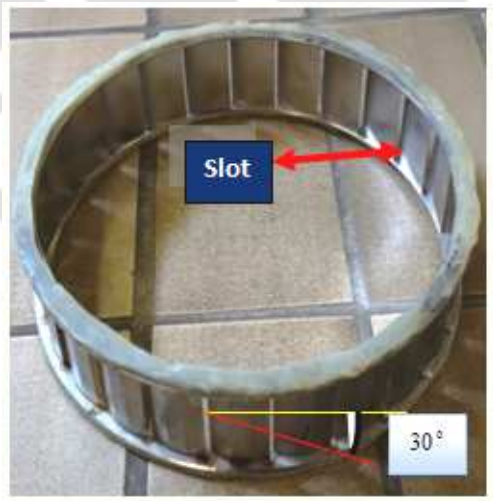

Fig.4. 3 Picture of the reactor with 24 slots.

Air is distributed through a hole of inner diameter of 25 mm to the vortex chamber. Total locations of the tubes are extended to the slots by drilling through holes on the

jacket. Total 24 such supply lines are provide in the system for uniform supply of air through the slots to the reactor/vortex chamber. A pictorial view of the air distribution system to the vortex chamber is shown in Fig. 4.4.

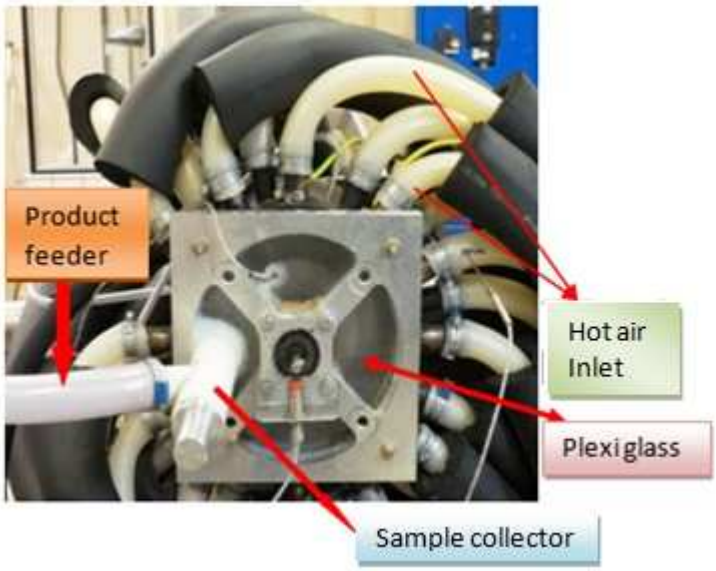

Fig.4. 4Picture of the air distribution with vortex chamber.

The centre of the reactor contains a diffuser chimney with inner diameter of 70 mm inside the reactor and 120 mm at the outside to dispose of the moisture and air. Figure 4.5 presents the location of chimney inside the reactor.

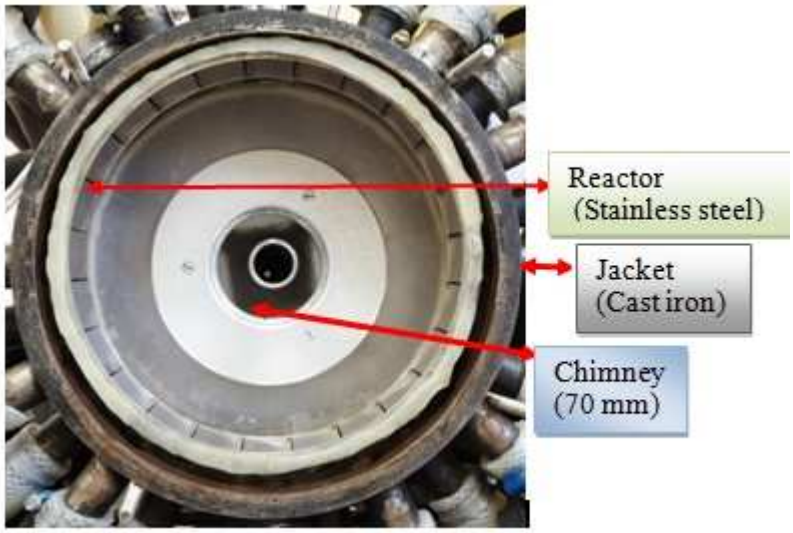

Fig.4. 5Picture of the vortex chamber with chimney from the front.

(a) Compressor

(b) Micro- flow controller

(c) Electrical heater

(c) Air distributor

(e) Feed materials hopper

(f) Cyclone separator

(g) Solid recuperator

(h) Vortex chamber with particles bed

Fig.4. 6Various components of the experimental set-up (a) Compressor, (b) Micro-flow controller, (c) Electric heater, (d) Air Distribution network, (e) Material feed hopper, (f) Cyclone separator, (g) Solid recuperator and (h) Pictorial view of solid circulation

The flat side of the reactor was fixed with plexi-glass for flow visualization. Air is compressed to in the rotary air compressor and heated to the desired temperature by passing the same through a 12 kW electrical heater. Hot air at the desired

temperature is then sent to an air distributor from where air is passed on to the gap between the stainless steel slots located just outside the vortex chamber (Fig. 4.1). Depending on the number of slot gaps in the system, same numbers of distribution tubes are used. The feed material at a particular flow rate is passed through another tube to feed into the vortex chamber simultaneously. A screw feed is used to facilitate the solid flow into the vortex chamber. Mixture of air, moisture, dirt and some feed materials go out through the diffuser chimney which in turn passes through a cyclone separator. The solids separate out and fall on the solid recuperator and air with moisture is released to the atmosphere. A pictorial view of the various components of the experimental set-up is presented in Fig. 4.6.

4.2.1 MODIFICATION OF SET-UP

Preliminary experiments with the aforementioned set-up were not found to be suitable for drying of cereal crops like paddy and wheat grains. Following drawbacks were observed:

1. Test of fluidization were conducted with 24, 36 and 72 slots for the vortex chamber diameter of 0.24 m and found that fluidization was unsatisfactory with 36 and 72 slots. This may be attributed to the insufficient air supply to the vortex chamber causing unbalanced centrifugal forces inside the reactor. However, a good fluidization was observed with 24 slots with 3 mm gap and same was considered for the present investigation.
2. It was observed in preliminary experiments that a significant amount of solid is lost (10-15%) through the existing diffuser chimney with 70 mm inside diameter (Fig. 4.5). Concept of distributor plate design was used and the chimney inlet was redesigned as shown in Fig. 4.7. In the modified design, percentage opening is reduced by 50%. However, effective diameter is kept same as the previous chimney and a distributor plate with 12 holes each of 12 mm diameter is incorporated to minimize the solid loss from the system. A sample calculation of the design is shown in Appendix B.

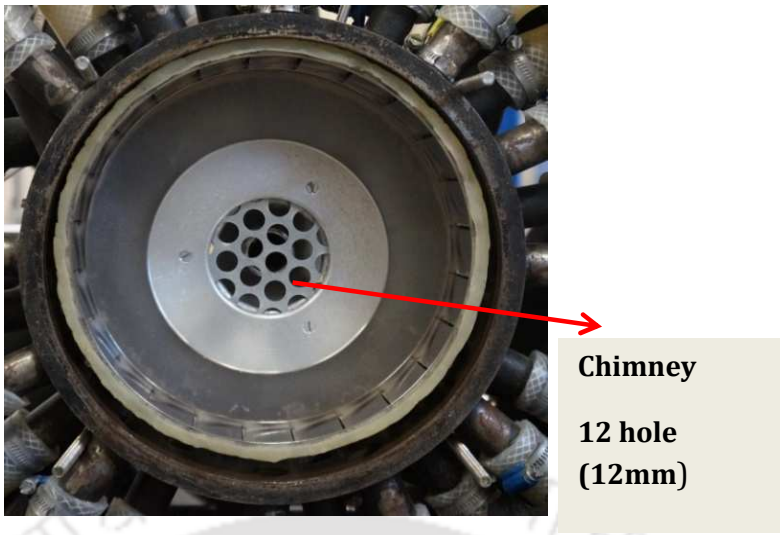

Fig.4. 7 Picture of vortex chamber with modification of chimney.

4.3 BUBBLING FLUIDIZED BED (BFB)

4.3.1EXPERIMENTAL SETUP ON CONVENTIONAL BUBBLING FLUIDIZED BED (BFB)

The schematic diagram of the BFB experimental set-up used for drying of cereal grains is shown in Fig.4.8.

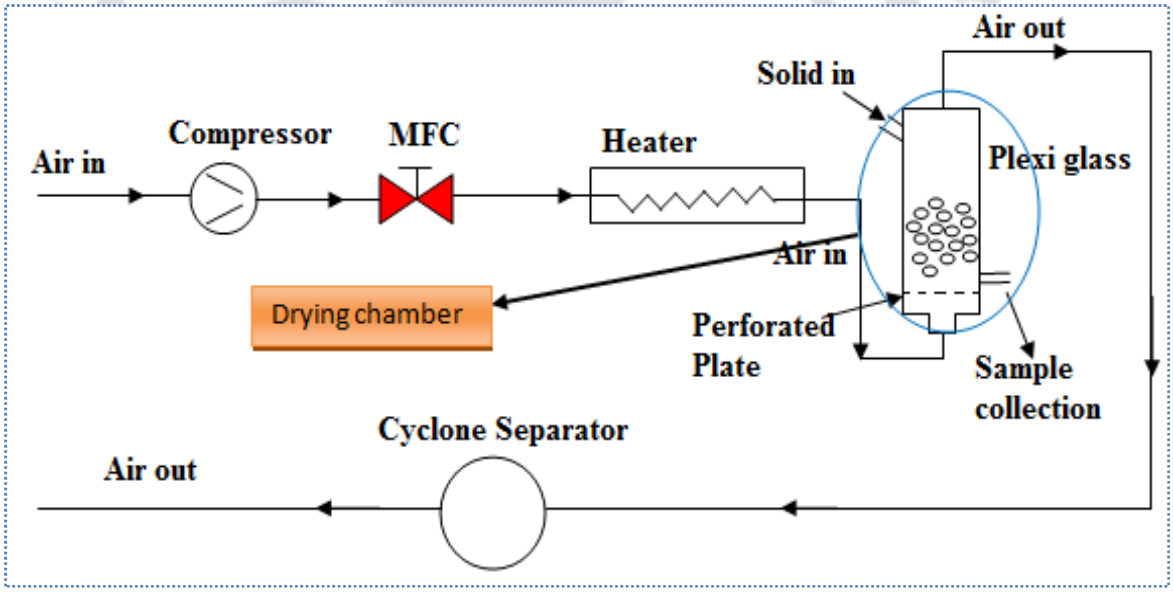

Fig.4. 8Schematic diagram of the bubbling fluidized bed (BFB) drying set-up. (a) Rotary air compressor, (b) Micro-flow controller, (c) electric heater, (d) air distributor, (e) BFB, and (f) cyclone separator.

The experimental set-up is similar to Fig. 4.1 except the reactor or vortex chamber and material feeding system. The vortex chamber of RFB-SG is replaced with a bubbling fluidized bed and feeding mechanism is maintained by manual feeding in the present set-up. The BFB dryer used in the present experiments is shown in details in Fig. 4.8.

It consists of a riser column made of plexi glass material with inner diameter of 0.10 m and height of 1.5 m. A fine wire mesh of 1 mm pore diameter was used as a distributor plate as shown at the bottom of the riser. The distributor wire mesh was clamped between two flanges with the help of nuts and bolts in which the top flange was fixed to the riser column. The top of the riser column was connected to an exhaust pipe which in turn was connected to the inlet of the cyclone separator (Fig. 4.8). A moisture probe was placed at the top of the riser to estimate of the moisture carried away by the out-going air.

4.3.2 INSTRUMENTATION AND CONTROL OF RFB-SG AND BFB DRYING UNITS

Both the RFB-SG and BFB drying set-ups are instrumented with pressure, temperature and humidity measuring sensors. Following are the sensors and control systems used for both the systems.

1. Air humidity sensor (Make: Rotronic HC2), was used at the outlet of both the RFB-SG as well as BFB units.

2. RTD temperature sensors, PT 100, were used at the inlet air passage, inside the bed/vortex chamber as well as at the outlets of both the set-ups (Figs. 4.9 and 4.6(h)). The positions of the sensors are just below the distributor plate and 26 cm above the distributor plate for the BFB unit whereas it was placed at a distance of 3 cm inside the vortex chamber from the top of the casing in case of the RFB-SG.

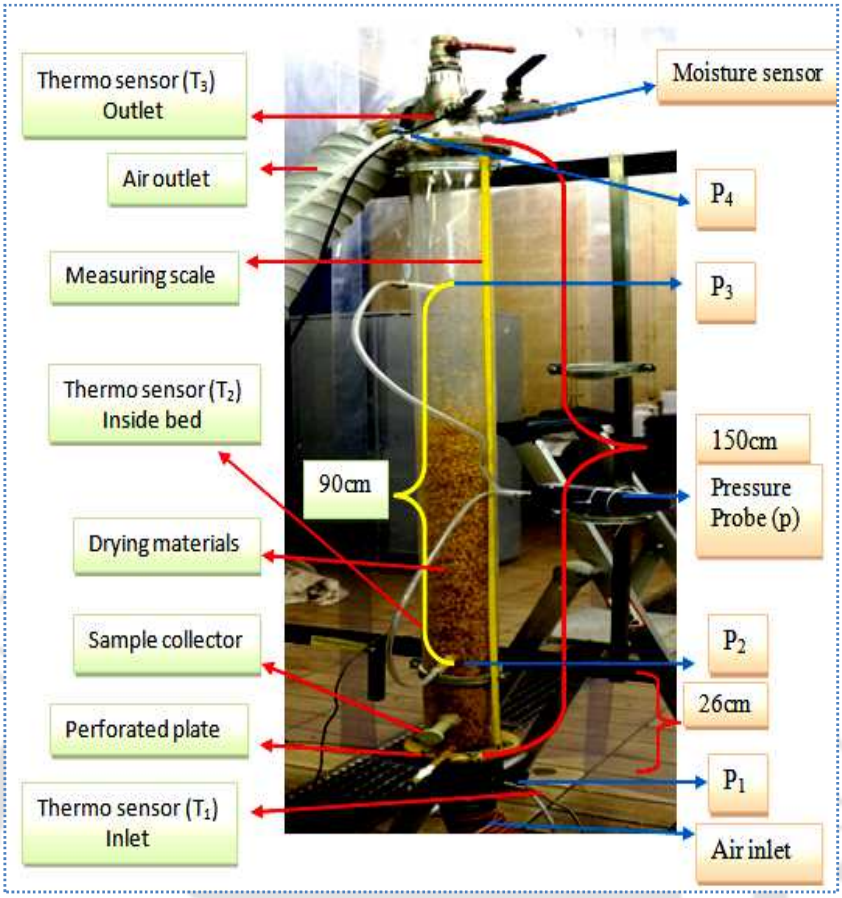

Fig.4. 9 Pictorial view of BFB drying unit.

3. Silicon Piezo-resistive pressure sensors were used to measure the pressure at various locations of the experimental set-ups(make: Gefran TSA, Belgium). One such sensor was used at the air inlet located at the apex of the vortex chamber and another one was located at the outlet to the chimney for the RFB-SG. In case of BFB, 4 (Four) such pressure sensors, namely, P_1,P_2, P_3 and P_4were used to measure the variation of pressure along the riser of the BFB. It may be mentioned here that pressure just above the distributor plate (P_1) and at the outlet (P_4) were measured with the help of LAB-VIEW software connected through a PID controller. The position of outlet (P_4) is at a height of 150 cm above the distributor plate. Measurement of pressure for the locations P_2 and P_3 were taken manually with the help of a digital meter (Make: DPI 800).

4. Weights of the sample to be dried were taken in a highly sensitive weighing balance (Make: Mettler AE-260, Delta Ranga).

5. Moisture measurement was done using a muffler furnace (Make: GFL 7104, D3006, Burgweldel). The weighed samples were kept in the furnace for 24 hours under controlled temperature of at 105^0C.

4.3.3 EXPERIMENTAL PROCEDURE FOR RFB-SG AND BFB

Prior to the starting of actual experiments, some trial runs are taken to have an idea about the control and measurement of operating parameters. The experiments are performed by following a standard procedure in order to have accurate data during experimentation.

In the first step, only hot air was fed to the drying chamber to obtain a stable gas flow pattern. Experiment is started only after ensuring a stable input reading. In second step, the paddy/wheat particles are fed to the drying chamber by auto controlled screw feeder to generate a fluidized bed of solids. During the experiments, samples are collected through the front plate at a particular interval of time to ensure the moisture content. Latter on the samples are weighted on a physical balance and kept inside the furnace at 105^0C for 24 hour. The samples are weighted again to determine the evolution with time of the solids moisture content. The air temperature and humidity are recorded at the inlet, outlet and inside the drying chamber with Rotronic HC2 and PT100 probes. The pressure drop across the drying chamber, the particles losses from the particle bed and rotational speed of the bed are also recorded online. The product uniformity is measured at particular interval of times through a moisture content distribution. Attrition of the paddy particles by shear is also measured at particular interval of times for different air flow rates.

The experiments in the vortex chamber are carried out with air flow rates of 400,500,600 and 700 Nm^3/h. The gauge pressure in the gas distribution chamber was varied between 200 and 300 mbar depending on the air flow rate. Inventory of 300, 400, 500 and 600 g on a dry basis are dried with air flow rates in between 400-700 Nm^3/h and at pressure between 200 and 300 mbar.

Similar methods are followed during the experimentation with BFB except the inventory is fed manually at one end of the riser at once. Inventory of 300, 400, 500

and 600 g on a dry basis are dried with air flow rates in between 125-175 Nm^3/h and at pressure 200-300 mbar.

In both drying chambers, the air inlet temperature was varied between 50 and 65°C to evaluate its influence on the drying rate.

Calculation of Moisture Content

Moisture content is calculated Zaman and Bala(2001), IRRI, (2005) as follows

$$MC_{wb} = \frac{m_i - m_f}{m_i} \times 100 \tag{4.1}$$

This is for weight basis moisture content calculation.

Similarly for dry basis MC

$$MC_{db} = \frac{m_i - m_f}{m_f} \times 100 \tag{4.2}$$

where m_i is initial weight of particles before drying, m_f is the final weight after drying. MC_{wb} and MC_{db} are the moisture content of weight basis and dry basis respectively.

4.3.4 PROCESS INTENSIFICATION

The drying rates of the dryers are quantitatively expressed in terms of process intensification (PI) factor as the ratio of the specific drying rates. The specific drying rate is defined as the quantity of particles dried perunit time and per cubic meter drying chamber (kg dry particles/m^3.s).

4.4 SUMMARY

The experimental procedure and instrumentation of two different types of dryers, viz., RFB-SG and BFB are described in the present Chapter. The detail description of procedure and measuring instruments are elaborated. Chapter 5 deals with results and discussion along with development of correlations for differential moisture removal based on the identified parameters influencing the drying process.

CHAPTER - 5

RESULTS AND DISCUSSION
PARAMETRIC STUDY ON DRYING IN RFB-SG AND BFB DRYERS

5.1INTRODUCTION

A parametric study on paddy and wheat drying was conducted in rotating fluidized bed in a static geometry (RFB-SG) and conventional bubbling fluidized bed (BFB) dryer at IMAP laboratory, UCL, Belgium. In this chapter, the focus is given on effect of various parameters on the drying characteristics along with an analysis of the uniformity of dried products. Finally a correlation is developed to establish the influence of different parameters on moisture removal rate from the products.

5.2 EXPERIMENTAL INPUT MATRIX FOR RFB-SG AND BFB DRYER

Table 5.1 presents the input parameters used for drying of paddy and wheat grains in RFB-SG and BFB dryers.

Table 5.1Input parameters for RFB-SG and BFB for drying of paddy and wheat grains

Sl. No	Particulars	RFB-SG	BFB
1	Ambient air temperature	16 - 18^{0}C	16 - 18^{0}C
2	Relative humidity (RH) in the laboratory	35 - 45%	35 - 45%
3	Inlet air temperature	50 - 65^{0}C	50 - 65^{0}C
4	Inventory (Paddy/Wheat grains)	300 - 600g	300 - 600g
5	Moisture content of paddy grains	44-52% (db) approx.	44 - 52% (db) approx.
6	Moisture content of wheat grains	64-72% (db) approx.	64 -72% (db) approx.
7	Controlled final moisture content	14 ± 1 % (db) approx.	14 ± 1 % (db) approx.
8	Input electrical energy from heater for air heating	12 kW_e	12 kW_e
9	Inlet air flow rate (from main duct)	400 - 700 Nm^3/h	125 - 175 Nm^3/h
10	Superficial Air velocity at inlet slit to the vortex chamber/riser	36 – 66m/s	5– 7m/s

5.3 DRYING CHARACTERISTICS IN RFB-SG

Drying characteristics of paddy and wheat grains in RFB-SG are discussed in the following sections.

5.3.1 EFFECT OF INLET AIR TEMPERATURE ON DRYING

Figs. 5.1 and 5.2 represent the variation of moisture removal rate with time for inventory of 600 g with inlet air flow rate of 400 Nm^3/h during the drying of paddy and wheat grains. Experiments were conducted for the inlet air temperature in the range of 50-65^{0}C in a step of 5^{0}C starting from 50^{0}C.

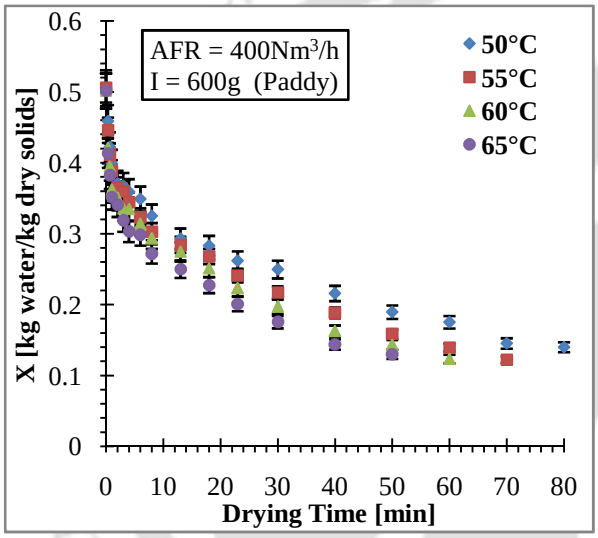

Fig.5. 1MC varies with drying time at different air inlet temperature (Paddy)

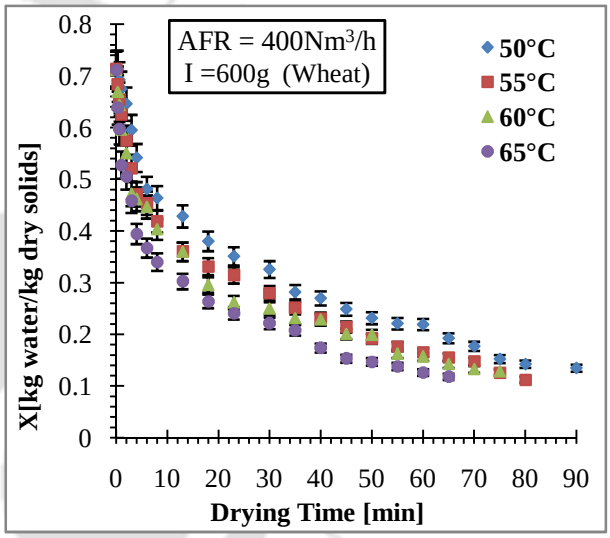

Fig.5. 2MC varies with drying time at different air inlet temperature (Wheat)

It is observed from both the figures that drying time and rate of drying decreases with increase in drying air temperature. Increase in inlet air temperature accelerates both the heat and mass transfer (i.e., moisture) leading to the decrease in drying time. Similar trend was reported by Basunia and Abe, (2001) and Chakraborty, (1994). It was observed that with increase in inlet air temperature by 30% decreases the drying time by 38% for paddy drying with reduction of drying time from 80 to 50 minutes. Similarly, decrease in drying time was observed to be 28% for wheat for the same percentage increase of inletair temperature (from 90 to 65 minutes). The variation in such decrease is attributed to the texture of the grains.

Figures 5.3-5.4 and Figs. 5.5 -5.6 present similar plots for inventories of 500g and 400g, respectively under similar air temperature range and air flow rate of 400 Nm^3/h.

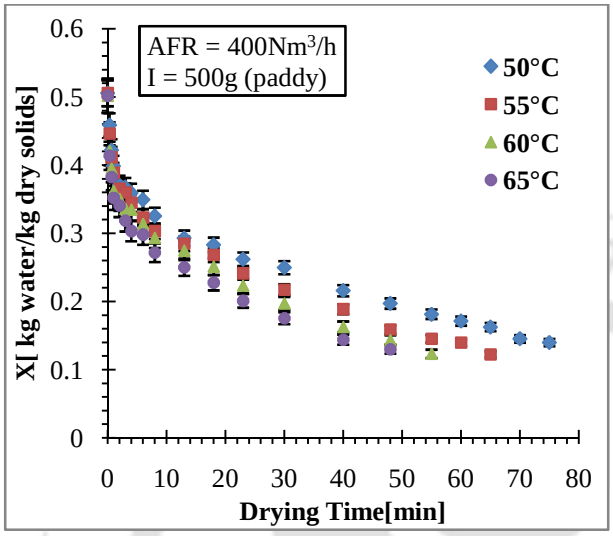

Fig.5. 3MC varies with drying time at different air inlet temperature (Paddy)

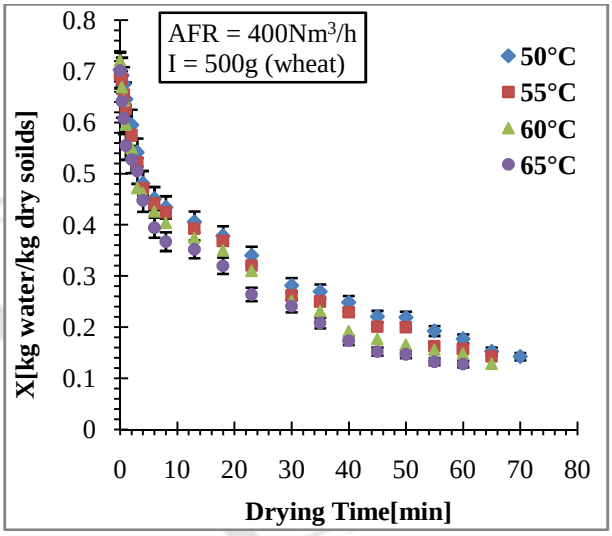

Fig.5. 4MC varies with drying time at different air inlet temperature (wheat)

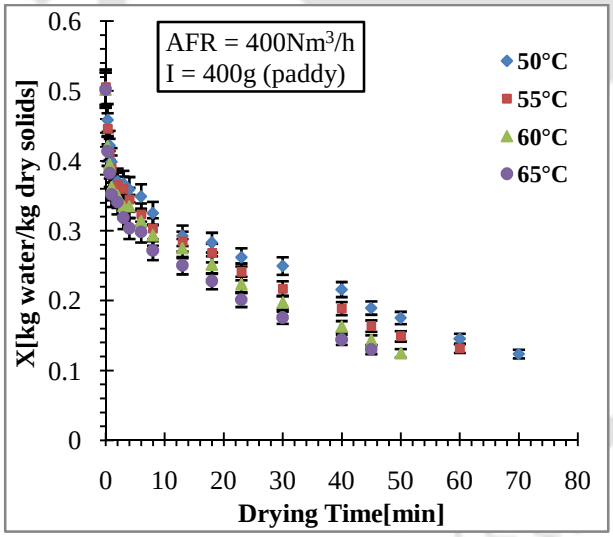

Fig.5. 5MC varies with drying time at different air inlet temperature (paddy)

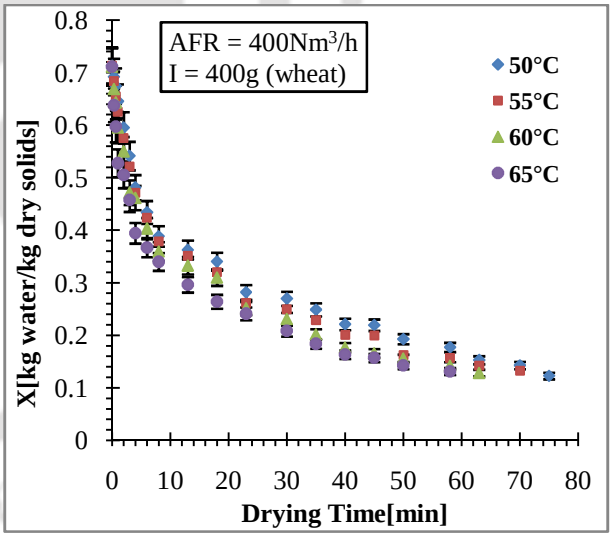

Fig.5. 6MC varies with drying time at different air inlet temperature (wheat)

It is observed from all these figures that drying time decreases with increase in inlet air temperature.

5.3.2 EFFECT OF AIR FLOW RATE (AFR) ON DRYING

Figures 5.7-5.8 shows the variation of MC with drying time with variation of air flow rate (AFR) from 400 to 700 Nm^3/h at inlet air temperature of 60^0C. Both the results are presented for inventory of 400 g of paddy as well as wheat grains. Wet paddy and wheat grains with initial MC $48 \pm 3.8\%$ and $68 \pm 4.32\ \%$, respectively were considered. The drying process was controlled so to maintain the final MC at $13 \pm 0.68\ \%$ and $13 \pm 0.72\ \%$ for paddy and wheat grains, respectively. Rapid initial drying was observed with removal of the superficial moisture in less than 1-2 minutes as observed from the figures. The drying time is reduced by about a factor of 2 with increase in the air flow rate from 400 to 700Nm^3/h.

Drying time changes with different air flow rates as shown in the figure below.

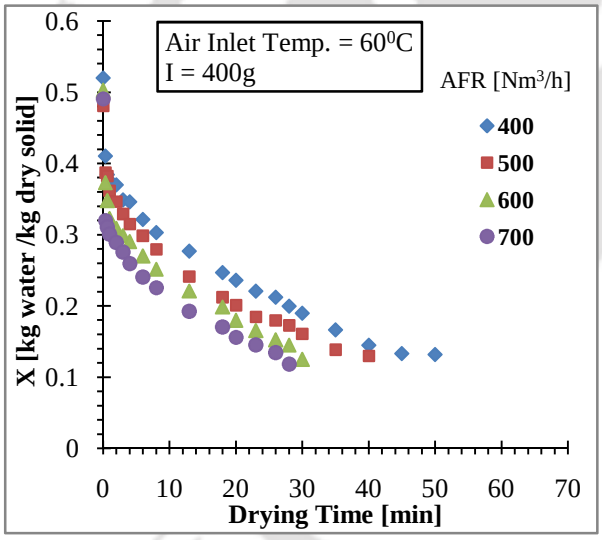

Fig.5. 7MC varies with drying time at different AFR of paddy

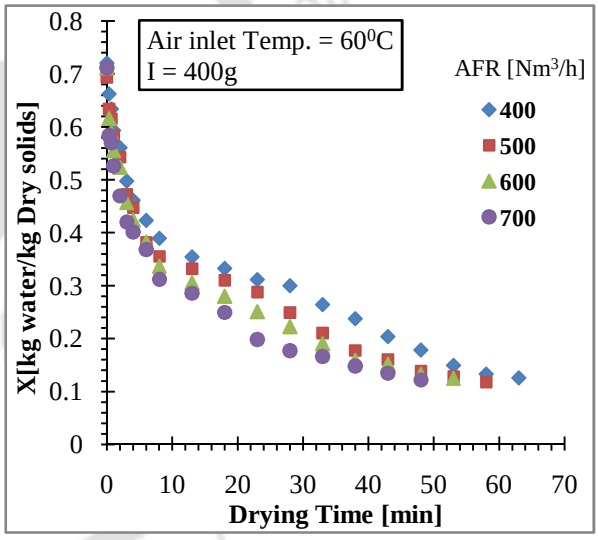

Fig.5. 8 MC varies with drying time at different AFR of wheat

It is observed from both the figures that increase in AFR results in decrease in drying time. This is attributed to the increase in centrifugal force with significant increase in acceleration due to gravity subsequently producing an increase of slip velocity between the gas and solid phases leading to high rate of heat and mass transfer. It may be further observed that percentage decrease in drying time for paddy grains is more than that of wheat grains which is due to the textural differences.Figure 5.9 and 5.10 present similar results for drying air temperature of 65^0C.

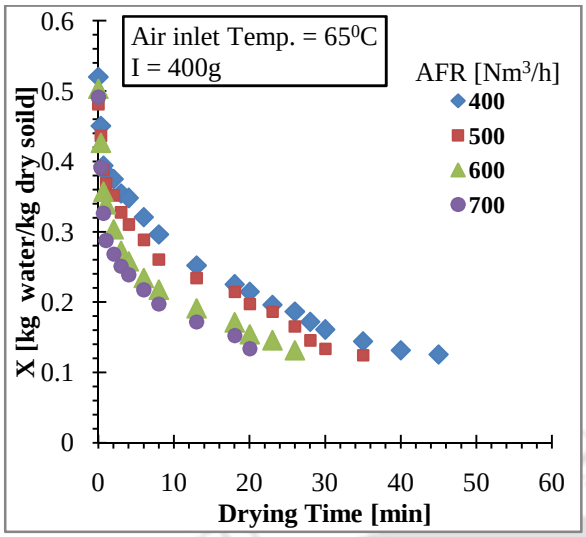

Fig.5. 9MC varies with Drying time at different AFR (paddy)

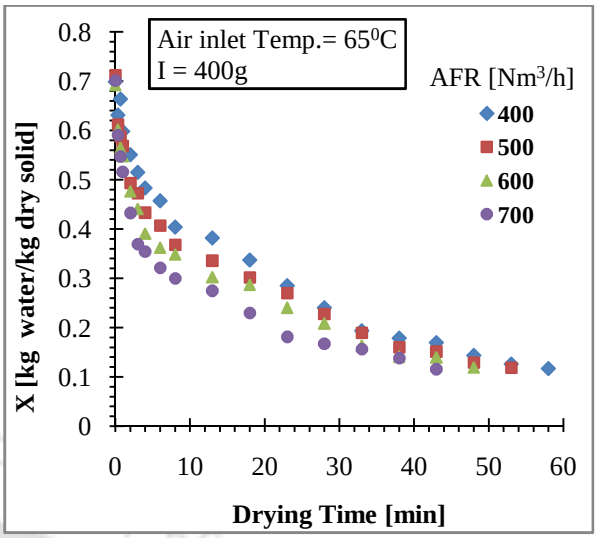

Fig.5. 10MC varies with Drying Time at different AFR (wheat)

Effect of drying air temperature on drying time with different AFR for inventory of 400 g each of paddy and wheat grains is presented in Figs. 5.11-5.12. It is observed from the figures that drying time decreases from 50 to 28 minutes (44%) and 45 to 20 minutes (55%) at air inlet temperature 60^{0}C and 65^{0}C, respectively for attaining the controlled final MC for paddy grains. Drying time was observed to be decreased by 24% and 28% for wheat grain as observed from Fig. 5.12.

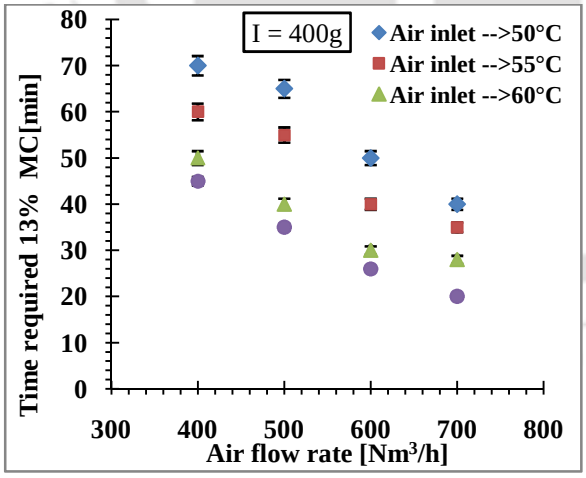

Fig.5. 11Time required to reach desired MC at different air inlet temperature and AFR at constant loading (paddy)

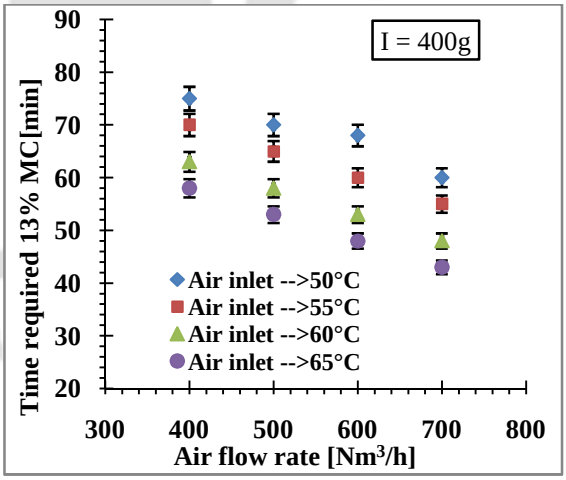

Fig.5. 12Time required to reach desired MC at different air inlet temperature and AFR at constant loading (wheat)

5.3.3 EFFECT OF LOADING/INVENTORY ON DRYING

To analyse the effect of inventory, all experiments were carried out at a constant air inlet temperature of 60^0C and air flow rate 400Nm^3/h. Different inventory of drying materials (paddy/wheat) was fed inside the drying chamber (vortex chamber) by screw feeder. Figure 5.13 and 5.14shows the drying time for an air flow rate of 400Nm^3/h, air inlet temperature of 60^0C and paddy loading between 300 and 600g.

The drying time increases from 45 to 60 minutes; however, the increase in the drying time was not proportional to the increase in loading. For an increase of 100% in the paddy loading, the drying time increased by 30% only. In case of wheat drying, the drying time increases from55 to 75 minutes, indicating 36% increase in drying time for loading of wheat by 100%. The increase in drying time was not large, even when the loading was doubled. This can be attributed to the formation of a dense and packed fluidized bed in the vortex chamber at a higher inventory; the dense bed facilitates better hot air contact during drying. However, improvement in heat and mass transfer rates at higher loading may be compromised with slight increase in the drying time.

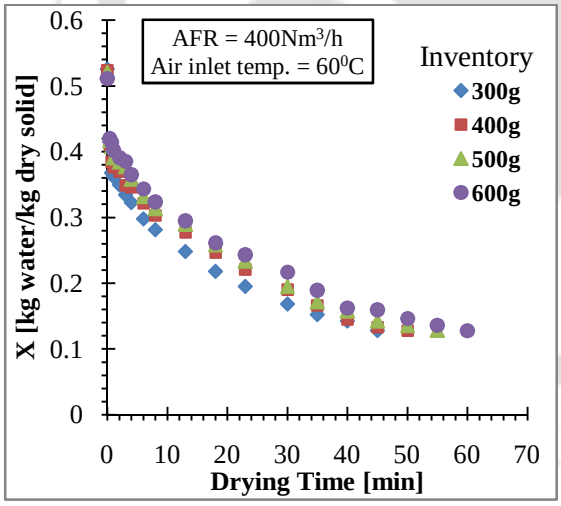

Fig.5. 13MC versus Drying time at different inventory (paddy)

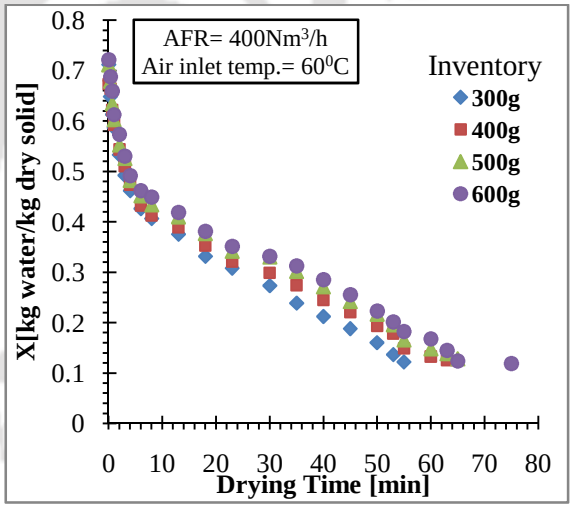

Fig.5. 14MC versus Drying time at different inventory (wheat)

5.3.4 VARIATION OF OUTLET AIR HUMIDITY

Specific humidity of air at the outlet of the RFB-SG was measured using a humidity sensor (Make: Rotronic HC2). The observations were made for the initial 10

minutes of drying process. The variation of the same for different air flow rates through the dryer with time is presented in Figs. 5.15-5.16. Higher air flow rate leads to more centrifugal force in the RFB-SG enabling air to capture more moisture from the wet paddy. As a result, the outlet humidity was high.

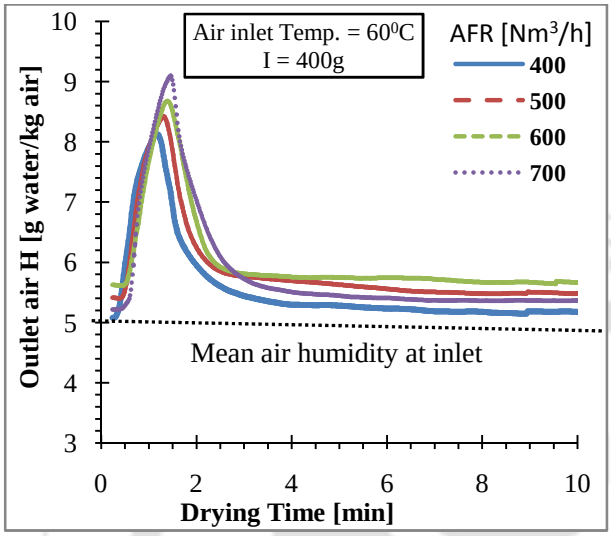

Fig.5. 15Outlet humidity varies with drying time at different AFR(Paddy)

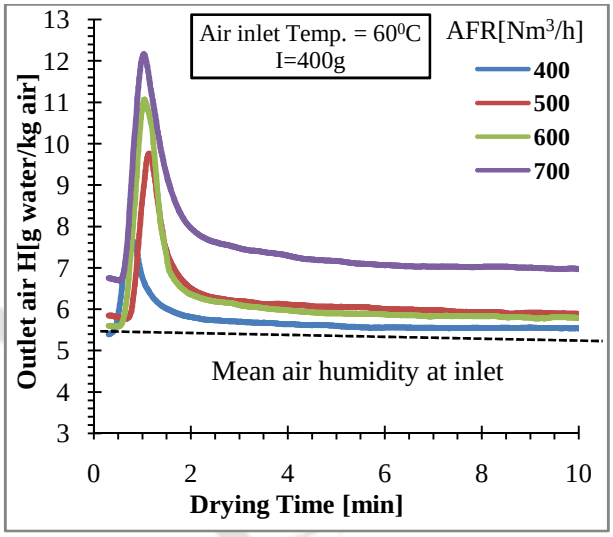

Fig.5. 16Outlet humidity varies with drying time at different AFR(Wheat)

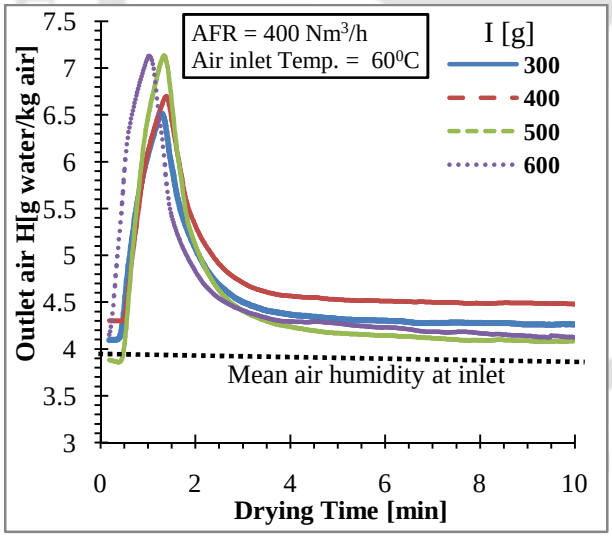

Fig.5. 17Outlet humidity versus drying time at different inventory of paddy

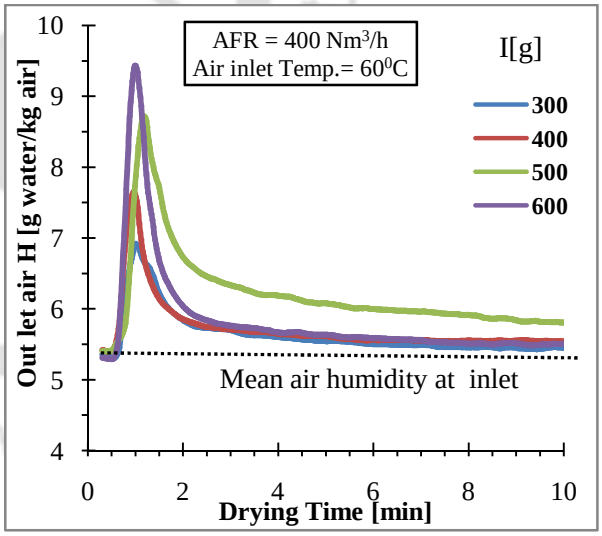

Fig.5. 18Outlet humidity versus drying time at different inventory of wheat

The figures show higher peaks at higher air flow rates resulting in better evaporation rate from the drying materials. Effect of inventory on specific humidity of outlet air is presented in Figs.5.17 and 5.18 for drying of paddy and wheat grains. It is observed that higher rate of evaporation for high loading in the dryer. The

phenomena indicate that most of the surface moisture from the grains is removed within first 2(two) minutes of operation. However, it takes considerable time to remove the internal moisture and specific humidity remains more or less constant during the process.

5.3.5 AIR OUTLET TEMPERATURE DURING DRYING

Effect on outlet air temperature form RFB-SG with drying time is presented in Fig. 5.19. It was observed that, a high air flow rate inside the vortex chamber initially decreases the outlet air temperature indicating rapid use of thermal energy for removing the surface moisture. However, outlet air temperature goes on increasing once the falling rate period is over. This is due to the convective heat and mass transfer from the core of the grain to the surface. From the figure it is clear that with increase in air flow rate the change of outlet air temperature is more significant.

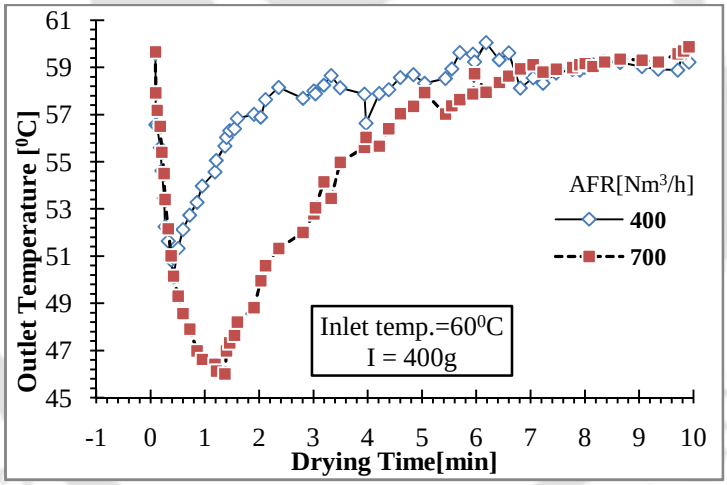

Fig.5. 19 Variation of outlet air temperature affecting drying time for different air flow rates

5.3.6 DRYING CURVE AND DRYING RATE CURVE

Figure 5.20 illustrates the drying phenomena of paddy grains in terms of gradient of drying curve as well as moisture removal rate for AFR of 700Nm^3/h for inlet air temperature of 65^{0}C. The loading rate considered is high (I=600 g). Similar observations are reported in literature Eliaers et al., (2013).

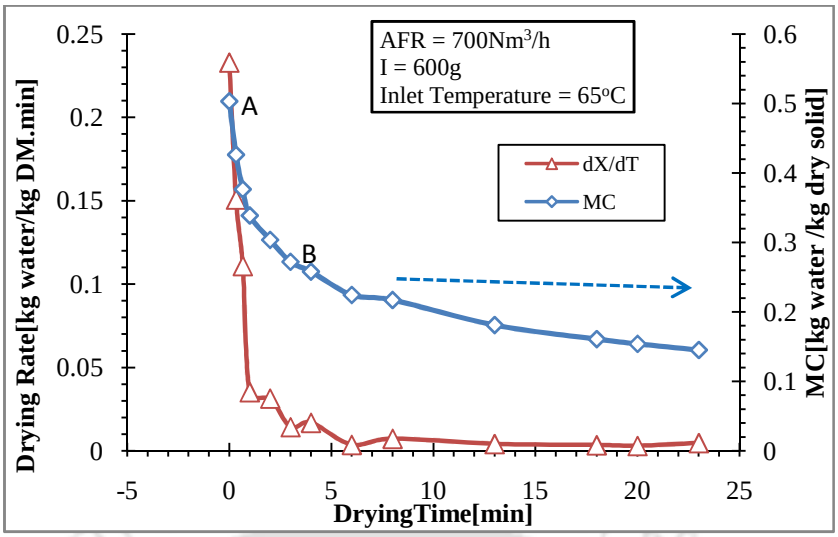

Fig.5. 20Drying rate varies with drying time and MC at inlet temperature of 65^0C

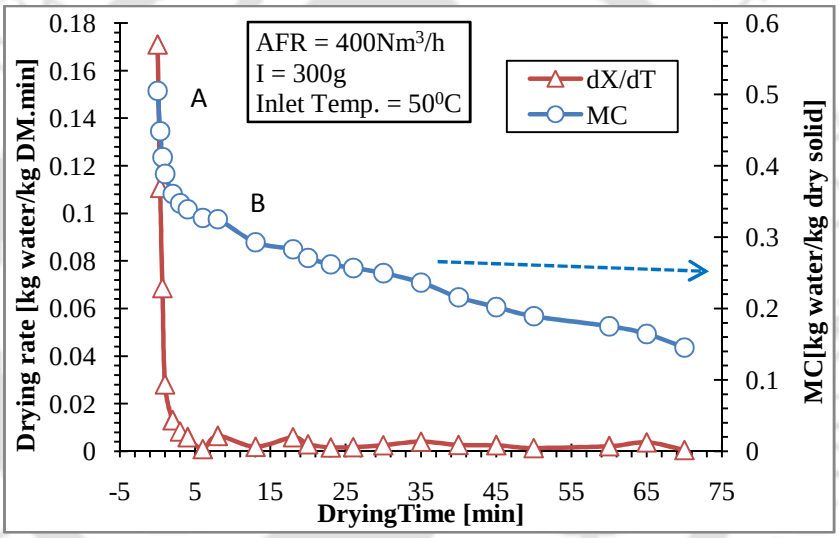

Fig.5. 21Drying rate varies with drying time and MC at inlet temperature 50^0C

It is observed from this figure that heat and mass transfer occurs simultaneously at a very fast rate causing faster removal of moisture from the paddy grains. Position "A" and "B" represents the initial controlled condition of grains and termination of constant rate period. Similar trends were observed for low inventory (I=300g), low inlet air temperature (50^0C) and low AFR ($400Nm^3$/h).

Figure 5.22 describes time independent curve i.e. krischer curve with drying curve. Drying rate versus MC is called time independent curve or Krischer Curve. This graph is similar to Kemp et al.,(2001). However, they Kemp et al., (2001) used relatively high temperature and study was based on a single particle showing shift of the curve from the present work.

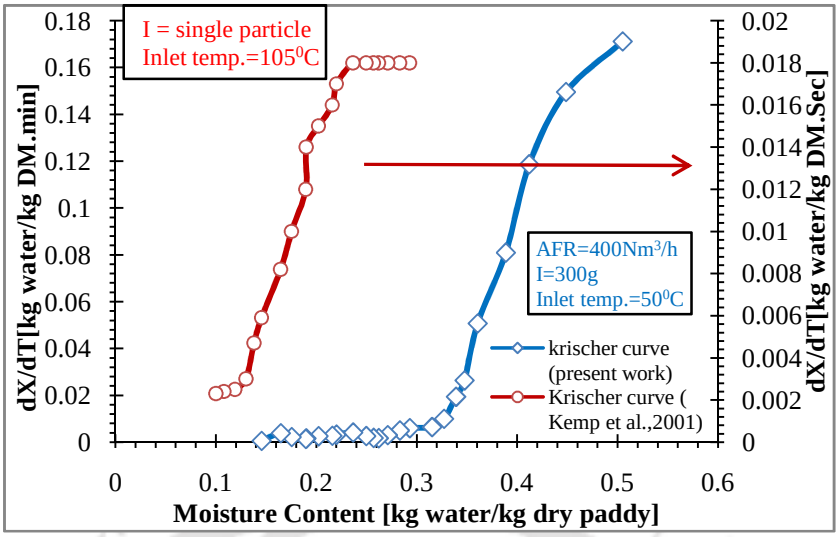

Fig.5. 22Drying rate varies with Moisture Content

5.4 DRYING CHARACTERISTICS IN BUBLLING FLUIDIZED BED (BFB)

Drying characteristics of paddy and wheat grains in BFB are discussed in the following sections. The input parameters are already given in Table 5.1.

5.4.1 EFFECT OF INLET AIR TEMPERATURE ON DRYING

The variation of moisture removal rate with time for inventory of 500g with AFR of 125Nm^3/h during the drying of paddy and wheat grains represent in Figs.5.23 and 5.24, respectively. Experiments were conducted for the inlet air temperature in the range of 50-65^{0}C in a step of 5^{0}C starting from 50^{0}C. The AFR is considered based on repeated trial for minimum fluidization.

It is observed from the figures that the moisture removal rate increases with increase in air temperature resulting in decrease of drying time. Increase in inlet air temperature accelerates both the heat and mass transfer from the grains leading to the decrease in drying time. Similar trend was reported by Watchacama et al., (2000) and Ozbey and Soylemez,(2005).

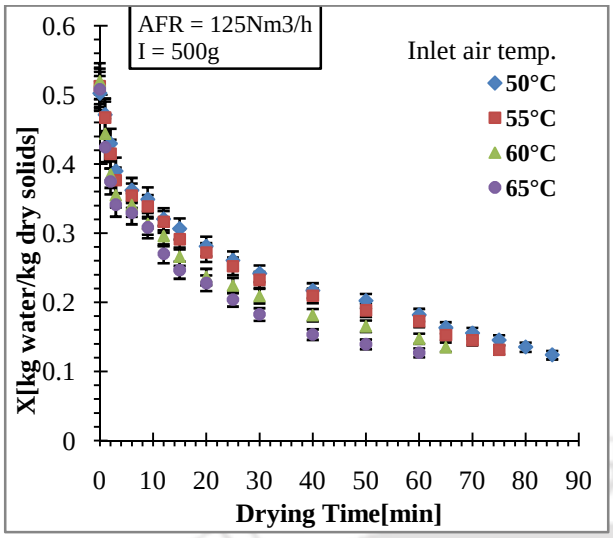

Fig.5. 23MC varies with drying time at different inlet temperature with constant inventory and AFR (paddy)

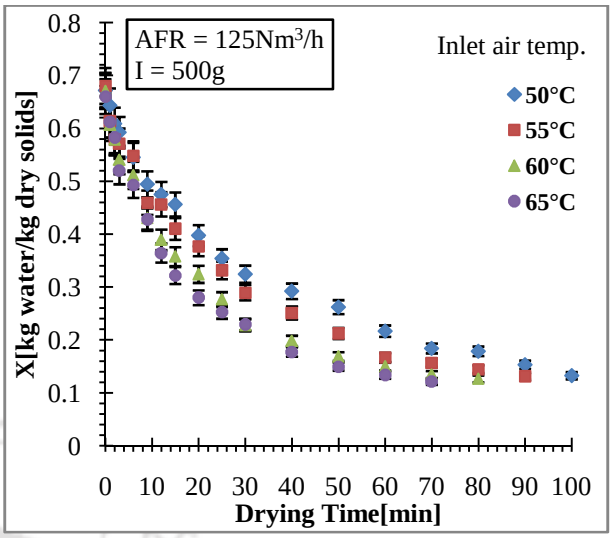

Fig.5. 24MC varies with drying time at different inlet temperature with constant inventory and AFR (wheat)

It is observed that with increase in inlet air temperature by 30% decreases the drying time by 25% for paddy decreasing the absolute drying time from 85 to 60 minutes. Similarly, decrease in drying time was observed to be 30% for wheat for the same percentage increase of inlet air temperature (from 100 to 70 minutes). The variation in such decrease is attributed to the texture of the grains.

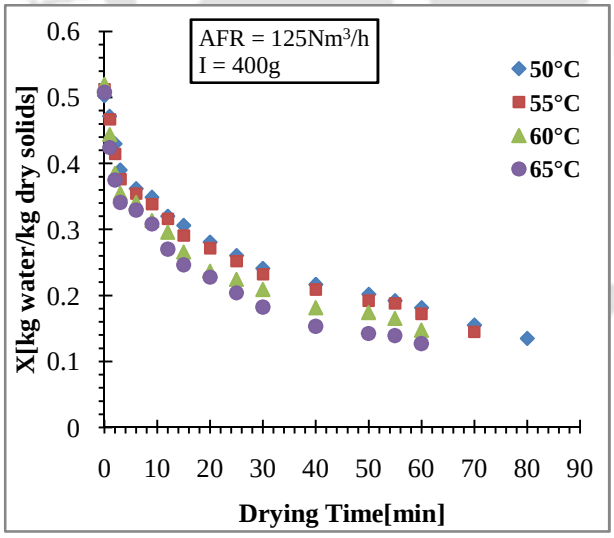

Fig.5. 25MC varies with drying time at different inlet temperature with constant inventory and AFR (paddy)

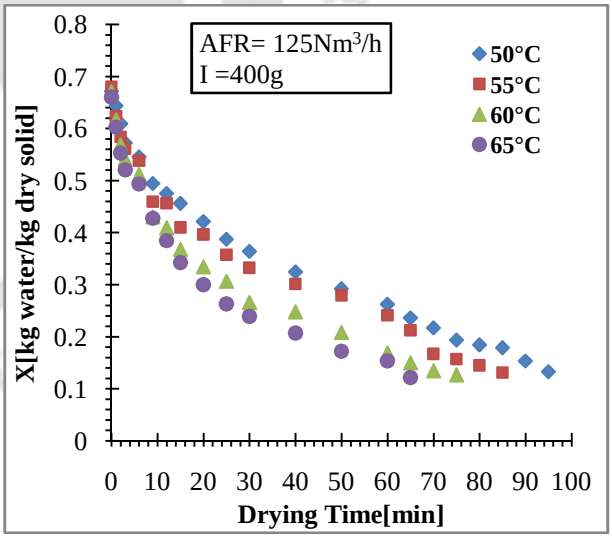

Fig.5. 26MC varies with drying time at different inlet temperature with constant inventory and AFR (wheat)

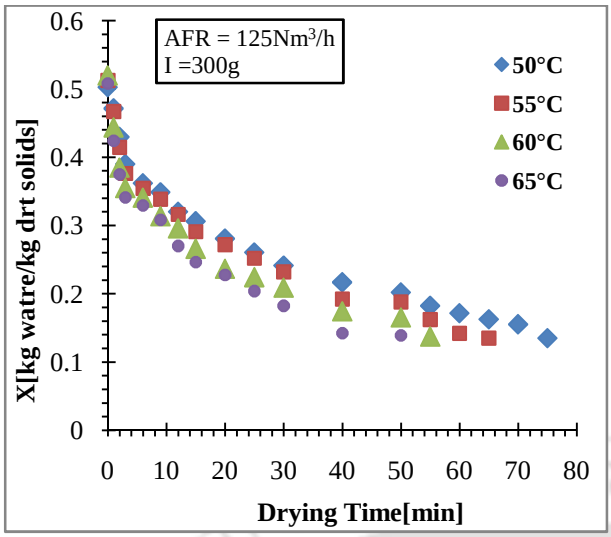

Fig.5. 27MC varies with drying time at different inlet temperature with constant inventory and AFR (paddy)

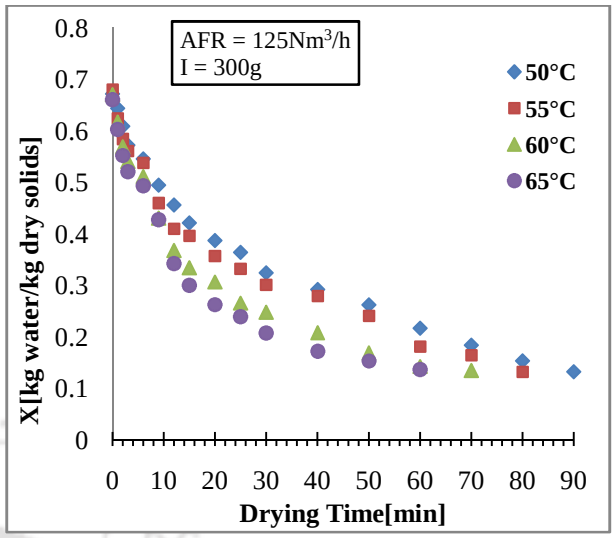

Fig.5. 28MC varies with drying time at different inlet temperature with constant inventory and AFR (wheat)

Figures 5.25-5.26 and Figs. 5.27 -5.28 present similar plots for inventories of 400g and 300g, respectively under similar air temperature range and air flow rate of 125 Nm^3/h. Moisture contain (MC) of paddy comes from 48±3.8% to 13±0.68% dry basis (db) and from 68±4.32 to 13±0.72 for wheat which is the safe limit of MC for storage of the grains atleast for 1(one) year IRRI, (2005).

5.4.2 EFFECT OF AFR ON DRYING WITH BFB DRYER

The variations of AFR from 125 to 175 Nm^3/h at inlet air temperature of 60^0C reflect the variation of MC with drying time as shown in Figs.5.29-5.30. Both the results are presented for inventory of 400 g of paddy as well as wheat grains. Wet paddy and wheat grains with initial MC 68 ± 4.32 %, respectively were considered. The drying process was controlled so as to maintain the final MC at 13 ± 0.68 % and 13 ± 0.72 % for paddy and wheat grains, respectively. Rapid initial drying was observed with removal of the superficial moisture in less than 2-5 minutes as observed from the figures. The drying time is reduced with increase in the air flow rate from 125 to 175 Nm^3/h.

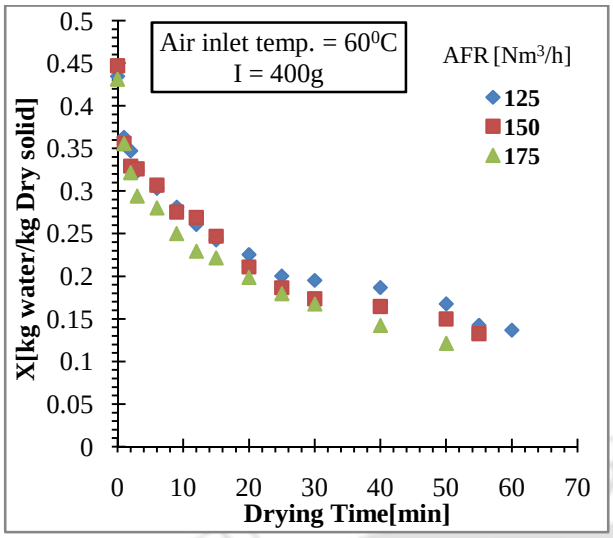

Fig.5. 29MC varies with drying time at different air flow ratewith constant inventory and inlet temperature (paddy)

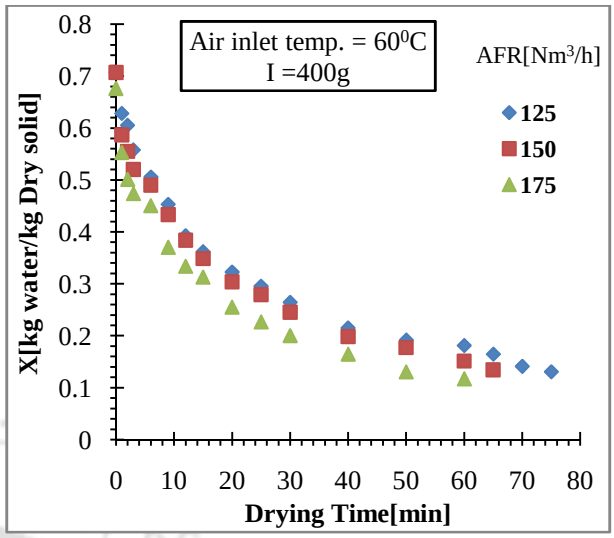

Fig.5. 30MC varies with drying time at different air flow rate with constant inventory and inlet temperature (wheat)

It is observed from both the figures that increase in AFR results in decrease in drying time. This is attributed to the increases the slip velocity gas and solids which inhibits bubbling leading to high rate of heat and mass transfer.

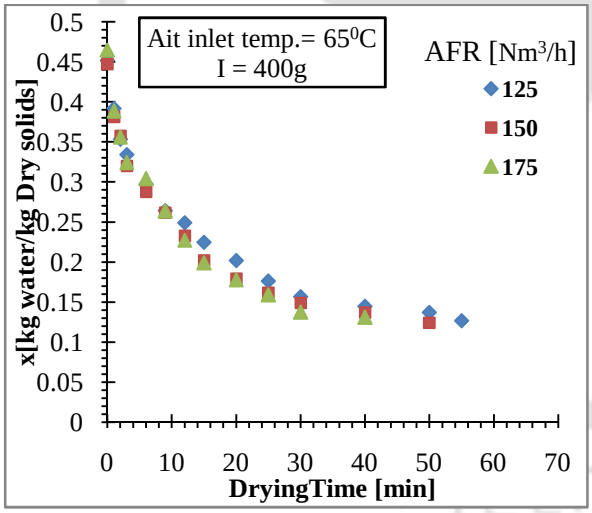

Fig.5. 31MC changed with drying time at different air flow rate with constant inlet temperature and inventory(paddy)

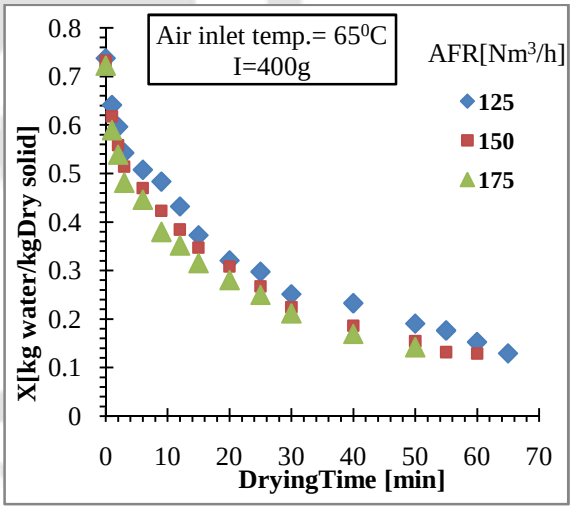

Fig.5. 32MC changed with drying time at different air flow rate with constant inlet temperature and inventory (wheat)

It may be further observed that percentage decrease in drying time for paddy grains is more than that of wheat grains which is due to the textural differences. Figure 5.31 and 5.32 present similar results for drying air temperature of 65^{0}C.Effect of

drying air temperature on drying time with different AFR for inventory of 400 g each of paddy and wheat grains is presented in Figs. 5.33-5.34.

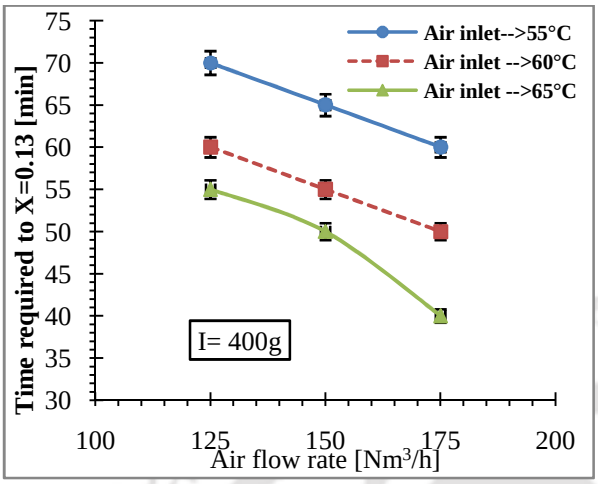

Fig.5. 33Time required to reached the desired MC with different AFR and inlet temperature at constant inventory (paddy)

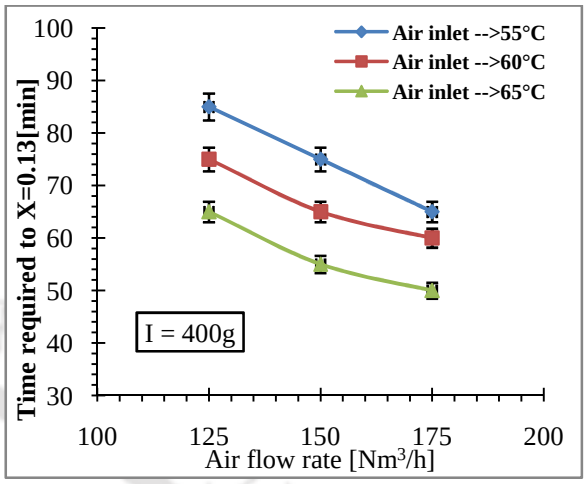

Fig.5. 34Time required to reached the desired MC with different AFR and inlet temperature at constant inventory (wheat)

It is observed from the figures that drying time decreases from 60 to 50 minutes (17%) and55 to 40 minutes (27%) at air inlet temperature 60^0C and 65^0C, respectively for attaining the controlled final MC for paddy grains. Drying time was observed to be decreased by 20% and 38% for wheat grain as observed from Fig. 5.34.

5.4.3 EFFECT OF LOADING /INVENTORY ON DRYING

All experiments were carried out at a constant air inlet temperature of 60^0C and air flow rate 125 Nm^3/h to analyse the effect of inventory on drying. Different inventory of drying materials (paddy/wheat) was fed inside the drying chamber manually in batches. Figure 5.35 and 5.36 shows the drying time for an air flow rate of 125 Nm^3/h, air inlet temperature of 60^0C with paddy and wheat loading 300-500g.

The drying time is observed to increase from 55 to 65 minutes for the range of loads; however, the increase in the drying time was not proportional to the increase in loading. For an increase of 66% in the paddy loading, the drying time increased by 18% only. In case of wheat drying, the drying time increases from 70 to 80 minutes, indicating an increase of drying time by 15% when the loading is increased 66%.

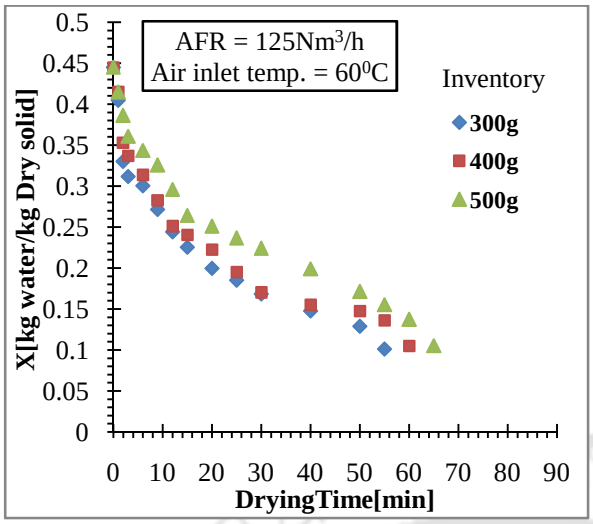

Fig.5. 35MC varies with drying time at different inventory with constant AFR and inlet temperature (paddy)

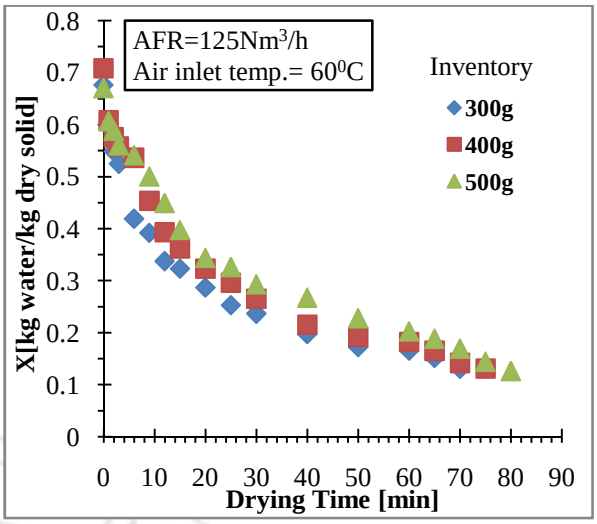

Fig.5. 36MC varies with drying time at different inventory with constant AFR and inlet temperature (wheat)

The increase in drying time is not significantly high in comparison to the increase in loading rate. This is due to the better mixing of grains in hot air environment producing a thin thermal boundary layer. However, improvement in heat and mass transfer rates at higher loading may be compromised with slight increase in the drying time.

5.4.4 EFFECT ON OUTLET AIR HUMIDITY FOR DRYING IN BFB

The humidity sensor (Make: Rotronic HC2) was used for measuring Specific humidity of air at the outlet of the BFB.The variation of the same for different air inlet temperature through the dryer with time is presented in Figs. 5.37 -5.38. Higher air inlet temperature leads to more thermal energy enabling air to capture more moisture from the wet paddy. As a result , the outlet humidity was high. The figures show higher peaks at higher air inlet temperature resulting in better evaporation rate from the drying materials.

Effect of air flow rate and inventory on specific humidity of outlet air is presented in Figs.5.39-5.40 and 5.41-5.42, respectively for drying of paddy and wheat grains. It is observed that higher rate of evaporation for high loading and higher AFR in the dryer. The phenomena indicate that most of the surface moisture from the grains is removed within first 2(two) minutes of operation. However, it takes considerable

time to remove the internal moisture and specific humidity remains more or less constant during the process.

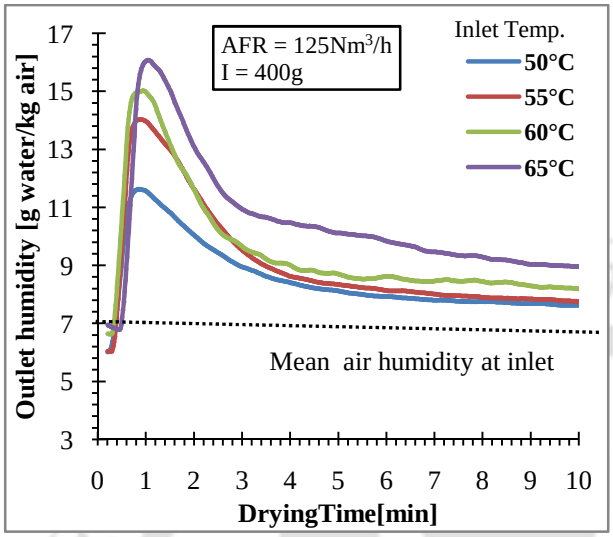

Fig.5. 37Humidity varies with drying time at different inlet temperaturewith constant AFR and inventory (paddy)

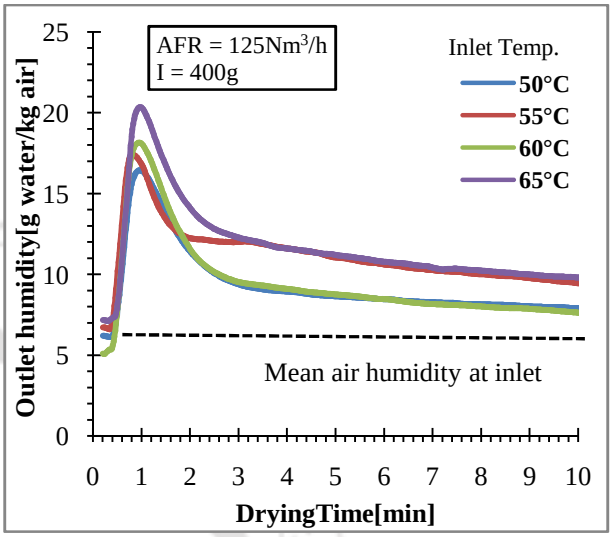

Fig.5. 38Humidity varies with drying time at different inlet temperature with constant AFR and inventory (wheat)

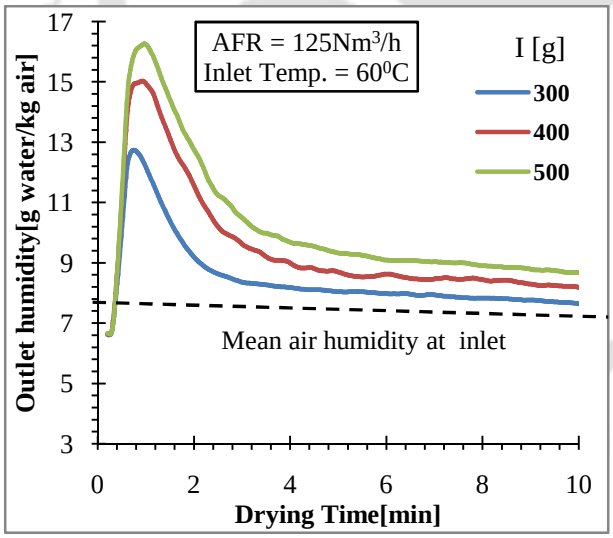

Fig.5. 39Humidity varies with drying time at different inventory with constant AFR and inlet temperature (paddy)

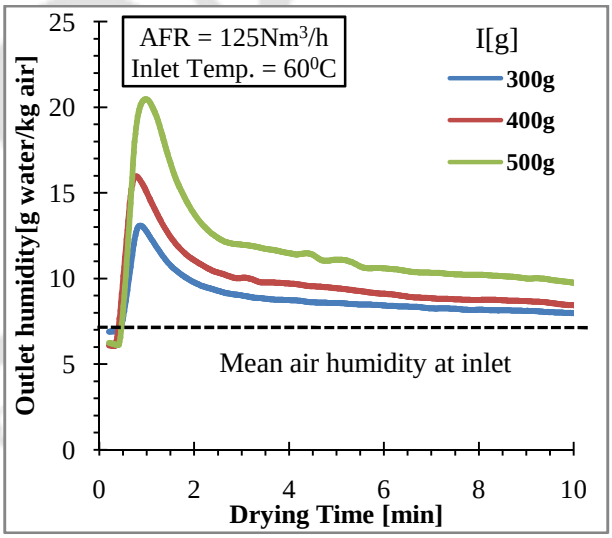

Fig.5. 40Humidity varies with drying time at different inventory with constant AFR and inlet temperature (wheat)

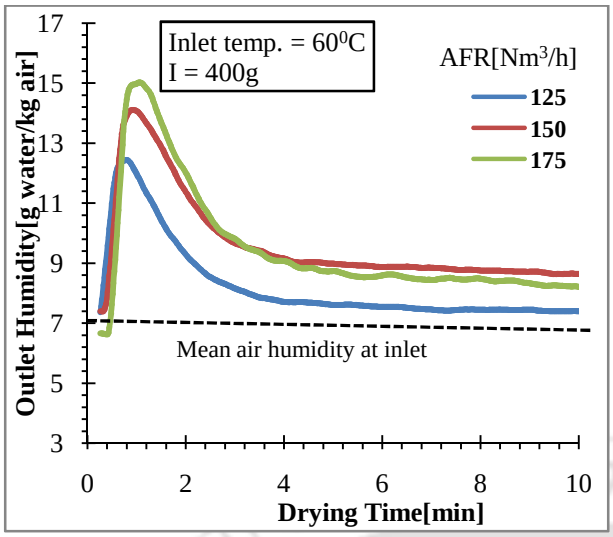

Fig.5. 41Humidity changed with drying time at different air flow rate with constant inlet temperature and inventory (paddy)

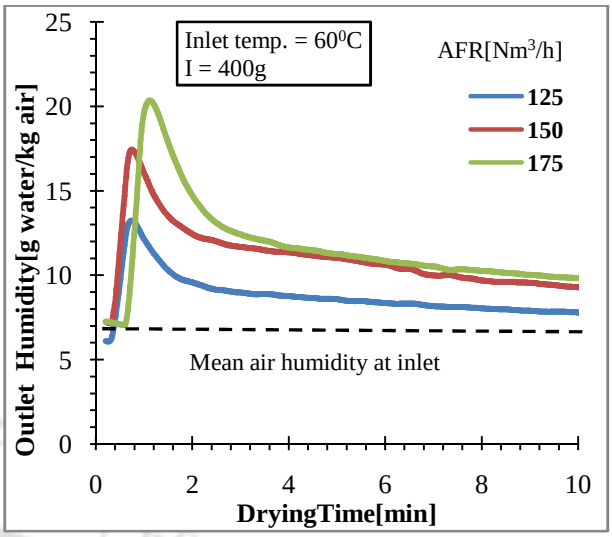

Fig.5. 42Humidity changed with drying time at different air flow rate with constant inlet temperature and inventory (wheat)

5.4.5 AIR OUTLET TEMPERATURE DURING DRYING

Effect on outlet air temperature form BFB with drying time is presented in Fig. 5.43. It was observed that, a high air flow rateinside the riser initially decreases the outlet air temperature indicating rapid use of thermal energy for removing the surface moisture.

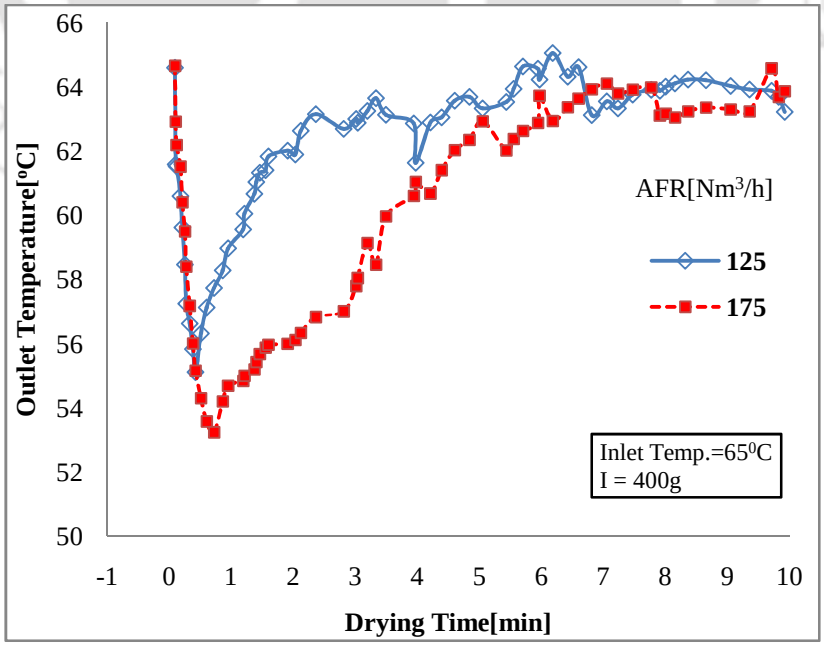

Fig.5. 43Variation of outlet air temperature affecting drying time for different air flow rates

However, outlet air temperature goes on increasing once the falling rate period is over. This is due to the convective heat and mass transfer from the core of the grain to the surface. From the figure it is clear that with increase in air flow rate the change of outlet air temperature is more significant.

5.5 UNIFORMITY OF DRYING AND QUALITY OF PADDY/ WHEAT GRAINS

5.5.1 UNIFORMITY OF DRYING FOR RFB-SG

Uniformity in drying of grains is highly essential for maintenance of quality and storage. The paddy/wheat grain samples were collected from RFB-SG port of vortex after13th and 26th minutes of drying. The bulk sample moisture was measured using proximate analysis using a muffle furnace. Moisture content of each particle in a matrix of 100 particles was measured individually, which is then compared with bulk sample moisture content at 13 minutes.

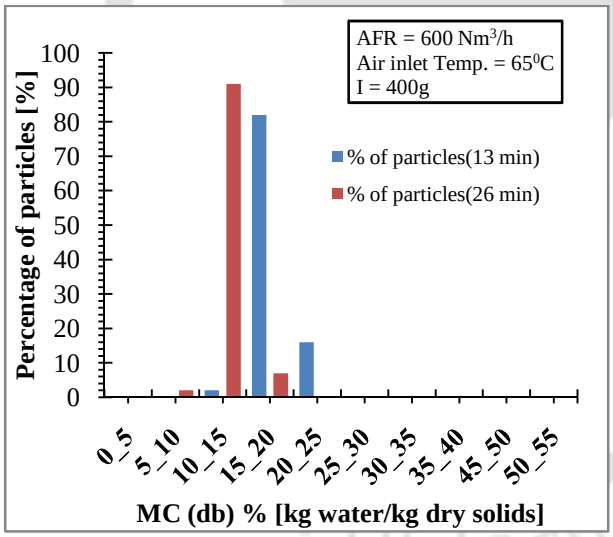

Fig.5. 44Percentage of particles having uniform MC versus bulk MC for two different time of drying (paddy)

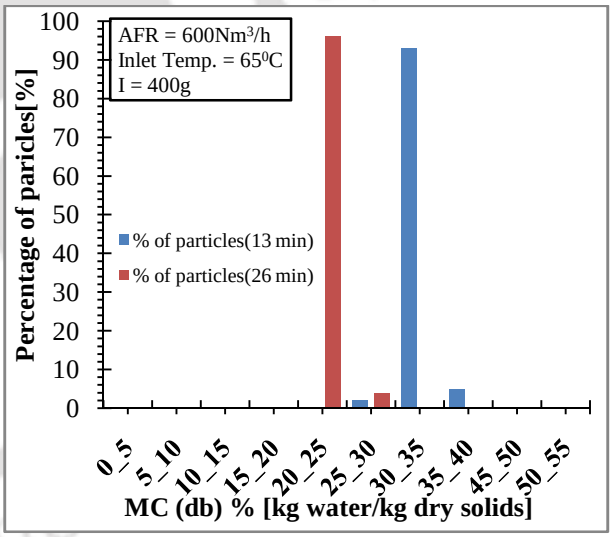

Fig.5. 45Percentage of particles having uniform MC versus bulk MC for two different time of drying (wheat)

It was found that 84% of particles had the same moisture content as measured from bulk sample. At 26th minutes, this value had increased to 94%. In case of wheat the measured uniformity was 88% and 95% at 13th and26th minutes, respectively. The increase in uniformity is due to the efficient mixing in the fast rotating particle bed.

However, the drying rate found to be relatively low compared to the mixing rate. Figure 5.44 and 5.45 presents the percentage of particles having MC (% db) for the drying time of 13th and 26th minutes for paddy and wheat grains, respectively. It is observed from Fig. 5.44 that more than 80% of paddy grains are having uniform bulk moisture content of in the range of 10 - 15 and 15 - 20% (db). However, more uniformity was observed when drying time increased to 26 minute. Similar results were obtained for wheat grains as shown in Fig. 5.45.

5.5.2 UNIFORMITY OF THE DRYING OF PADDY AND WHEAT (BFB)

Figures 5.46 and 5.47 presents the percentage of grains attaining a range of final MC(db)for the drying time of 13thand26thminutes, respectively. It is observed from Fig. 5.46that more than 90% of paddy grains are attaining uniform bulk MC of in the range of 15-20% (db). However, more uniformity was observed when drying time is increased to 26 minutes. Similar results are obtained for wheat grains as shown in Fig. 5.47.

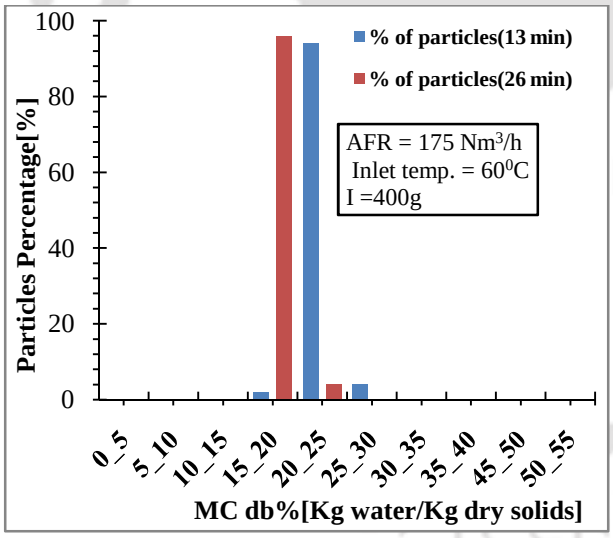

Fig.5. 46Percentage of particles with MC at different time for paddy

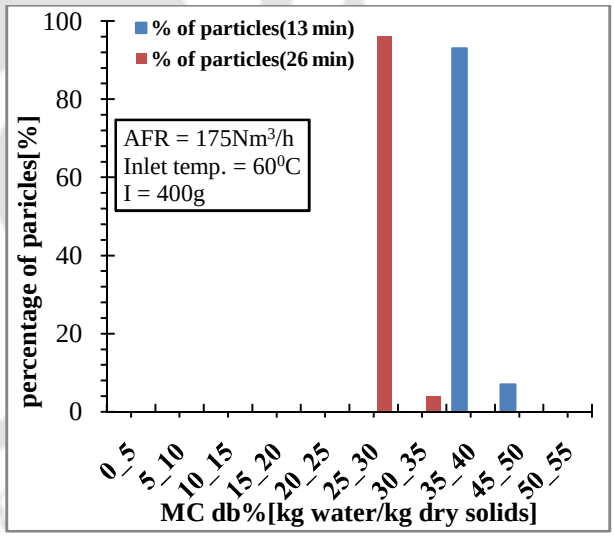

Fig.5. 47Percentage of particles with MC at different time for wheat

5.5.3 PRODUCT QUALITY

After drying, the quality of product should be checked. Shear and normal stresses in the fast rotating particle bed can lead to attrition and damage to the paddy shell. In this case, different air flow rates were used for drying the paddy in RFB-SG. After drying, the damaged percentages of the particles were measured. Figure 5.48 present

the fraction of grains damaged with time for given operating conditions and different air flow rates.

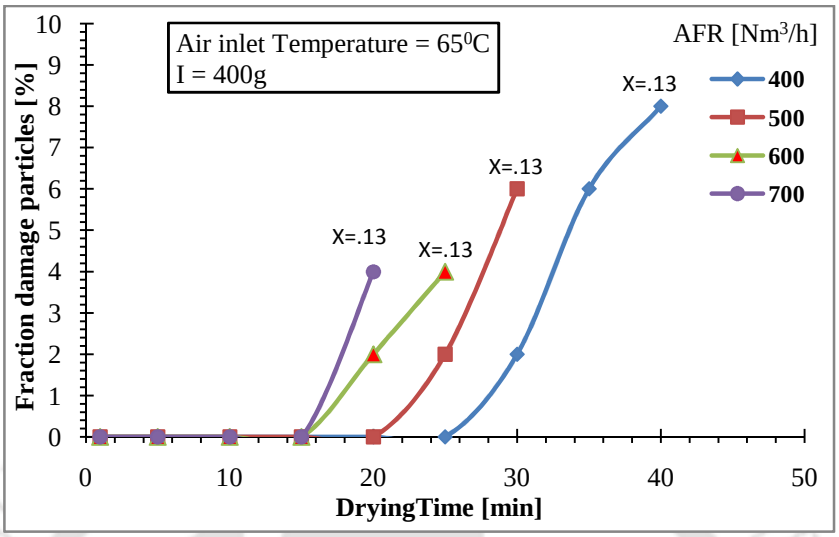

Fig.5. 48Percentage of damage particles versus drying time at different air flow rate with constant air inlet temperature

As expected, attrition occurs faster at higher air flow rates. However, when the air flow rate is high, there is a formation of boundary layer; also, less time is needed to reach the desired moisture content of X= 0.13 (kg H_2O/kg dry paddy). Owing to both these factors, the damage percentage is very less at high flow rates compared to lower air flow rates. Percentage of damaged particles is given in Table 5.2.

Table 5.2 Percentage of damaged particles at different AFR

Air flow rate(Nm^3/h)	Damage (%)
400	8
500	6
600	4
700	4

Paddy and wheat samples were tested at **Centre wallon de Recherches agronomiques, Belgium**for the analysis of dry matter and total protein content. The samples were ground after removal of husk using a Foss-Cyclotec mill with a grid of 1.0 mm. The moisture content was determined using a Near Infrared Reflectance spectrometer (Foss NIRSystems 5000). Test results for moisture, dry matter and protein are given in Table 5.3.

Table 5.3 Moisture/dry matter content and protein Kjeldahl of paddy and wheat before and after drying.

Sample	Moisture	Dry matter	Protein Kjeldahl	
Drying Product (paddy/wheat)	%	%	N*6.25% [g/100 g Product]	N*6.25% DM [g/100 g dry matter]
Original dry paddy	12.1	87.9	5.9	6.8
BFB dried paddy	11.6	88.4	5.9	6.7
RFB-SG dried paddy	10.5	89.5	6.1	6.9
Original dry Wheat	12.2	87.8	10.4	11.8
BFB dried wheat	11.3	88.7	11.0	12.4
RFB-SG dried wheat	10.9	89.1	11.1	12.5

It is observed from the Table that the protein content is not affected by the drying treatment. Moisture content and dry matter are remained qualitatively unchanged before and after drying.

5.5.4 PROCESS INTENSIFICATION (PI) FACTOR

The specific drying rate is an important factor pertaining to drying. It is defined as the quantity of paddy/wheat dried par unit time and per cubic meter drying chamber. It can be calculated based on either the air humidity or the paddy moisture content as shown [Eq. 5.1 and 5.2], respectively.

$$\text{Sp. Drying rate} = \frac{\dot{m}_{\text{dry paddy}}}{V}(MC_{\text{paddy-in}} - MC_{\text{paddy-out}}) \quad (5.1)$$

$$\text{Sp. Drying rate} = \frac{\dot{m}_{\text{dry air}}}{V}(H_{\text{air-out}} - H_{\text{air-in}}) \quad (5.2)$$

The improvement of drying characteristics can be quantified by means of process intensification (PI) factor, which is defined as the ratio of the specific drying rates in the RFB-SG and BFB. The merit of a dryer can be quantified by means of PI [Eq. (5.3)].

$$\text{PI factor} = \frac{(\text{sp . drying rate})\ \text{RFB} - \text{SG}}{(\text{sp . drying rate})\ \text{BFB}} \qquad (5.3)$$

The PI factor depends on the diffusion limitation within the pores of the paddy particles. Using [Eqs. 5.1-5.3], PI factor in the range of 14 to 16 was obtained for RFB-SG dryer in comparison to the BFB dryer. From this PI factor, it is inferred that a dense and packed as well as uniform bed formed inside the RFB-SG dryer due significantly high rotational speed of gas-solid mixture. Further, the gas - solid slip velocities are higher in RFB-SG than that in the BFB dryer resulting in higher coefficient of interfacial mass and heat transfer rate.

5.6 COMPARATIVE STUDY ON DRYING CHARECTERISTICS BETWEEN RFB-SG AND BFB

5.6.1 EFFECT OF AIR INLET TEMPERATURE ON DRYING OF PADDY GRAINS

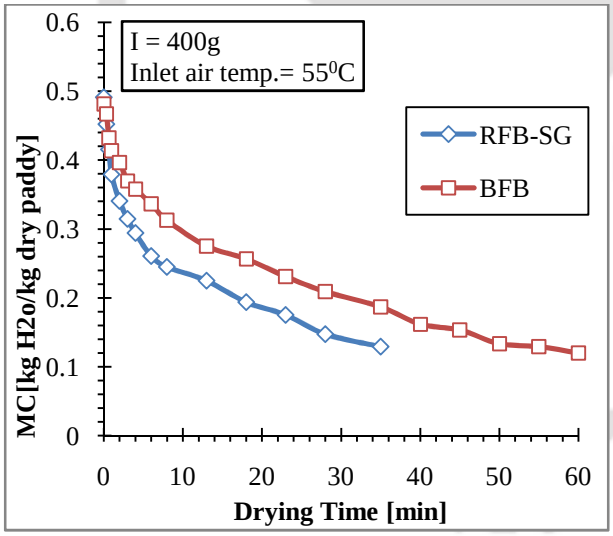

Fig.5. 49Variation of MC with drying time in RFB-SG and BFB dryers air inlet temperature 550C and inventory I= 400g

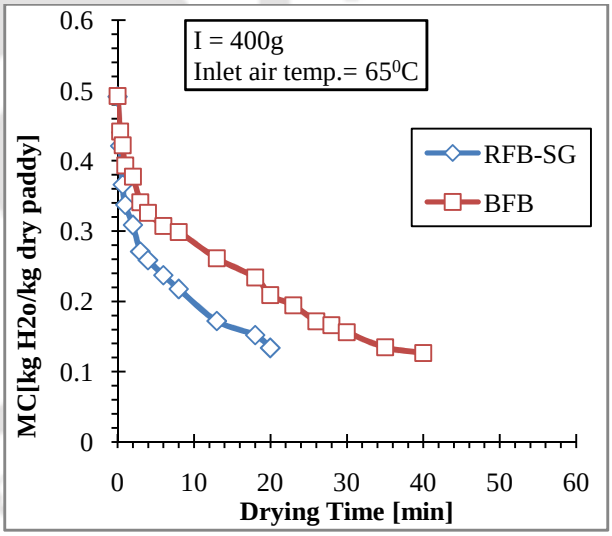

Fig.5. 50Variation of MC with drying time in RFB-SG and BFB dryers at air inlet temperature 650C and inventory I= 400g

Figures 5.49 and 5.50 shows the drying time in batch drying of 400g paddy (db) to reach the desired moisture content of X=0.13 (kg H_2O/kg dry paddy) for different air inlet temperatures. It may be noted that the gas flow rates were 700Nm^3/h and

175Nm^3/h for RFB-SG and BFB dryer, respectively. The air flow rate of the BFB was limited to 175 Nm^3/h to avoid particle entrainment. These figures are presented for two different drying air temperatures, viz. 55^{0}C to 65^{0}C. It is observed that the drying time decreased with increase in inlet air temperature. However, the drying time of RFB-SG dryer was nearly half of the drying time of BFB dryer so as to reach the final moisture content X=0.13 (kg H_2O/kg dry paddy.

5.6.2 EFFECT OF LOADING/INVENTORY ON DRYING

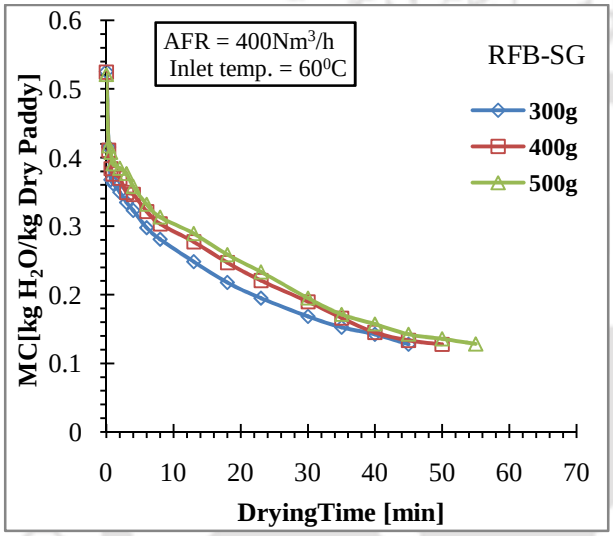

Fig.5. 51Effect of inventory on variation of MC with drying time for RFB-SG dryer

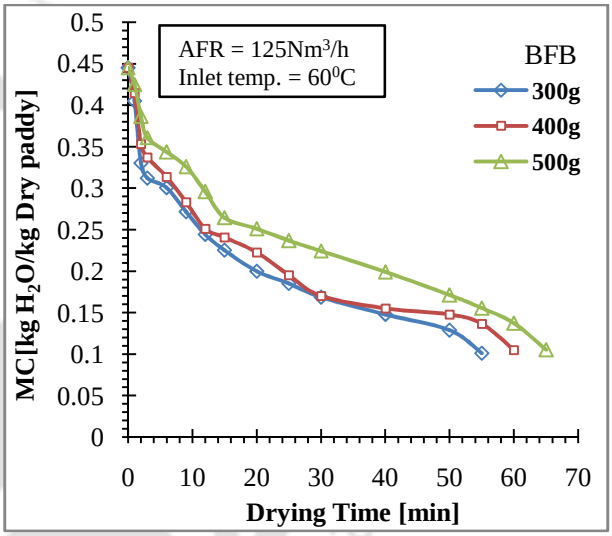

Fig.5. 52Effect of inventory on variation of MC with drying time for BFB dryer

Figure 5.51 describes the drying process at air flow rate of 400Nm^3/h for RFB-SG. Similarly, drying process for BFB dryer is presented in Fig. 5.52 for air flow rate of 125Nm^3/h. Air inlet temperature of 60^{0}C at different inventories in the range of 300-500g was maintained for experiments in both the dryers. When the inventory was increased from 300 g to 500 g, the drying time increased from 45 to 55 minutes (22% increase) for RFB-SG dryer whereas drying time increased from 55 to 65 minutes (18% increase) in case of BFB dryer.

5.6.3 COMPARISON OF DRYING TIME WITH CHANGE IN INVENTORY PER UNIT VOLUME OF THE REACTOR FOR RFB-SG AND BFB DRYERS

Figure 5.53, shows the comparison of drying time with inventory/reactor volume at different air inlet temperatures viz. 55^{0}C and 65^{0}C for both the RFB-SG and BFB

dryers. It is observed that the drying time for RFB-SG dryer is much less compared to BFB dryer for both the air inlet temperature. Table 5.4 presents the increase in drying time for both of the dryers with two different inlet air temperatures with different inventories. The drying time increases with increase in inventory. However, it has been notice that the drying time is comparatively higher for BFB dryer for the same inventory.

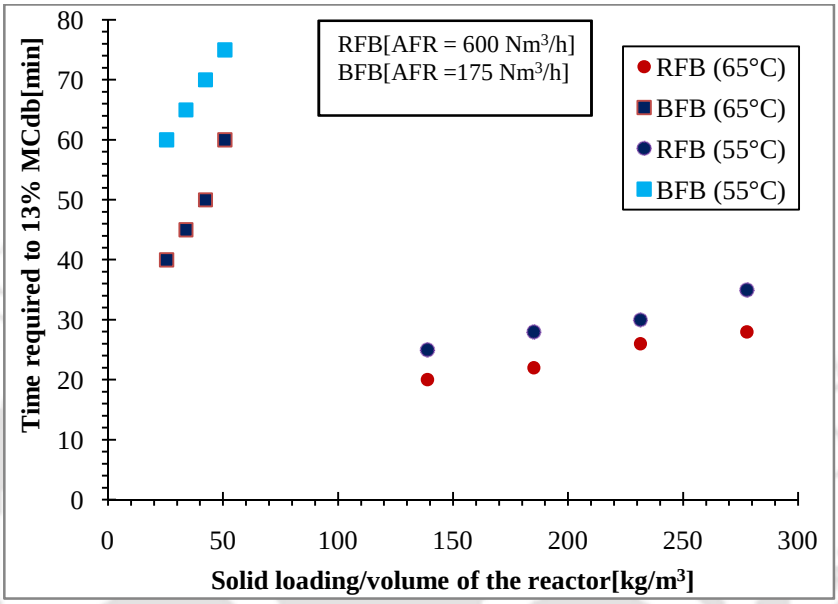

Fig.5. 53Effect of solid loading/volume of the reactor (kg/m^3) on drying time

Table 5.4 Increase in drying time for solid loading per unit volume of reactor

Inlet air temp. (^{0}C)	BFB (Increasing drying time)	RFB-SG (Increasing drying time)
55	60%	40%
65	50%	30%

The shorter drying time and smaller equipment size when using a vortex chamber of RFB-SG dryer comes with an increased air flow rate. The air consumption and utilization efficiency is therefore to be analysed further.

5.6.4 COMPARISON OF AIR CONSUMPTION FOR RFB-SG AND BFB DRYER

Figure 5.54 shows that the function of the paddy loading required to reach the desired moisture content for both RFB-SG and BFB dryers. Because of the increased drying rate and resulting drying time , the total amount air required with the vortex chamber was less than double the amount of air required with the BFB dryer, despite the 3.4 times higher air flow rate fed to the vortex chamber of RFB-SG dryer.

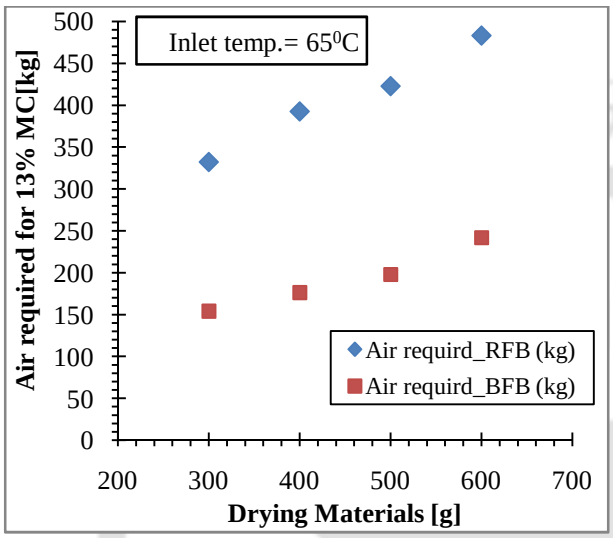

Fig.5. 54Air required versus solid loading for drying to reach the desired MC

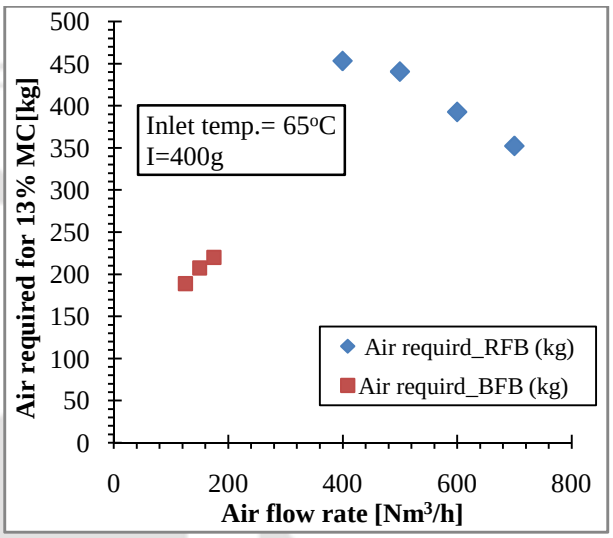

Fig.5. 55Air required versus air flow rate for drying to reach the desired MC

Similarly, Fig. 5.55 compares for given paddy loading, for BFB and RFB-SG dryer the total amount of air required to reach the desired moisture content as function of the air flow rate. Whereas with the BFB dryer, the total amount of air required increased with the air flow rate, it decreases with RFB-SG dryer. In BFB dryer, bubbling increases with increasing air flow rate. This is not the case of RFB-SG in a vortex chamber. In the RFB-SG, the slip velocity and related coefficients of interfacial mass, heat and momentum transfer increases when increasing the air flow rate without introducing or increasing the bubbling because of increasing particles bed rotation.

5.6.5 COMPARISON OF SPECIFIC DRYING RATE FORRFB-SG AND BFB DRYER

Figure 5.57 directly compares with the paddy drying performance of a BFB and a RFB-SG in a vortex chamber. Figure shows the average specific drying rate [kg H_2O/kg dry paddy.min], that is, averaged over the time required to reach the desired paddy moisture content of 0.13 [kg H_2O/kg $_{dry\ paddy}$], as a function of paddy loading for an air inlet temperature of 65^0C and air flow rate of 175 and 600Nm^3/h for respectively the BFB and RFB-SG dryer.

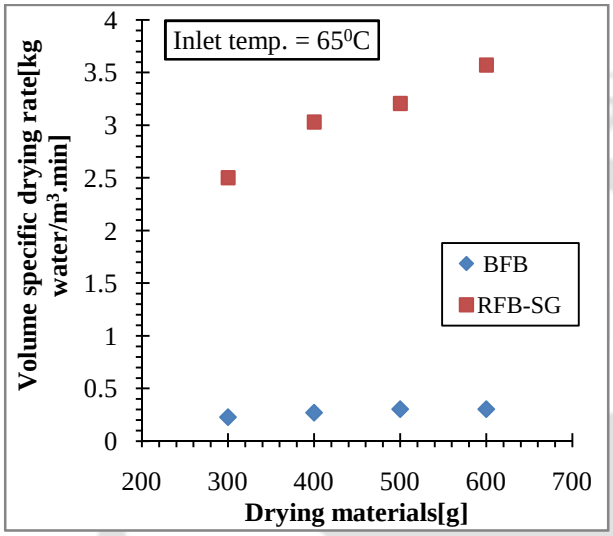

Fig.5. 56Volume specific drying rate versus Inventory at constant inlet temperature

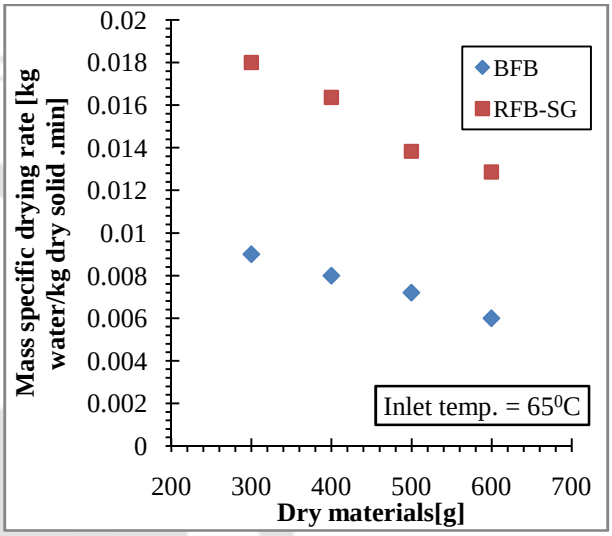

Fig.5. 57Mass specific drying rate at constant inlet temperature versus inventory

The vortex chamber technology indeed allows operation at much higher air flow rate to reach high-g operation. The significantly increased average specific drying rate that is achieved with the vortex chamber results for m intensified inter facial mass and heat transfer at the particle scale and improved the uniformity. The process intensification benefit related to the intensified interfacial momentum transfer i,e the denser ad more uniform particle bed and related more efficient interfacial mass and heat transfer at the bed or the chamber scale, remains even when strong intra-particle diffusion limitation occur. The decrease of average specific drying arte with increasing the paddy loading is explained by an increasing part of the particles bed being contacted with already humidified and cooler air. The higher specific drying rate in the vortex chamber explains the steeper slope of the curve.

5.7 DEVELOPMENT OF FINAL MOISTURE CONTENT CORRELATION FOR RFB-SG AND BFB DRYERS

5.7.1CORRELATION FOR RFB-SG

From the experiments, it was observed that the final moisture content of the paddy grain, ΔMCp (moisture contain of paddy) is a function of the following variables.

$$\Delta MCp = f(T_a, \phi_{am}, \rho_{da}, \rho_{dp}, \phi_{wp}, t, m_{wp}, V, \vartheta_{fc}) \quad (5.4)$$

where,

T_a = Temperature of the inlet fluidizing air

ϕ_{am} = Moisture of the ambient air

ρ_{da} = Density of dry air

ρ_{dp} = Density of dry paddy grain

ϕ_{wp} = Moisture of the wet paddy

t = Drying time

m_{wp} = Mass of the wet paddy

V = Velocity of the fluidizing air

ϑ_{fc} = Volume of the fluidization chamber

ρ_{ma} = Density of moist air

ΔMCp = IMC - FMC

In order to decrease the number of variables, some new terms have been introduced, which may be varied during the experiments. In this case, ρ_{ma}(density of the moist air) is the function of T_a, ϕ_{am} and ρ_{da}. Hence, ρ_{ma} is introduced replacing T_a, ϕ_{am} and ρ_{da} .

Now the above equation changes to

$$\Delta MCp = f(\rho_{ma}, t, m_{wp}, V, \vartheta_{fc}) \quad (5.5)$$

Dimensional analysis of [Eq. (5.6)] is made using Buckingham π theorem.A correlation between differences of MC of product with other parameters is obtained as follows:

$$\Delta MCp = C \left(\frac{m_{wp}}{\rho_{ma}.\vartheta_{fc}}\right)^a \left(\frac{V.t}{\vartheta_{fc}^{1/3}}\right)^b \quad (5.6)$$

From the results discussed in the preceding sub-sections, a set of 48 experimental data points was analysed with the help of **FindFit function** using **Mathematica (**version 5.2) of software and with maximum iterations 1000 for RFB-SG and BFB dryers for paddy as well as wheat grain drying. The value of constants (C, a and b) in [Eq. (5.3)] are estimated for both the dryers for paddy and wheat drying.

In RFB-SG dryer for paddy grain drying, the coefficients of correlations are found to be

C= 104.609, a = -0.0227364, b = -0.0969066

Thus correlation for paddy drying in RFB-SG is

$$\Delta MCp = 104.509 \left(\frac{m_{wp}}{\rho_{ma}.\vartheta_{fc}}\right)^{-0.0227354} \left(\frac{V.t}{\vartheta_{fc}^{1/3}}\right)^{-0.0959066} \quad (5.7)$$

In this correlation is valid for the following range of parameters.

$$131.17 < \frac{m_{wp}}{\rho_{ma}.\vartheta_{fc}} < 263.27$$

$$9{,}622 < \frac{V.t}{\vartheta_{fc}^{1/3}} < 26{,}015$$

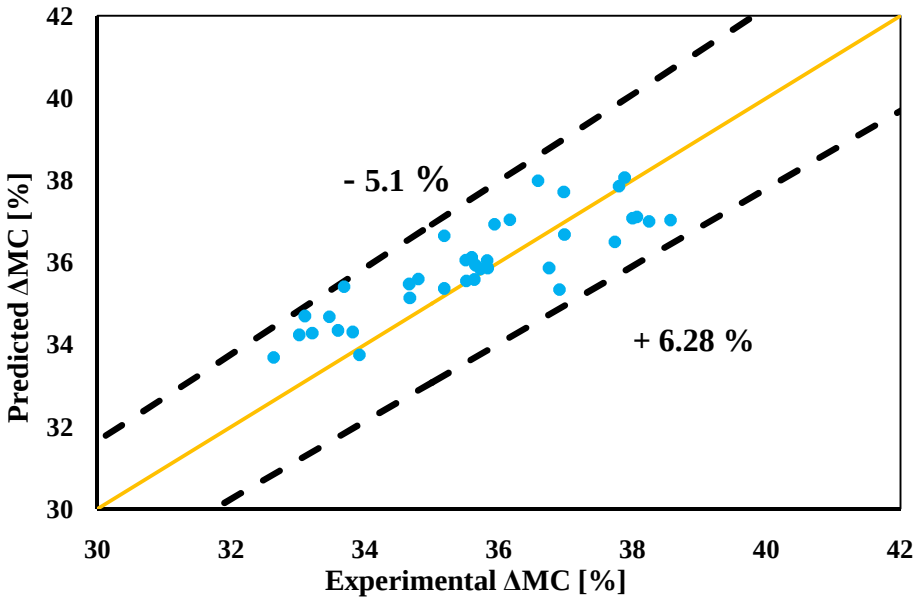

Fig.5. 58Comparison of theoretical and experimental MC difference [%]

The theoretical value of ΔMCp deviates from the experimental data by ±7% as shown in the Fig. 5.58.

Similarly, following correlation is developed for paddy drying in BFB dryer

$$\Delta MCp = 57.6895 \left(\frac{m_{wp}}{\rho_{ma}.\vartheta_{fc}}\right)^{0.0530522} \left(\frac{V.t}{\vartheta_{fc}^{1/3}}\right)^{-0.082461} \quad (5.8)$$

This correlation is valid for following range of parameters.

$$25.09 < \frac{m_{wp}}{\rho_{ma}.\vartheta_{fc}} < 41.89$$

$$1{,}179 < \frac{V.t}{\vartheta_{fc}} < 2{,}404$$

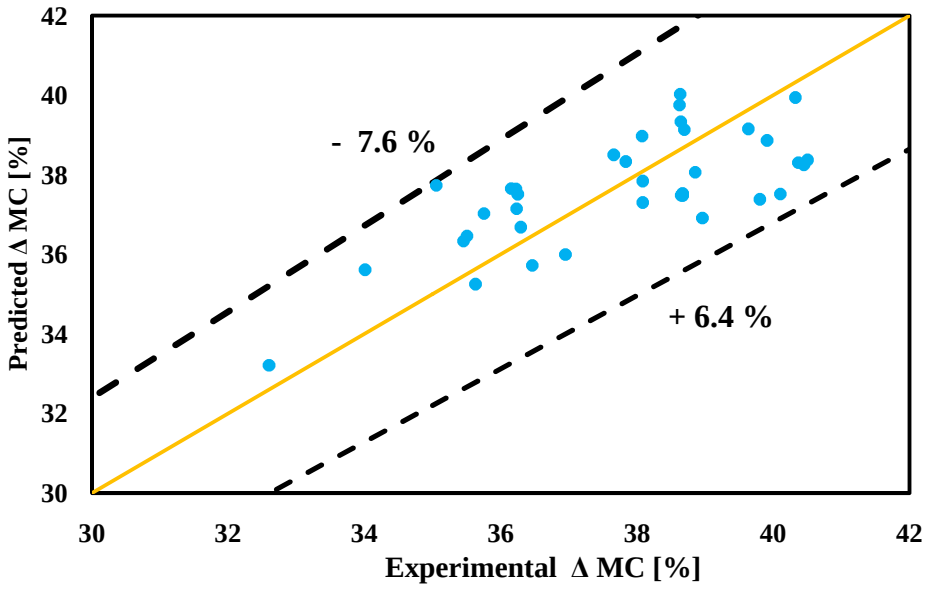

Fig.5. 59Comparison of theoretical and experimental MC differences [%]

Theoretical value of MCp predicated using the correlation [Eq. (5.9)] is in the range of ±6% of the experimental value for the given range of non-dimensional numbers as shown in Fig. 5.59.

5.7.2 Similar correlations are developed for wheat drying in RFB-SG as follows

$$\Delta MCp = 76.3605 \left(\frac{m_{wp}}{\rho_{ma}.\vartheta_{fc}}\right)^{-0.017526} \left(\frac{V.t}{\vartheta_{fc}^{1/3}}\right)^{-0.0220619} \quad (5.9)$$

In this correlation, the π terms ranges are as follows

$$131.15 < \frac{m_{wp}}{\rho_{ma}.\vartheta_{fc}} < 263.01$$

$$14{,}581.16 < \frac{V.t}{\vartheta_{fc}^{1/3}} < 31{,}215.96$$

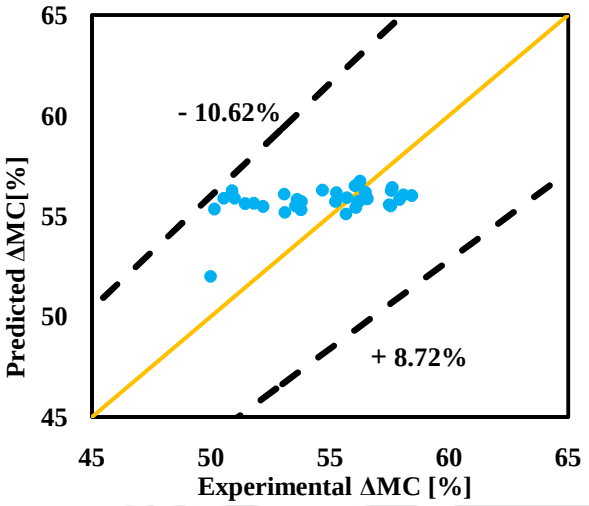

Fig.5. 60Comparison of theoretical and experimental MC differences [%] of RFB-SG (wheat)

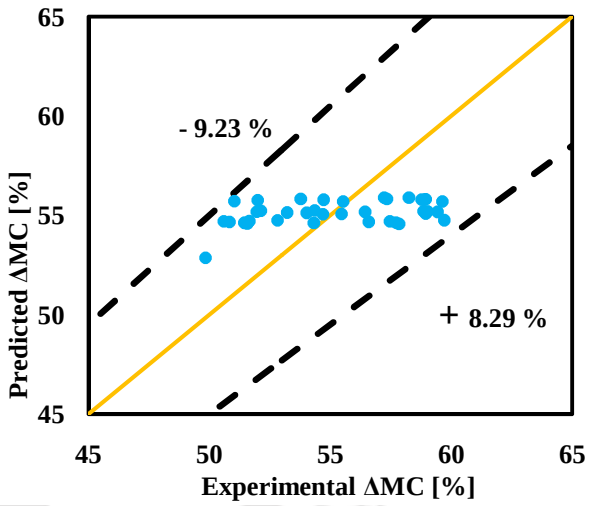

Fig.5. 61Comparison of theoretical and experimental MC differences [%] of BFB (wheat)

Theoretical value of ΔMCp predicated using the correlation [Eq. (5.9)] is in the range of ±8% of the experimental value as shown in Fig. 5.60.

Similar correlations are developed for wheat drying in BFB as follows

$$\Delta MCp = 60.2464 \left(\frac{m_{wp}}{\rho_{ma}.\vartheta_{fc}}\right)^{0.0425184} \left(\frac{V.t}{\vartheta_{fc}^{1/3}}\right)^{-0.00808605} \quad (5.10)$$

In this correlation, the π terms ranges are as follows

$$25.12 < \frac{m_{wp}}{\rho_{ma}.\vartheta_{fc}} < 41.93$$

$$1{,}444 < \frac{V.t}{\vartheta_{fc}^{1/3}} < 2{,}565.18$$

Using the correlation value [Eq.(5.9)], the theoretical value of ΔMCp is varied by ±6% from experimental value shown in Fig.5.61.

Table 5.5presents the summary of correlations developed along with applicable ranges.

Drying Product/ Dryer	Correlation	Range (correlation)
Paddy (RFB-SG)	$\Delta MCp = 104.509 \left(\frac{m_{wp}}{\rho_{ma}.\vartheta_{fc}}\right)^{-0.0227354} \left(\frac{V.t}{\vartheta_{fc}^{1/3}}\right)^{-0.0959066}$ [5.4]	$131.17 < \frac{m_{wp}}{\rho_{ma}.\vartheta_{fc}} < 263.27$ $9{,}622 < \frac{V.t}{\vartheta_{fc}^{1/3}} < 26{,}015$
Paddy (BFB)	$\Delta MCp = 57.6895 \left(\frac{m_{wp}}{\rho_{ma}.\vartheta_{fc}}\right)^{0.0530522} \left(\frac{V.t}{\vartheta_{fc}^{1/3}}\right)^{-0.082461}$ [5.5]	$25.09 < \frac{m_{wp}}{\rho_{ma}.\vartheta_{fc}} < 41.89$ $1{,}179 < \frac{V.t}{\vartheta_{fc}} 2{,}404$
Wheat (RFB-SG)	$\Delta MCp = 76.3605 \left(\frac{m_{wp}}{\rho_{ma}.\vartheta_{fc}}\right)^{-0.017526} \left(\frac{V.t}{\vartheta_{fc}^{1/3}}\right)^{-0.0220619}$ [5.6]	$131.15 < \frac{m_{wp}}{\rho_{ma}.\vartheta_{fc}} < 263.01$ $14{,}581.16 < \frac{V.t}{\vartheta_{fc}^{1/3}} < 31{,}215.96$
Wheat (BFB)	$\Delta MCp = 60.2464 \left(\frac{m_{wp}}{\rho_{ma}.\vartheta_{fc}}\right)^{0.0425184} \left(\frac{V.t}{\vartheta_{fc}^{1/3}}\right)^{-0.00808605}$ [5.7]	$25.12 < \frac{m_{wp}}{\rho_{ma}.\vartheta_{fc}} < 41.93$ $1{,}444 < \frac{V.t}{\vartheta_{fc}^{1/3}} < 2{,}565.18$

5.8 SUMMARY

In this chapter, different drying parameters were taken to find out the drying time and moisture content of agricultural products i,e paddy and wheat. In both RFB-SG and BFB dryers increase in air flow rates and inlet temperature resulted in drying rate. Consequently, the dried products had lesser percentage of damage of kernels with better quality in final product. However, air flow rate is restricted in BFB dryer to avoid entrainment of grains.

Finally a correlation was developed using Buckingham π theorem to predict the amount of moisture removed (difference in initial and final moisture content) with different parameters. The theoretical prediction agreed well with the experimental results with a deviation of ±6 - 10%. Thermo-economic analyses of different dryers are discussed in the next Chapter.

CHAPTER - 6

THERMO-ECONOMIC ANALYSIS OF DRYERS

6.1 INTRODUCTION

Energy, exergy and economic analysis of drying with RFB-SG and BFB dryers are presented in this chapter. A comparative study of energy and exergy was performed with data obtained from the experiments with different drying parameters. The energy analysis was carried out to calculate (a) the energy gain by the drying air from an electric heater, (b) energy used during moisture removal process from different inventory and air flow rate, and (c) energy utilization ratio (EUR). Similarly, exergy analysis was performed to determine the exergy of inlet drying air, outlet air and exergy utilized by the drying the chamber. Overall efficiency and drying efficiency were calculated and compared. Finally, economic analysis of the processes is presented.

6.2 THEORY OF ENERGY AND EXERGY

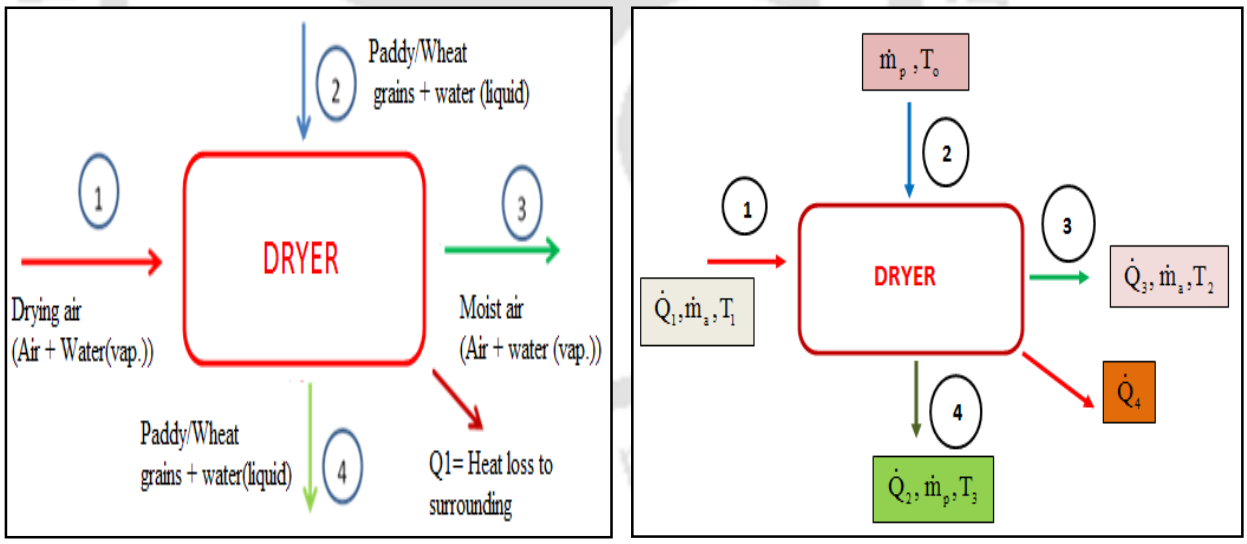

(a) **(b)**

Fig.6. 1(a) Schematic diagram of the drying process (b) Schematic diagram for energy analysis.

Figures 6.1(a)-(b) presents energy balance of the system in general. The drying chamber (vortex chamber for RFB-SG and riser for the BFB dryer) is considered as a system. Fig. 6.1(a) presents the inputs and outputs of the drying chamber. Fig.

6.1(b) depicts the mass, temperature and heat energy at each of the inlet and outlet sections.

6.2.1MASS BALANCE EQUATIONS

In the above diagram, there are three components such as product(paddy or wheat grains), drying air and water content inside the product and the drying air. The mass balance equations of the elements are given by Dincer and Sahin, (2004).

$$\text{Products: } (\dot{m}_p)_2 = (\dot{m}_p)_4 = \dot{m}_p \tag{6.1}$$

$$\text{Air: } (\dot{m}_a)_1 = (\dot{m})_3 = \dot{m}_a \tag{6.2}$$

$$\text{Water: } \omega_1 \dot{m}_a + (\dot{m}_{pw})_2 = \omega_3 \dot{m}_a + (\dot{m}_{pw})_4 \tag{6.3}$$

where $\dot{m}_a$, $\dot{m}_p$, $\dot{m}_w$ and ω are mass of air, mass of product, mass of water and water vapour, respectively.

An energy analysis of the drying of paddy grains in a RFB-SG is calculated using the equations described Celma, (2009).

The relative humidity (ϕ) is given by Celma, (2009) is

$$\phi = \frac{w\ p}{(0.622 + w)\, p_{sat,T}} \tag{6.4}$$

where w denotes the specific humidity, p is the atmospheric pressure and $p_{sat,T}$ is the saturated vapour pressure of the drying air.

The enthalpy of the drying air is given by

$$h = C_{pda}\, T_1 + w\, h_{sat,T} \tag{6.5}$$

where C_{pda} is the specific heat of the drying air and inlet temperature of the drying air is T_1 and $h_{sat,T}$ is the enthalpy of saturated vapour. The inlet and outlet temperature of the dryer is measured by thermo-sensors (Model: RTDPT100, class B). The energy gain by the inlet drying air $\dot{Q}_{1da}$ is calculated using the following equation.

$$\dot{Q}_{1da} = \dot{m}_{da} C_{pda} (T_1 - T_o) \tag{6.6}$$

where T_1 and T_o are the inlet and ambient temperature of the dryer, respectively. Energy utilized by the dryer can be calculated as

$$\dot{Q}_{dc} = \dot{m}_{da} (h_{dci,T} - h_{dco,T}) \tag{6.7}$$

where $h_{dci,T}$is enthalpy input at the inlet to the drying air and $h_{dco,T}$ is the enthalpy of the outlet air.

Similarly, energy utilization ratio can be estimated by using the following equation

$$EUR_{dc} = \frac{\dot{m}_{da} (h_{dci,T} - h_{dco,T})}{\dot{m}_{da} C_{pda} (T_1 - T_o)} \tag{6.8}$$

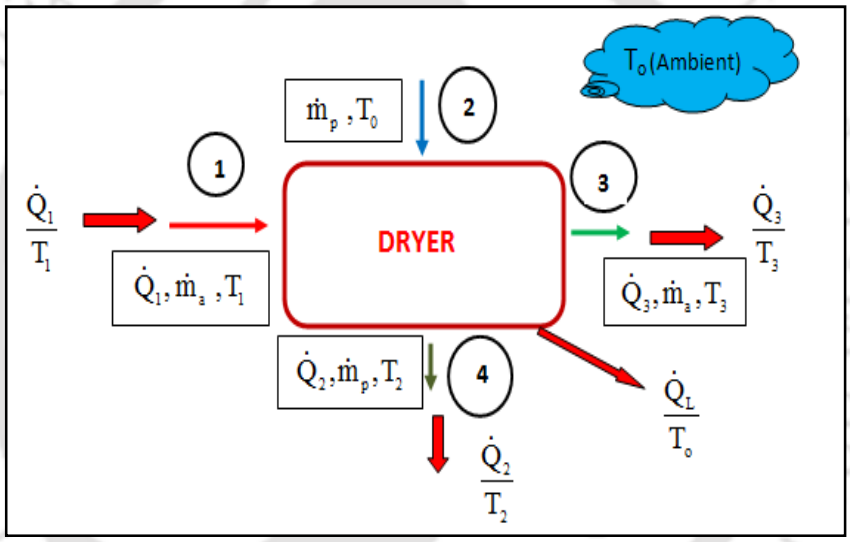

Fig.6. 2Schematic diagram of exergy analysis.

The exergy analysis of the system is based on the second law of thermodynamics. Exergy analysis deals with the evaluation of the available energy at different locations in the drying system. Heat, mass and entropy transfer with heat are shown in Fig. 6.2. Temperature at each of the inlets and outlets to the drying chamber are shown in the figure. The exergy of the system is calculated using the following equation Eq. (6.9), Nag, (2005).

$$E_x = \dot{m}_{da} c_p \left[(T_1 - T_o) - T_o \ln \frac{T_1}{T_o} \right] \tag{6.9}$$

Where E_x is exergy of the system, $\dot{m}_{da}$ is the mass of dry air, C_p specific heat of drying air, T_1 is the temperature of the drying air and T_o is the ambient temperature. Applying the Eq.(6.9), the inflow and outflow of exergy can be calculated depending on the ambient, inlet and outlet temperature of the drying chamber. So the exergy of inflow and outflow for the drying chamber are

$$\dot{E}_{x\,dci} = \dot{m}_{da}\, c_p \left[(T_{dci} - T_o) - T_o \ln \frac{T_{dci}}{T_o} \right] \tag{6.10}$$

$$\dot{E}_{x\,dco} = \dot{m}_{da}\, c_p \left[(T_{dco} - T_o) - T_o \ln \frac{T_{dco}}{T_o} \right] \tag{6.11}$$

where $T_{dci}=T_1$ and $T_{dco}=T_3$ are the input and output temperature of the drying chamber ,respectively.

Now exergy utilized can be calculated as

$$\sum \dot{E}_u = \sum \dot{E}_{Xdci} - \sum \dot{E}_{X\,dco} \tag{6.12}$$

According to exergy analysis carried out by Dincer and Sahin, (2003) for the drying process, the exergy efficiency can be defined as the ratio of exergy used for the drying the products to exergy of the processed drying air supplied the system.

Exergy efficiency is given as,

$$\eta_{ex} = \frac{\text{Exergy utilized in the evaporation of moisture in the products}}{\text{Exergy of the air sup plied}} \tag{6.13}$$

6.3 ECONOMIC ANALYSIS OF RFB-SG AND BFB DRYER

RFB-SG dryer has offered many advantages over open sun drying and also different mechanical dryers. It operates with high gravitational force. The volume of the dryer is relatively smaller compared to the BFB dryer. Drying time was also observed to be least to reach the safe moisture content. The following subsection provides an economic assessment of RFB-SG and BFB dryers.

6.3.1 COST OF DRYING

Drying of paddy/wheat grains cost depends on many factors such as depreciation, cost of interest, repair cost and opportunity cost, etc. Variable cost consists of fuel, labourer and cost of electricity. Drying cost can either be stated as annual cost or as

cost per unit of weight depending on the purpose of drying. Total drying cost comprises of fixed and variable cost as given below

where:

C_{Dr} = Total drying cost

C_F = Fixed cost

C_V = Variable cost

To determine the drying cost the following three steps are considered

1. Numerical value of input parameters
2. Determination of variable cost
3. Determination of the fixed cost

6.3.2 NUMERICAL VALUE OF INPUT PARAMETERS

A good understanding of the postharvest system is required to assign numerical value for the economic analysis **(www.knowledgebank.irri.org)**. In the present work data are estimated based on experimental investigations except for dryer life and repair and maintenance. These two data are assumed based on literature. Tables 6.1-6.2 present the numerical value of input parameters for paddy and wheat grains, respectively.

Table 6.1Assumptions for drying cost calculation for paddy

Calculation parameters	RFB-SG dryer	BFB dryer
Dryer service life	10 year	10 year
Capacity per hour	6kg	4kg
Drying time	18 minutes	45 minutes
Dryer utilization	300 days/year (paddy/ wheat)	300 days/year (paddy/ wheat)
Initial MC(db)(paddy/wheat)	50%/70%	50%/70%
Final controlled MC(db)	13-14%	13-14%
Weight after drying	3.5kg	2.4kg
Wet Paddy per 100kg (price)	1100/- (INR)	1100/- (INR)
Dry Paddy per 100kg (price)	1600/- (INR)	1600/- (INR)
Interest rate	8.5%	8.5%
Price per kWh	2.25/- (INR)	2.25/- (INR)
Unskilled Labour wage per day	150/- (INR)	150/- (INR)
Repair and maintenance	4% of investment	4% of investment

Table 6.2Assumptions for drying of wheat for cost calculation.

Calculation parameters	RFB-SG dryer	BFB dryer
Dryer service life	10 year	10 year
Capacity per hour	5kg	3kg
Drying time	38 minutes	55 minutes
Dryer utilization	300 days/year (paddy/ wheat)	300 days/year (paddy/ wheat)
Initial MC(db)(paddy/wheat)	50%/70%	50%/70%
Final controlled MC(db)	13-14%	13-14%
Weight after drying	2.15kg	1.45kg
Wet Paddy per 100kg (price)	1200/- (INR)	1200/- (INR)
Dry Paddy per 100kg (price)	2000/- (INR)	2000/- (INR)
Interest rate	8.5%	8.5%
Price per kWh	2.25/- (INR)	2.25/- (INR)
Unskilled Labour wage per day	150/- (INR)	150/- (INR)
Repair and maintenance	4% of investment	4% of investment

6.3.3 OPERATING COSTS/VARIABLE COSTS

The operating cost is that which occurs only when the dryer is actually operated. This includes the cost of labour, electricity and fuel, and some minor other costs.

$$C_{ope} = C_{electricity} + C_{labor} + C_{others} \quad (6.14)$$

where

C_{ope} = Operating cost

$C_{electricity}$ = Electricity cost

C_{labor} = Labour cost

C_{others} = Other relating cost for operation the dryer

6.3.4 FIXED COST

The fixed cost mainly comprises of the investment cost of the system which depends on dryer capacity, local content as well as state of the art technology. The use of the existing structure and local available materials can reduce the fixed cost. The installation cost depends on several factors. Thus fixed cost Mohapatra, (2012).

$$C_{Fix} = C_{repair} + C_{depr} + C_{interest} + C_{other} \quad (6.15)$$

where

C_{Fix}= Fixed cost

C_{repair} = Annual repair cost

$C_{interest}$ = Annual interest cost

C_{depr} = Annual deprecation cost

C_{other} = Other annual cost

6.3.5 PAYBACK PERIOD

A quantitative yardstick to measure the effectiveness of the system is the payback period. Payback period is based on determining the number of year required for the invested capital to be recovered. It can be calculated using the Eq.6.19.

$$N^{*} = \frac{A}{S} \tag{6.16}$$

where

N^{*} = Payback period (year)

A= Total capital cost (Rs)

S = Net annual saving cost (Rs/year)

$$S = C - B \tag{6.17}$$

C = Annual profit (cash inflow)

B = Operating cost with annual maintenance (cash outflow)

6.4 RESULTS AND DISCUSSION

6.4.1 ENERGY UTILIZED BY RFB-SG DRYER

Figures 6.3-6.4 present the energy utilized and EUR with different inlet air temperature for air flow rate from 400 to 600Nm^3/h. The bar diagrams are plotted for four different inlet air temperature, i.e. 50 to 65^0Cin a step of 5^0C increase. Results are plotted for inventories ranging from 400-600 g. These results are presented for drying of paddy grains in RFB-SG dryer.

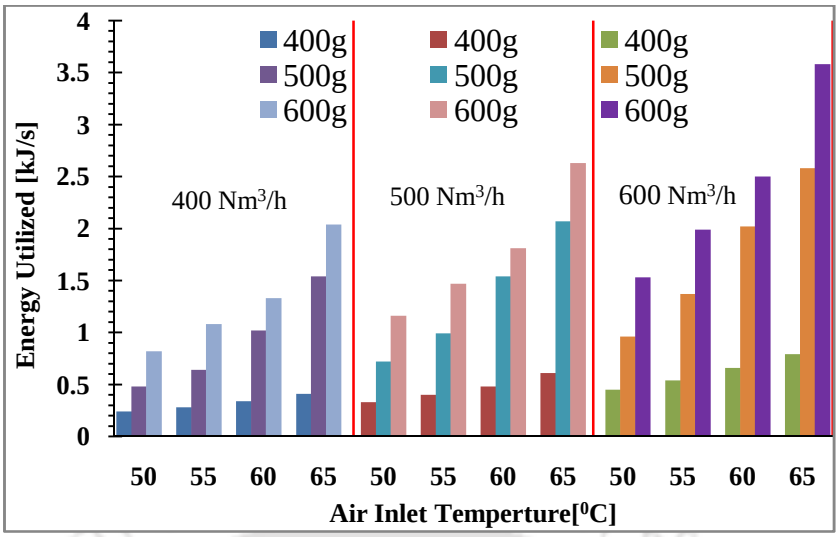

Fig.6. 3 Influence on the energy utilization of paddy drying at different drying air inlet temperature, air flow rate and inventory

It is observed from the Fig. 6.3 that the maximum value of energy utilized is 3.58 kJ/s at inlet air temperature 65^0C for drying air flow rate of 600Nm^3/h and loading of drying materials 600 g. Similarly the minimum value of energy utilized is found to be 0.24 kJ/s at inlet air temperature 50^0C with drying air flow rate 400Nm^3/h and loading of 400 g of inventory. Energy utilization is more at higher air flow rate and temperature contributing to substantial absorption of heat by the drying materials resulting in significant removal of moisture.

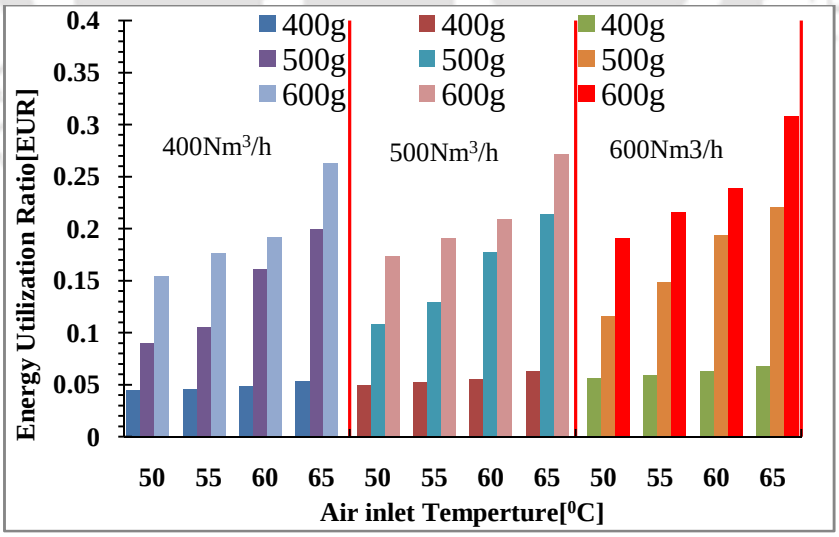

Fig.6. 4 Variation of energy utilization ratio (EUR) with inlet air temperature for paddy drying in RFB-SG dryer.

The energy utilization ratio (EUR) increases with increase in air inlet temperature, air flow rate as well as inventory as shown in Fig. 6.4.

The least value of energy utilization ratio is found to be 4.5% for air inlet temperature 50^0C, drying air flow rate 400Nm^3/h and inventory of 400 g. Similar to Fig. 6.3, the maximum value of EUR is30.8% for the air inlet temperature of 65^0C with drying air flow rate of 600Nm^3/h and 600 g of inventory. It is observed that for a constant inventory more energy is utilised at higher air flow rate and air temperature as enhancing both the heat and mass transfer rates. Effect of formation of high turbulence due to high superficial velocity of air resulted in uniform and fast drying in RFB-SG dryer.

It is further observed that the thermal energy released by the electrical heater is more effectively utilized by the drying air at high air flow rate, temperature and loading.

6.5 EXERGY ANALYIS OF RFB-SG DRYER

The exergy analysis of paddy drying in a RFB-SG was performed by using experimental data collected for different drying conditions. Here, variation of exergy utilized as well as exergy efficiencies are presented for the following experimental matrix as given in Table 6.3.

Table 6.3 Experimental Matrix for exergy analysis

Sl. No	Inventory (grams)	Air inlet Temperature (^{o}C)	Air flow rate (Nm^3/h)
1	400	50,55,60,65	400,500,600
2	500	50,55,60,65	400,500,600
3	600	50,55,60,65	400,500,600

Appendix G presents the exergy inflow and outflow for different air inlet temperature as well as air flow rates for drying of paddy grains in RFB-SG dryer. Figure 6.5 shows exergy utilized for paddy drying in a batch drying process in different drying conditions. The effect of air flow rate, air inlet temperature and different loading was observed in exergy analysis. The exergy utilized increased with increasing drying air flow rate, air inlet temperature and loading of wet materials.

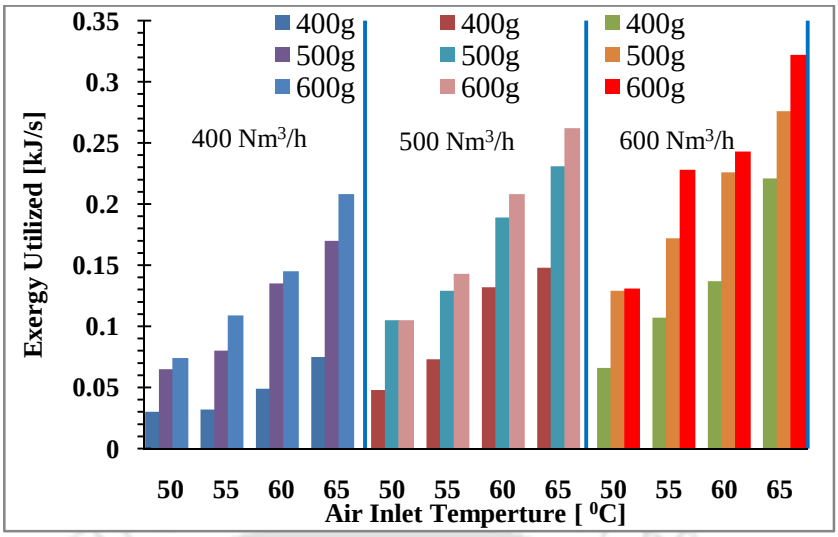

Fig.6. 5Influence on the exergy utilized of paddy drying at different conditions of drying air inlet temperature, air mass flow rate and loading

The maximum exergy utilized is 0.322 kJ/s at 600Nm^3/h air flow rate for air inlet temperature 65^{0}C and loading of 600 g inventory. It can be inferred that a large portion of supplied exergy is utilized for drying the materials. The minimum value of exergy utilized is 0.03kJ/s at 400Nm^3/h air flow rate with air inlet temperature 50^{0}C and loading 400 g. The low exergy utilisation value indicates that only a small amount of exergy is used leaving a substantial amount of energy through the outlet of the dryer. Thus there is a scope to improve the drying efficiency by reducing the energy losses

6.5.1 EXERGY EFFICIENCY

Effect of air flow rate and inlet temperature on exergy efficiency is presented in Fig. 6.6. It is observed that exergy efficiency increases with air flow rate, air inlet temperature and inventory. This is attributed to the better heat and mass transfer mechanism prevailing in RFB-SG dryer. Present results are in good comparison with Dincer and Sahin, (2004).

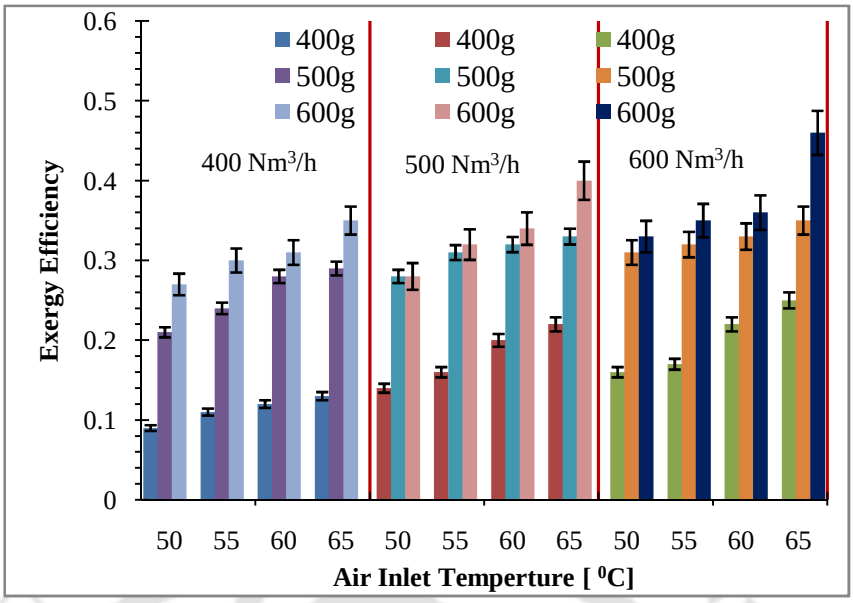

Fig.6. 6Influence on the exergy efficiency of paddy drying at different conditions of drying air inlet temperature, air mass flow rate and loading

6.6COMPARATIVE STUDY ON ENERGY ANALYSIS OF RFB-SG WITH BFB DRYER

Figures 6.7 and 6.8 present the energy utilization in paddy drying at different air flow rates and inlet air temperatures for RFB-SG and BFB dryers, respectively.

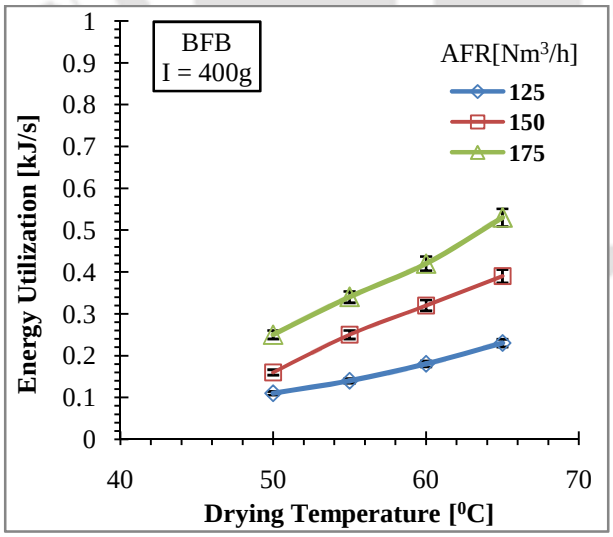

Fig.6. 7Energy utilized varies with inlet drying temperature at different air flow rate for BFB

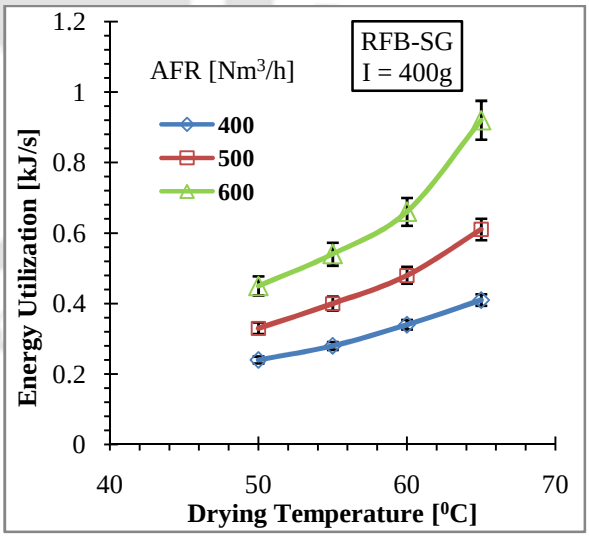

Fig.6. 8Energy utilized varies with inlet drying temperature at different air flow rate for RFB-SG

Both The figures are given for inventory of 400 g. However, air flow rate for BFB dryer is limited to a maximum of 175 Nm^3/h to avoid entrainment. It is observed from both the figures that energy utilization is higher for high air flow rate. Further, energy utilization increases with drying air temperature. In case of RFB-SG dryer the maximum value of energy utilization was 0.92kJ/s at inlet air temperature 65^0C, drying gas flow rate $600Nm^3/h$ and the minimum value of energy utilization was 0.24kJ/s at inlet air temperature 50^0C, drying gas flow rate $400Nm^3/h$ and loading of drying materials 400 g.

In case of BFB, the maximum value of energy utilization was 0.53kJ/s at inlet air temperature 65^0C, drying gas flow rate $175Nm^3/h$ and the minimum value of energy utilization was 0.11kJ/s at inlet air temperature 50^0C, drying gas flow rate $125Nm^3/h$ and loading of drying materials 400 g. For the same inlet temperature, the energy utilisation increases more rapidly with loading for RFB-SG dryer, when compared to BFB dryer as shown in Fig. 6.8.

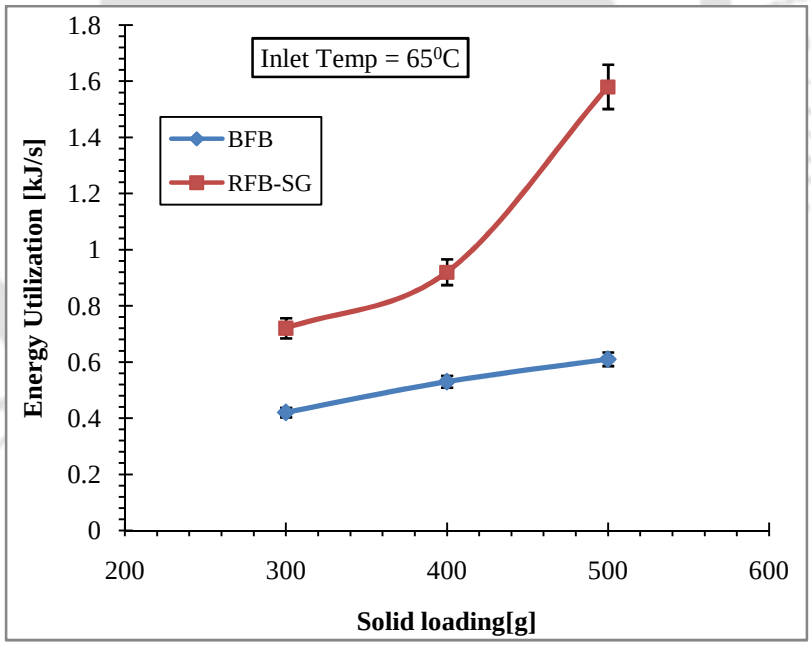

Fig.6. 9Energy utilized variation with solid loading at constant inlet temperature for RFB-SG and BFB dryer

Comparison of energy utilization with inventory loading at inlet air temperature of 65^0C is shown in Fig. 6.9. It is observed that RFB-SG dryer utilizes energy more effectively than the BFB dryer.

6.6.1ENERGY UTILIZATION RATIO (EUR)

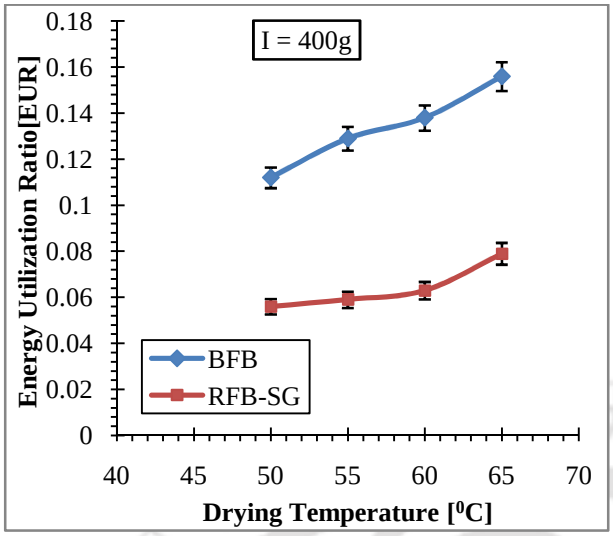

Fig.6. 10EUR varies with drying Temperature at constant inventory for both the dryer

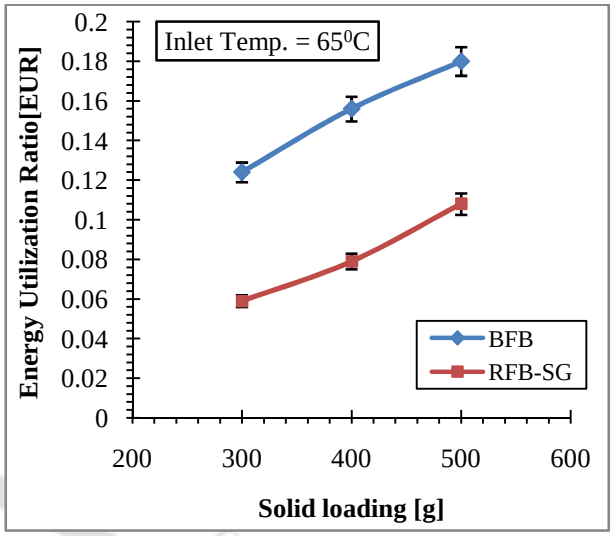

Fig.6. 11EUR varies with solid loading at constant inlet temperature for both the dryer

EUR increases with increase in inlet air temperature and loading for both the RFB-SG and BFB dryers (Figs. 6.10-6.11). However, EUR of BFB dryer is higher than that of RFB-SG dryer even though the energy utilisation values were greater for RFB-SG. This is due to the fact that the BFB dryer is operated at a lower energy input (lower air flow rate) than the RFB-SG dryer.

6.6.2EXERGY ANALYSIS

Exergy inflow for both the RFB-SG and BFB dryers are given in Appendix G. Figures 6.12 and 6.13 describe the influence on the exergy utilized for paddy drying in both the dryers. The maximum exergy utilized is 0.221kJ/s and 0.122 kJ/s with inlet air temperature of 65^{0}C and loading of 400 g for RFB-SG and BFB dryer, respectively. However, air flow rate maintained to achieve the maximum energy utilization for RFB-SG dryer is 600 Nm^3/h whereas same is found to be 175Nm^3/h for BFB dryer.

Similarly, the minimum value of exergy utilized is 0.066 kJ/s and was 0.046 kJ/s for RFB-SG and BFB dryer for inlet air temperature of 50^{0}C considering other parameters to be same that for achieving the maximum value of exergy utilization.

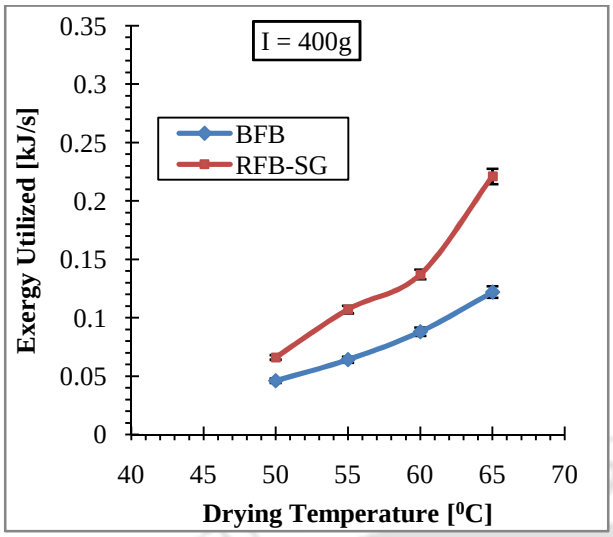

Fig.6. 12Exergy utilized variation with drying temperature at constant inventory for both the dryer

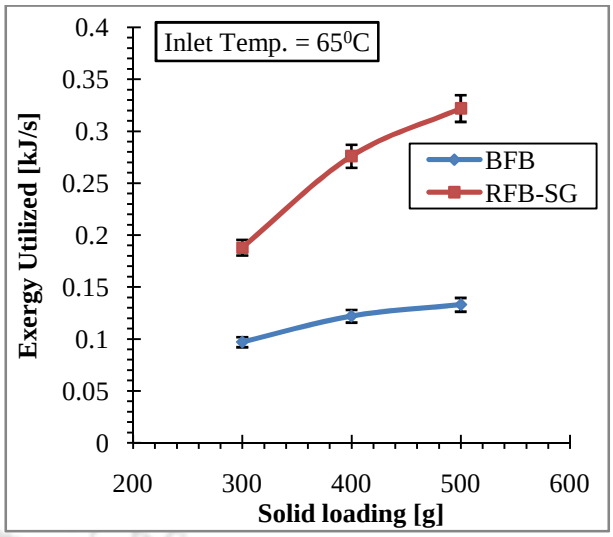

Fig.6. 13Exergy utilized variation with different inventory at constant inlet temperature for both the dryer

6.6.3 EXERGY EFFICIENCY

Figures 6.14-6.16 describe the variation of exergy efficiency for both the dryers. Effect of drying air temperature is presented in Fig. 6.14. Effect of solid loading and air flow rate are given in Figs. 6.15 and 6.16, respectively. It is observed from all the three figures that exergy efficiency is higher for BFB dryer in comparison to the RFB-SG dryer.

From Fig. 6.14, it is observed that the exergy efficiency increases with increase in inlet air temperature. The increase is 32% and 56% for BFB and RFB-SG dryer, respectively. Effect of loading on exergy efficiency is presented in Fig. 6.15. It is seen that, for an increase of 66.6% in inventory, the exergy efficiency increases by 35% and 66% for BFB and RFB dryers, respectively. From Fig 6.16, it is observed that the exergy efficiency of RFB-SG dryer increase by 169% for 50% increase of air flow rate. However, same is quite low (17% increase) for BFB dryer for increase in air flow rate by 40%.

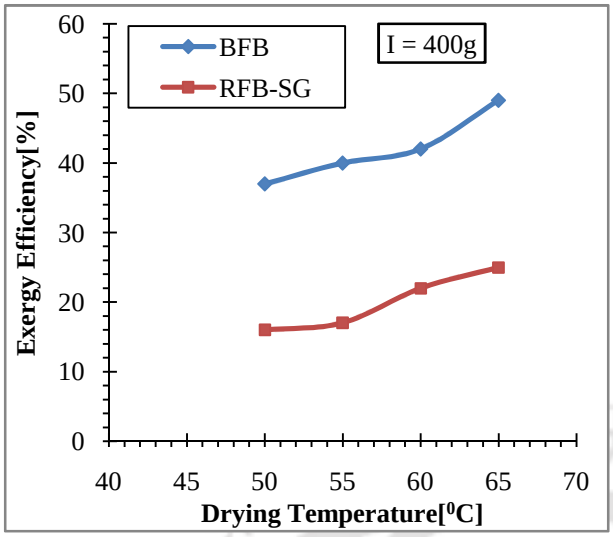

Fig.6. 14Exergy efficiency varies with drying temperature at constant inventory for both the dryer

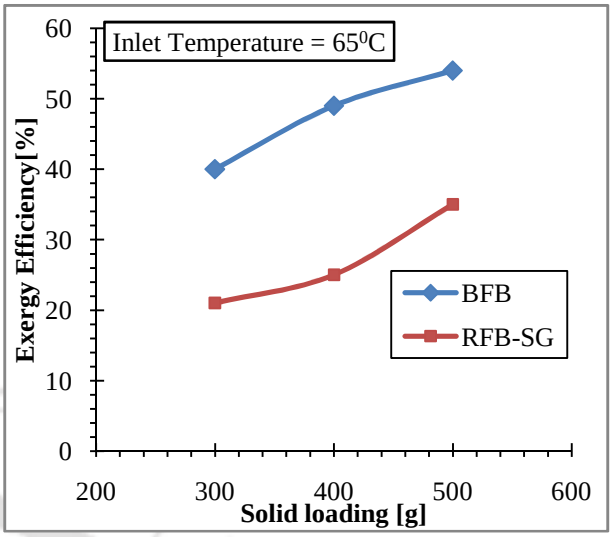

Fig.6. 15Exergy efficiency varies with solid loading at constant inlet temperature for both the dryer

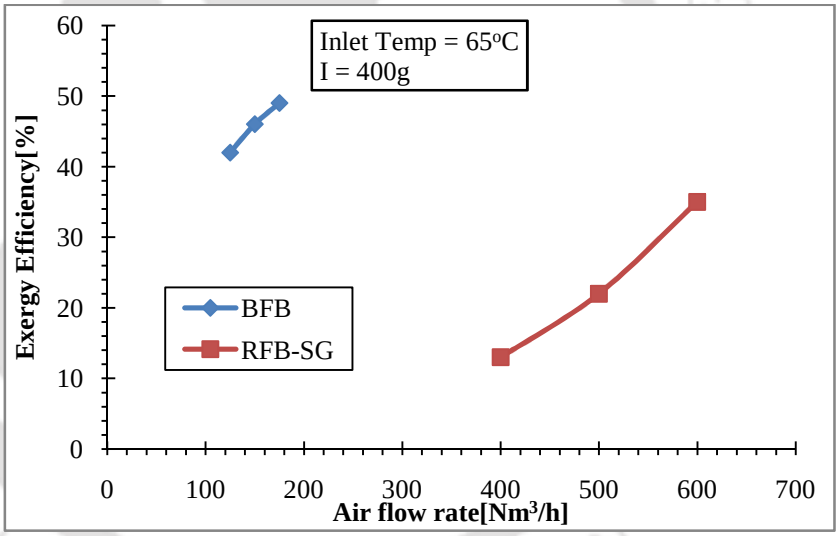

Fig.6. 16Exergy efficiency versus air flow rate at constant inventory and air inlet temperature for both the dryer

6.6.4 ECONOMIC ANALYSIS OF DRYERS

The sample calculations regarding economic evaluation of the dryers is described in Appendix H. Drying cost and payback period for both RFB-SG and BFB dryer are given in Table 6.4. It is found from the table that the drying cost per kg of paddy/wheat grains as well as the payback period for RFB-SG is lower than that of BFB dryer. Minimum payback period is found to be 2.9 years for RFB-SG dryer if utilized for drying of paddy grains alone.

Table 6.4 Drying cost per kg and payback period in year are described.

Dryer	Paddy		Wheat	
	Drying Cost per kg (Rs)	Payback Period (years)	Drying Cost per kg (Rs)	Payback Period (years)
RFB-SG	2.49	2.9	2.99	3.7
BFB	2.71	4.4	3.60	6.5

6.7 UNCERTAINTY ANALYSIS

In the present experimentation, various measuring device were used. The individual accuracies of measuring devices based on the specification provided by the manufacture and observed during the experiments are given in the Table-6.5

Table 6.5 Uncertainty values of different experimental parameters

Experimental Parameters	Uncertainty Values (%)
Air flow rate	±2
Temperature	±1.5
Air humidity	±3.7
Initial moisture content	±4.5
Final moisture content	±0.6
Inventory	±2.5 - ±4.5

By consider the individual uncertainties of the measuring device; the overall uncertainty of different experimental parameters was carried out. The detail calculations of overall uncertainty are presented in the appendix C.

6.8 SUMMARY

In the present Chapter, thermo-economic analysis of RFB-SG and BFB dryer is accomplished for drying of paddy/wheat grains. Energy utilized, energy utilization ratio, exergy utilized, exergy efficiency and overall drying efficiency are calculated. Comparisons reveal that RFB-SG dryer is superior to the BFB dryer in terms of energy and exergy utilization. From economic analysis, it is found that the drying cost and payback period is lower for RFB-SG than the BFB dryer. The conclusions and scope of the future work is described in chapter 7.

CHAPTER -7

CONCLUSIONS AND SCOPE FOR FUTURE WORK

7.1 BACKGROUND

Rotating fluidized bed in a static geometry (RFB-SG) was reported in literature for implementing processes like coating of particles and drying of hard beech wood. There is no attempt for agricultural products drying in this dryer as it has operated in high 'g' as well as centrifugal force. The present research work focus on the RFB-SG dryer to reduce the post-harvest losses of agricultural products like paddy and wheat grains and to maintain the quality of the final drying product. Parametric study on the RFB-SG dryer available at IMAP laboratory at UCL, Belgium was conducted. The experimental setup was modified to make it suitable to use for grain drying. Results obtained were compared with a BFB dryer. Paddy and wheat grains were dried from average moisture content of 48±3.8 % and 68±4.32 % to 13±0.68% and 13±0.72 % safe storage moisture content, respectively. The quality of the drying product was tested at Centre Wallon de Researches Agronomiques, Belgium. The quality in terms of nutritional value was found to be satisfactory.

7.2 CONVENTIONAL BUBBLING FLUIDIZED BED DRYER (BFB)

The experiments were done at IMAP laboratory, UCL Belgium. BFB was operated in single acceleration due to gravity 'g'. Drag force was balance with gravitational force, so drying materials were floating and behave as fluid. The fluid velocity was depending on the air flow rate. If air flow rate was increased the fluid velocity increased the minimum fluidization velocity i,e higher then terminal velocity as a result the particles are entrained by the fluid through and out of the reactor. All experiments were performed with change of different drying parameters. Different air inlet temperature, air flow rate and inventory were used to find out the drying characteristics of paddy and wheat.

- The moisture removal/drying rate were increased when air flow rate, air inlet temperature and loading of drying materials increased. The drying time was 35 minutes when air flow rate 175Nm^3/h, air inlet temperature 65^0c and

inventory 300g of paddy. In the same inlet drying condition, the drying time of wheat was 45 minutes. The initial moisture content of paddy and wheat was 48±3.8% (db) and 68±4.32% (db) decreased the safe storage final moisture content 13±0.68%, 13±0.72% respectively.

- The air inlet temperature was increased from 50^0C to 65^0C with step of 5^0C at constant 400g loading and air flow rate 175Nm^3/h. The drying time was decrease from 70 to 40 minutes (43%).
- Air flow rate was increased from 125Nm^3/h to 175Nm^3/h at constant air inlet temperature 65^0C and inventory 400g. The drying time was decreased from 55 to 40 minutes (27%).
- The inventory was increased from 300g to 500g at constant air flow rate 125Nm^3/h and air inlet temperature 60^0C. The drying time increased from 55 to 65 minutes (18%).
- Energy utilized, energy utilization ratio (EUR), exergy utilized and exergy efficiency were increase with increase of air inlet temperature, air flow rate and loading. The EUR and exergy efficiency was varied from and 5.8 – 18% and 29 to 54 %, respectively.
- Dryer efficiency of BFB dryer was 5.8% to 18% depend on different inlet parameters. Drying efficiency was 3.95% to 6.8%.
- Qualities of the drying products were satisfactory.

7.3 ROTATING FLUIDIZED BED IN A STATIC GEOMETRY (RFB-SG)

In conventional, gravitational fluidized bed, the heat, mass and moment transfer rates are limited because the gas-solid slip velocity cannot exceed the terminal velocity of the particles in the earth gravitational field. If increasing the air flow to enhance mass and heat transfer rates leads to dramatic decrease of the solid volume faction in conventional fluidized bed. The conventional fluidized bed dryer do not allow fluidizing fine or light cohesive particles because of the prevailing van der Waals forces. To deal with these issues, rotating fluidized bed in a static geometry dryer has been preferred. Rotating fluidized bed is operated in a high ‘g’ (acceleration due to gravity). This is achieved by the fast rotation of particles in a cylindrically shaped vessel or vortex chamber.

- The moisture removal/drying rate were increased when air flow rate, air inlet temperature and loading of drying materials increased. The drying time was 18 minutes when air flow rate 700Nm^3/h, air inlet temperature 65^0c and inventory 300g of paddy. In the same inlet drying condition, the drying time of wheat was 38 minutes. The initial moisture content of paddy and wheat was 48±3.8% (db) and 68±4.32% (db) decreased the safe storage final moisture content 13±0.68%, 13±0.72%, respectively.
- The air inlet temperature was increased from 50^0C to 65^0C with step of 5^0C at constant 400g loading and air flow rate 700Nm^3/h. The drying time was decrease from 40 to 20 minutes (50%).
- Air flow rate was increased from 400Nm^3/h to 700Nm^3/h at constant air inlet temperature 65^0C and inventory 400g. The drying time was decreased from 45 to 20 minutes (55%).
- The inventory was increased from 300g to 600g at constant air flow rate 600Nm^3/h and air inlet temperature 60^0C. The drying time increased from 28 to 40minutes (43%).
- Energy utilized, energy utilization ratio (EUR), exergy utilized and exergy efficiency were increase with increase of air inlet temperature, air flow rate and loading. The EUR and exergy efficiency was varied from 4.5 – 32.8% and 9 to46%, respectively.
- Dryer efficiency of RFB-SG dryer was 4.5% to 30.8% depend on different inlet parameters. Drying efficiency was 2.31% to 4.12%. Initial 5 minutes drying was very fast. The drying efficiency was 15.32% compare to 11.21% for BFB
- The RFB-SG dryer was very small volume and less drying time in compare to conventional bubbling fluidized bed (BFB). Qualities of the drying products are satisfactory.

7.4 COMPARISON OF RFB-SG WITH BFB DRYING

- A faster rate of drying was achieved with RFB-SG dryer in comparison to the BFB dryer. Drying time is 18 minute in RFB-SG dryer while same was found to be 35 minutes for BFB dryer. Thus there is decrease of 52% in drying time using RFB-SG dryer.
- Specific drying rate ($kg/m^3.s$) for RFB-SG dryer is 0.8 which is 13 times higher than the BFB dryer.
- Energy utilization was estimated to be 0.24to 3.58 kJ/s for RFB-SG dryer whereas same was found to be in the range of 0.11-0.61 kJ/s for the BFB dryer.
- Process intensification factor of RFB-SG was found to be excellent (14 to 16) in compare to BFB justifying the drying capacity of RFB-SG dryer.
- Drying efficiency for the RFB-SG and BFB dryer were found to be 4.12% and 6.8%, respectively. However, as most of the drying is completed within 5 minutes of operation, RFB-SG provides better efficiency.
- Based on the performance evaluation correlations are developed for both the dryers and specifically for paddy and wheat drying independently. These correlations can help in finding moisture removal rate without experiments. The variation of the theoretical and experimental results are within the accuracy limits of ±4% to ±8% .
- Economic analysis reveals that the cost of drying and payback period is lowest for RFB-SG dryer.

7.5 SCOPE FOR FUTURE WORK

In the present investigation, different drying parameters were taken and drying characteristics was determined. The important research findings are discussed. However, there is lot of scope for further research on RFB-SG dryer. Some of the future work is given below:

- So far the RFB-SG dryer is restricted to laboratory research. A scaled-up commercial model and work towards the same will be a novel research.
- Minimization energy and exergy loss can be studied. For more efficient use of hot air the concept of cascaded vortex chambers may be studied.
- Research with modification may be carried out for application to spray drying.
- This dryer is reported to be successful for coating of the particle. Attention may be given for its application towards pharmaceutical industry.

REFERENCES

Ambrosio-Ugri M. C. B. and Taranto O. P., (2007), "Drying in the Rotating pulsed fluidised bed",Brazilian Journal of Chemical Engineering, Vol. 24, No. 01,pp. 95 – 100.

Amer B.M.A, Hossain M.A, Gottschalk K., (2010), "Design and performance evaluation of a new hybrid solar dryer for banana", Energy Conversion and Management, Vol. 51, pp. 813–820.

Anwar S.I. and Tiwari G.N., (2001), "Convective heat transfer coefficient of crops in forced convection drying - an experimental study", Energy Conversion and Management, Vol, 42. PP. 1687-1698.

Ahmadzadeh, A., Arastoopour, H., Teymour, F., & Strumendo, M. (2008),

"Population balance equations application in rotating fluidized bed polymerization reactor" chemical engineering research and design, 86(4), 329-343.

Akpinar, E., A. Midilli, and Y. Bicer.(2003),"Single layer drying behaviour of potato slices in a convective cyclone dryer and mathematical modeling."Energy conversion and management, 44.10, pp.1689-1705.

Akpinar E. Kavak, Midilli A., Bicer Y., (2006), "The first and second law analyses of thermodynamic of pumpkin drying process",Journal of Food Engineering, Vol. 72, pp. 320–331.

Akpinar E. Kavak , Midilli A. , Bicer Y. , (2005), "Energy and exergy of potato drying process via cyclone type dryer", Energy Conversion and Management, Vol.46 , pp. 2530–2552.

Abdollahi_M, Guyy C, Chaoukiz J, (2010), "Biomass gasification in rotating fluidized bed", 13th International Conference on Fluidization - New Paradigm in Fluidization Engineering, http://dc.engcon_ntl.org/uidization xiii/89.

Akbulut, A., and Durmuş, A. (2010), "Energy and exergy analyses of thin layer drying of mulberry in a forced solar dryer" Energy, 35(4), 1754-1763.

Ayensu Akwasi (1997)**,** "Dehydration of food crops using a solar dryer with convective heat flow",Solar Energy,Vol. 59, Nos. 4-6, pp. 121-126.

Bala B. K. and Woods J. L., (1994), "Simulation of the indirect natural convection solar drying of rough Rice",Solar Energy, Vol. 53. No. 3, pp. 259-266.

Bena Benon and Fuller R. J., (2002), "Natural Convection solar Dryer with Biomass Backup heater", Solar Energy, Vol. 72, No. 1, pp. 75–83.

Basunia M.A. and Abe T., (2001), "Thin-layer solar drying characteristics of rough rice under natural Convection',Journal of Food Engineering, vol.47, pp. 295-301.

Bennamoun, L., & Belhamri, A. (2008), "Mathematical description of heat and mass transfer during deep bed drying: Effect of product shrinkage on bed porosity. Applied Thermal Engineering, 28(17), 2236-2244.

Bakker-Arkema, F. W., & Salleh, H. M. (1985). "In store drying of grain: the state of the art. ACIAR Proc. Preserving Grain Quality by Aeration & In-store Drying, 15, 24-30.

Chakraverty, A (1981). Post harvest technology of cereals, pulses and oilseeds. Oxford and IBH, Third Edition

Chakraverty, A., & Ojha, T. P. (1975). Effects of various drying air temperatures, exposure time and moisture levels of paddy on milling quality of rice. Journal of agricultural engineering.

Chungu, A. S., and V. K. Jindal. (1993) "Modeling of rough rice drying in thin vertical columns." Drying Technology, 11.6 1337-1351.

Chinenye, Ndukwu Macmanus.(2009) "Effect of Drying Temperature and drying air Velocity on the Drying Rate and Drying constant of Cocoa Bean." Agricultural Engineering International: the CIGREjournal. Manuscript 1091

Celma, A. R., & Cuadros, F. (2009). "Energy and exergy analyses of OMW solar drying process", Renewable Energy, 34(3), 660-666.

De Wilde Juray and De BroquevilleAxel (2010), "A rotating chimney for compressing

rotating fluidized beds",Powder Technology, Vol, 199, pp. 87–94.

De Wilde Juray and De Broqueville Axel, (2008), "Experimental investigation of a rotating fluidized bed in a static geometry", Powder Technology, vol. 183,pp. 426–435.

De WildeJuray and De Broqueville Axel(2007), "Rotating Fluidized Beds in a Static Geometry: Experimental Proof of Concept",AIChE *Journal* , Vol. 53, No. 4pp 793–810

Dongbang, W., Pirompugd, W., and Triratanasirichai, K. (2010)"The drying kinetics of chilies using a rotating fluidized bed technique. American Journal of Applied Sciences, 7(12), 1599-1606.

Dutta Abhishek , Ekatpure Rahul P. , Heynderickx GeraldineJ., deBroqueville Axel Marin GuyB (2010), "Rotating fluidized bed with a static geometry: Guidelines for design and operating conditions", Chemical Engineering Science, Vol.65, pp. 1678–1693.

DeBroqueville Axel, DeWilde Juray, (2009), "Numerical investigation of gas solid heat transfer in rotating fluidized beds in a static geometry", Chemical Engineering Science, Vol. 64, pp. 1232 - 1248

Diamente L. M. and Munro P. A. (1993), "Mathematical modelling of the thin layer solar drying of sweet potato slices." Solar Energy, Vol. 51(4), pp. 271–276.

Daud, W. R. W. (2008) "Fluidized bed dryers—Recent advances. Advanced Powder Technology, 19(5), 403-418"

Doungporn, Siri, Nattapol Poomsa-ad, and Lamul Wiset (2012)"Drying equations of Thai Hom Mali paddy by using hot air, carbon dioxide and nitrogen gases as drying media." Food and Bioproducts Processing 90.2: 187-198.

Dincer, I., and Sahin, A. Z. (2004)"A new model for thermodynamic analysis of a drying process. International Journal of Heat and Mass Transfer, 47(4), 645-652.

El-Sebaii A.A., Aboul-Enein S., Ramadan M.R.I., El-Gohary H.G.,(2002), "Experimental investigation of an indirect type natural convection solar dryer', Energy Conversion and Management, Vol.43, pp. 2251–2266

Ertekin, C., and O. Yaldiz. (2004)"Drying of eggplant and selection of a suitable thin layer drying model." Journal of food engineering 63.3 349-359.

Eliaers, Philippe. Pati, Jnyana R. Dutta, Subhajit., De Wilde, Juray. (2015), "Modeling and simulation of biomass drying in vortex chambers", Chemical Engineering Science, vol. 123, pp. 648-664.

Eliaers, P., and De Wilde, J. (2013), "Drying of biomass particles: experimental study and comparison of the performance of a conventional fluidized bed and a rotating fluidized bed in a static geometry. Drying Technology, 31(2), 236-245.

Forsona F.K., Nazhab M.A.A., Akuffo F.O., Rajakarunab H. (2007)**,** "Design of mixed mode natural convection solar crop dryers: Application of principles and rules of thumb",

Renewable Energy, Vol.32, pp .2306–2319.

Forson F.K**., Nazha M.A.A , Rajakaruna H.** (2007), "Modelling and experimental studies on a mixed-mode natural convection solar crop-dryer", Solar Energy , Vol.81, pp 346–357.

Froment, G. F., Bischoff, K. B., & De Wilde, J. (1990) Chemical reactor analysis and design (Vol. 2). New York: Wiley.

Gbaha P., H. Yobouet Andoha,, J. Kouassi Sarakaa, B. Kame´nan Kouab, S.Toure , (2007), "Experimental investigation of a solar dryer with natural convective heat flow", *Renewable Energy*, Vol. 32, pp. 1817–1829.

Garnavi. L., Kasiri. N., Hashemabadi. S.H. (2006), "Mathematical modelling of a continuous fluidized bed dryer", International Communications in Heat and Mass Transfer, Vol. 33, pp. 666–675.

G.-H. Qian, I. Bágyi, R. Pfeffer, H. Shaw and J. G. Stevens, (1999), "Particle mixing in rotating fluidized beds: inferences about the fluidized state", AIChE J. Vol.45, pp. 1401–1410.

G.-H. Qian, I. Bagyi, I. W. Burdick, R. Pfeffer, H. Shaw and J. G. Stevens, (2001), "Gas–solid fluidization in a centrifugal field", AIChE J. Vol.47, pp.1022–1034.

Golmohammadi, M., Assar, M., Rajabi-Hamaneh, M., and Hashemi, S. J. (2015) " Energy efficiency investigation of intermittent paddy rice dryer: Modeling and experimental study" Food and Bio products Processing, 94, 275-283.

Gidaspow, D. (1994). Multiphase flow and fluidization: continuum and kinetic theory descriptions. Academic press.

Hacıhafızog˘ lu Oktay, Cihan Ahmet, Kahveci Kamil, (2008), "Mathematical modelling of drying of thin layer rough rice",Turkeyfood and bio products processing, Vol.86, pp.268–275.

Henderson, S. M., and S. Pabis. (1961) "Grain drying theory I. Temperature effect on drying coefficient." Journal of Agricultural Engineering Research 6.3 169-174.

Hustrulid, A. (1963) "Comparative drying rates of naturally moist, remoistened, and frozen wheat." Transactions of the ASAE 6.4 304-0308.

Henderson, S. M. (1957) "Milled rice yields." California Agriculture 11.(6)15.

Izadifar, M., and D. Mowla. (2003) "Simulation of a cross-flow continuous fluidized bed dryer for paddy rice." Journal of Food Engineering 58.4 325-329.

International Rice Research Institute, (www.irri.org)

Jain Dilip, and Tiwari G.N. (2004), "Effect of greenhouse on crop drying under natural and forced convection I: Evaluation of convective mass transfer coefficient", Energy Conversion and Management, vol.45, pp.765–783.

Jain Dilip (2007), "Modelling the performance of the reversed absorber with packed bed thermal storage natural convection solar crop dryer", Journal of Food Engineering, vol.78, pp. 637–647.

Jangam V. Sachin (2011),"An overview of Recent Developments and Some R&D Challenges Related to drying of Foods", Drying technology, Vol.29, pp. 1343-1357.

Kudal H. N., Pangavhane D. R., Parishwad G. V. (2009), "Study of Photovoltaic Powered Forced Circulation Solar Tunnel Bagasse Dryer", International Journal of

Engineering Studies, ISSN 0975- 6469 ,Vol.1(4), pp. 279–293.

Karbassi A., Mehdizadeh Z. (2008)"Drying Rough Rice in a Fluidized Bed Dryer, J. Agric. Sci. Technol. Vol. 10: 233-241

Kochetov, L. M., Sazhin, B. S., & Karlik, E. A. (1969),"Experimental determination of the optimal ratios of structural dimensions in the whirl chamber for drying granular materials" Chemical and Petroleum Engineering, 5(2), 106-108.

Kunii, D. And 0. Levenspiel,(1969) Fluidization Engineering. John Wiley, 8, 44-5.

Kemp, I. C., Fyhr, B. C., Laurent, S., Roques, M. A., Groenewold, C. E., Tsotsas, E., and Kind, M. (2001). "Methods for processing experimental drying kinetics data" Drying Technology, 19(1), 15-34.

Laohavanich Juckamas and Wongpichet Seree (2008), "Thin layer drying model for gas-fired infrared drying of paddy", Songklanakarin J. Sci. Technology, Vol.30 (3), pp. 343-348.

Luangmalawat, P., Prachayawarakorn, S., Nathakaranakule, A., and Soponronnarit, S. (2008). "Effect of temperature on drying characteristics and quality of cooked rice." LWT-Food Science and Technology, 41(4), 716-723.

Levenspiel, O. (1999). Chemical reaction engineering. Industrial & engineering chemistry research, 38(11), 4140-4143.

Laohavanich, J., and Wongpichet, S. (2009). Drying characteristics and milling quality aspects of paddy dried with gas-fired infrared. Journal of food process engineering, 32(3), 442-461.

Madhlopa A. and Ngwalo G. (2007), "Solar dryer with thermal storage and biomass-backup heater", *Solar Energy*, vol. 81, pp. 449–462.

Midilli .A. and Kucuk. H. (2003)**, "**Energy and exergy analyses of solar drying process of Pistachio", Energy,Vol.28, pp 539–556.

Mujumdar, A.S. (2004), "Dehydration of Products of Biological Origin.", Science

Publishes, UK.

Ministry of Agriculture, Government of India (www.agricrop.nic.in)

Nygaard DF, and Pellett PL, (1986), "Dry Area Agriculture, Food Science and Human Nutrition", Pargamon Press.

Nitz, M., and Taranto, O. P. (2007)"Drying of beans in a pulsed fluid bed dryer: Drying kinetics, fluid-dynamic study and comparisons with conventional fluidization" Journal of Food Engineering, 80(1), 249-256.

Nakamura.Hideya, Kondo.Tetsufumi, Watano.Satoru, (2013), "Improvement of particle mixing and fluidization quality in rotating fluidized bed by inclined injection of fluidizing air", Chemical Engineering Science, Vol.91, pp. 70–78.

Nakamura H. and Watano S., (2008), "Fundamental particle fluidization behaviour and handling of nano- particles in a rotating fluidized bed", Powder Technology. Vol.186, pp 130–136.

Nag.P.K, (2008) Power plant Engineering, Tata,McGrow Hill, Third edition

Mohapatra S.S and Mahanta P, (2011), "Experimental investigation of an indirect type of natural convection dryer for thin layer paddy drying." International journal of mechanical Engg. And research, vols. 1, pp 47-54.

Mohapatra S.S and Mahanta P, (2011), "Performance Evaluation of Quality Drying in a Natural Convection Grain Dryer.", Applied Mechanics and Materials, vol.110, pp 2094-2100.

Moon, S. J., Kevrekidis, I. G., and Sundaresan, S. (2006). Particle simulation of vibrated gas-fluidized beds of cohesive fine powders. Industrial & engineering chemistry research, 45(21), 6966-6977.

Özbey, M., and M. S. Söylemez. (2005) "Effect of swirling flow on fluidized bed drying of wheat grains." Energy conversion and management 46.9 1495-1512.

Pangavhane Dilip R., Sawhney R.L., Sarsavadia P.N. (2002), "Design, development and

performance testing of a new natural convection solar dryer", Energy, Vol.27, pp. 579–590.

Prasad J., Vijay V.K., Tiwari G.N., Sorayan V.P.S., (2006), "Study on performance evaluation of hybrid drier for turmeric (Curcuma longa L.) drying at village scale", Journal of Food Engineering, Vol.75 pp 497–502.

Prommas. Ratthasak, Rattanadecho. Phadungsak , Cholaseuk .Dulyachot,(2010), "Energy and exergy analyses in drying process of porous media using hot air", International Communications in Heat and Mass Transfer, Vol.37, pp 372–378.

Pati, Jnyana R ., Hotta, Santosh K., Mahanta, P. (2015)"Effect of Waste Heat Recovery on Drying characteristics of Sliced Ginger in a Natural Convection Dryer"procedia engineering, Vol. 105, pp. 145-152

Prachayawarakorn. Somkiat, Tia .Warunee, Poopaiboon .Korakot, Soponronnarit. Somchart (2005), "Comparison of performances of pulsed and conventional fluidised-bed dryers", Journal of Stored Products Research, Vol.41, pp 479–497.

Quevedo, J., Pfeffer, R., Shen, Y., Dave, R., Nakamura, H., and Watano, S. (2006). Fluidization of nano agglomerates in a rotating fluidized bed. AIChE journal, 52(7), 2401-2412.

Ronoh E.K., Kanali C.L., Mailutha J.T., Shitanda D (2009), " Modeling Thin Layer Drying of Amaranth Seeds under Open Sun and Natural Convection Solar Tent Dryer", International: the CIGRE journal. Manuscript, Vol. XI. 1420 -1428.

Rowe D.M. and Min Gao. (1998), "Evaluation of thermoelectric modules for power generation", *Journal of Power Sources*, Vol.73 pp. 193–198

Sankat CK, (2004), "Drying Technologies For Caribbean Agro-Industry Using Solar Energy", Solar Assisted Drying Systems, Scientific and Cultural Organization –ISESCO.

Sankat CK and Castaigne F. (2004), "Foaming and drying behaviour of ripe bananas", Lebensm.-Wiss. U.-Technnology, Vol. 37, 517–525.

Shi .M.H., Hao .Y.L. , Din .Y.T.,(1998) "An Experimental Investigation on the Drying of Sliced Food Products in Centrifugal Fluidized Bed", J. of Thermal Science, Vol.7, No.3,

pp. 181-185.

Sobrino, C., Almendros-Ibáñez, J. A., Santana, D., and De Vega, M. (2008), "Fluidization of Group B particles with a rotating distributor" Powder Technology, 181(3), 273-280.

Sreekumar A, **ManikantanPE**, **Vijayakumar KP**. (2008), "Performance of indirect solar cabinet dryer", Energy Conversion & Management; Vol. 49, pp. 1388–95.

SharmaS.D., Buddhi D., Sawhney R.L., Sharma Atul, (2000), "Design, development and performance evaluation of a latent heat storage unit for evening cooking in a solar cooker",

Energy Conversion & Management, vol. 41, pp. 1497-1508.

Sharma A, Tyagi VV, Chen CR, and Buddhi D, (2009), "Review on thermal energy storage with phase change materials and applications", Renewable and Sustainable Energy Reviews, Vol. 13 (2), pp. 318-345.

Sarker, M. S. H., Ibrahim, M. N., Aziz, N. A., and Punan, M. S. (2015) "Energy and exergy analysis of industrial fluidized bed drying of paddy" Energy, 84, 131-138.

Sarsavadia, P. N., Sawhney, R. L., Pangavhane, D. R., and Singh, S. P. (1999). Drying behaviour of brined onion slices. Journal of Food Engineering, 40(3), 219-226.

Soponronnarit, S., Swasdisevi, T., Wetchacama, S., and Wutiwiwatchai, W. (2001). Fluidised bed drying of soybeans. Journal of Stored Products Research, 37(2), 133-151.

Silva-Moris, V. A., and Rocha, S. C. S. (2003). Development of a vibro fluidized bed and fluid-dynamic study with dry and wet adipic acid.Brazilian Journal of Chemical Engineering, 20(4), 423-434.

Triratanasirichai Kittichai, Dongbang Watcharin, Pirompugd Worachest, (2011), "Mathematical Modeling of Drying Characteristics of Chilies in a Rotating Fluidized Bed Technique", American Journal of Applied Sciences, Vol. 8 (10), pp.979-983.

Tabassum, M. A., and V. K. Jindal.(1992), "Effect of drying conditions on moisture removal rate and head yield of Basmati-370." Pakistan Journal of Agricultural Research,

13.4 312-319.

Waldo Rosales Trujillo, De WildeJuray (2012)'Fluid catalytic cracking in a rotating fluidized bed in a static geometry: a CFD analysis accounting for the distribution of the catalyst coke content', Powder Technology, Vol.221, pp. 36–46

Wetchacama. Somboon, Soponronnarit Somchart , Jariyatontivait .Wuttikon (2000)

"Development of a Commercial Scale Vibro-Fluidized Bed Paddy Dryer",Kasetsart J. (Nat. Sci.), Vol.34: pp 423 - 430.

Wimberly, J.E., (1983), Technical Handbook for the Paddy Rice postharvest Industry in developing countries", International Rice Research Institute,Philippines.

Wongpornchai, S., Dumri, K., Jongkaewwattana, S., and Siri, B. (2004) "Effects of drying methods and storage time on the aroma and milling quality of rice (Oryza sativa L.)", Food chemistry, 87(3), 407-414.

Wen, C. Y., and Yu, Y. H. (1966),"A generalized method for predicting the minimum fluidization velocity", AIChE Journal, 12(3), 610-612.

Yadollahinia, A. R., M. Omid, and S. Rafiee.(2008), "Design and fabrication of experimental dryer for studying agricultural products." Int. J. Agri. Bio, 10 61-65.

Y.A.Cengal and M.A.Boles, (2006), Thermodynamics: an Engineering Approach, McGraw Hill (Fifth edition).

Chen, Y. M. (1987),"Fundamentals of a centrifugal fluidized bed". AIChE journal, 33(5), 722-728.

Zaman, M.A., Bala, B.K.,(2001), " Thin layer solar drying of rough rice" Journal of

Food Eng. 47(4), 295-301.

Appendix A

Specifications of Various Equipments Used

Centrifugal type of blower with high pressure is used. It was installed to supply air to the vortex chamber/riser to fluidize the solids particles and other instruments are used for experimentation described below.

Specification of Blower

Robuschi Benelux B.V. 6956 AX spankeren

Air Capacity: 1200Nm^3/h

Pressure difference- : 800mbar

Power Consumption- : 45kw; (3×380V)

Mass flow controller
Bronkhorst Model F-106EI

Gefran, Olen, Blegium

Accuracy : ±0,5% Rd plus ±0,1% FS

Settling time: standard: 1...2 seconds

Operating temp. : -10...+90°C

Power supply : +15...24 Vdc

Material : stainless steel 316L

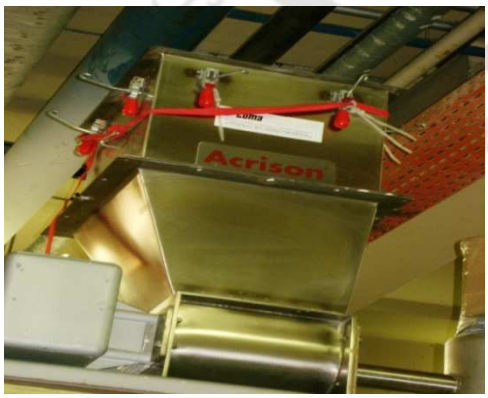

Acrison model AI-105-00 (Screw feeder)

TBMA, Woldelgem, Belgium

Model Ref : 105-00

Inlet mm : 165 x 200

Std DC Motor kW: 0.37

Approx. Kgs : 90

Feed Range l/h : 0.5-980

PT 100(RTD Class B) (Thermo sensor)

Range : 50^0C - 400^0C

Precission : ±0.3^0C

Tip length: 10cm(3.9inches)

Tip diameter: 5mm/0.2"

Max temperature : 400^0C Tip/ 280^0C wire

It is a 3 wires probe.

GEFRAN BV-25, BV-50 (Pressure Probe)

Ranges : 0 - 0.05 bar to 0 - 60 bar

Operating temp. range : -20 - 85°C

Accuracy: ± 0.15% FSO typical

Fill Fluid: silicone oil

Sartorius, (Weighing Mechine)
Vilvoorde, Belgium

Model-F61S-D2

Model-F300S-D2

Std deviation : ±0.01g

Linearity : ±0.03 g

METTLER(Physical Balance)
Type- AE260s

Delta Range , V(100-120,200-220)

Weighing capacity : 50mg - 250g

Pan size : 8 cm diameter

Precision : ± .1mg

KAMENEV Liege, (Electric Heater)

Belgium (Electric resistance)

Power : 12kw(3×380)

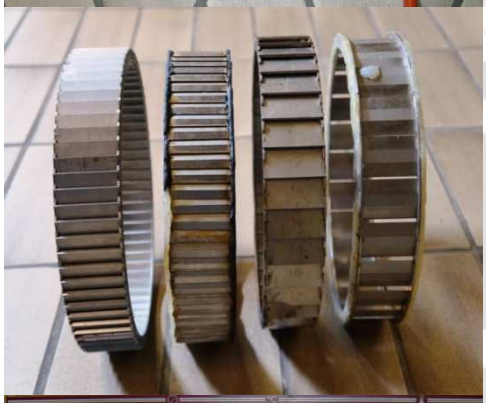

Rings placed inside the Vortex chamber

No of slots and size

72 ×0.2mm

36× 0.5mm

24 ×3mm

GFL-7104, D3006(Furnace)

Burgweldel

Power supply : Volt -240, 50Hz

A=3.4, 0.75kw

Fastime 01 (Stop watch)

Weighing : 37g

Accuracy : ±0.01second

Appendix B

Modification of the chimney of RFB-SG dryer

The chimney of the vortex chamber was 7cm in diameter. When the system operated with the air flow rate 600Nm3/h, the velocity of air passed through the chimney was 51.8m/s. In this condition, there is lots of paddy and wheat particles lost by the chimney. Initially, the size of the chimney was reduced to 5cm and the velocity of air passed through the chimney reached to 100.47 m/s. In this case, the particle lost by the chimney was decreased but it not totally illuminated. Finally, the area of the chimney was maintained constant as it was with 7cm diameter chimney but was replaced with 5cm diameter using 12 holes perforated plate and each hole has 12mm diameter. Now, the loss of particles during drying is very less compare to previous case.

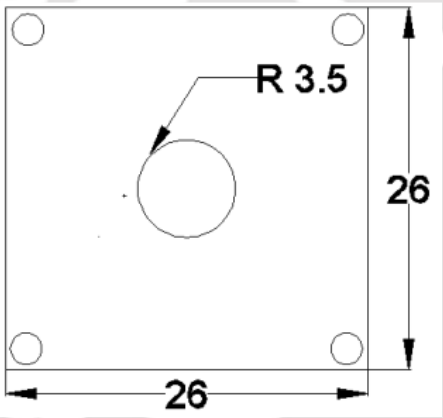

B1(a) Chimney of the vortex chamber with 3.5cm radius

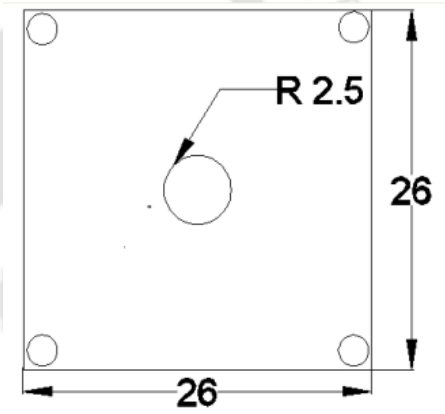

B1(b) Chimney of the vortex chamber with 2.5cm radius after decreasing

After modification the vortex chamber chimney with 13 holes contents 0.6 mm radius.

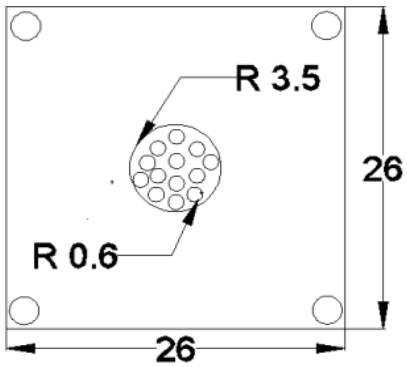

Fig. B.2: Schematic of chimney for RFB-SG with modification

Appendix C

Uncertainty Analysis

Uncertainty analysis also measure the 'goodness' of a result and without such a measurements, it is impossible to judge the fitness of the value as a basis for making decision relating to health, safety, commerce or scientific excellence. Some form of analysis must be performed on all the experimental data. The analysis may be a simple verbal appraisal of the results or it may take the form of complex theoretical analysis of the error involved in the experiment and matching of the data with fundamental physical principle. A method of estimating uncertainty in experimental has been presented by [Moffat,(1985)]. The method is based on careful specification of the uncertainty in the various primary experimental measurements at different experimental setup. For example, a certain pressure reading might be expressed as

$$P = 100kN/m^2 \pm 1kN/m^2 \qquad (C.1)$$

Here, ± notation is used to designate the uncertainty; the designation is stating the degree of accuracy with which the measurements has been made. Suppose a set of measurements is made than, the uncertainty in each measurement may be expressed with the same odds. These measurements are used to calculate some desired results of the experiments, to estimate the uncertainty in the calculated results on the basis of the uncertainty in the primary measurements. The results R are a given function of the independent variable x_1, x_2, x_3, x_4....x_n. Thus

$$R = R(x_1, x_2, x_3, x_4....x_n) \qquad (C.2)$$

Let w_R be the uncertainty in the results and w_1, w_2,w_3...w_n be the uncertainty in the independent variables. If the uncertainties in the independent variables are all given with the same odds, then the uncertainty in the results having these odds is given as,

$$W_R = \left[\left(\frac{\partial R}{\partial X_1} W_1 \right)^2 + \left(\frac{\partial R}{\partial X_2} W_2 \right)^2 + ... + \left(\frac{\partial R}{\partial X_n} W_n \right)^2 \right]^{1/2} \qquad (C.3)$$

In the experimental investigations, uncertainty assessment deals with the accuracies involved in the instruments and subsequently its effects in the global measurements.

The instruments used in the present investigation include thermo-sensor, moisture sensor, mass flow controller, physical balance, moisture content and electric heater.

Calculation of Moisture Content

Moisture content is calculated (Zaman and Bala(2001), IRRI, (2005) as follows

$$MC_{wb} = \frac{m_i - m_f}{m_i} \times 100 \quad \text{(C.4)}$$

This is for weight basis moisture content calculation.

Similarly for dry basis MC

$$MC_{db} = \frac{m_i - m_f}{m_f} \times 100 \quad \text{(C.5)}$$

where m_i is initial weight of particles before drying, m_f is the final weight after drying. MC_{wb} and $MC_{db}$are the moisture content of weight basis and dry basis respectively.

$$MC_{db} = f(W_f, W_i)$$

Therefore, uncertainty in moisture measurement Bekweith et al.,(2003)

In percentage= $\frac{Error}{MC_{db}} \times 100\%$

$$= \pm 100 \times \sqrt{\left(\frac{a_1}{W_f}\right)^2 + \left(\frac{a_2}{W_i}\right)^2}$$

Here, a_1 and a_2 are uncertainties associated with independent variables W_f and W_i, respectively.

For paddy bed inventory of 500g

W_i =500±8g, a_2 = ±8g

W_f= 298±6g, a_1= ±6g

Thus uncertainty of moisture content percentage is

$$= \pm 100 \times \sqrt{\left(\frac{6}{298}\right)^2 + \left(\frac{8}{500}\right)^2} = \pm 2.87\%$$

Similarly, other loading of paddy and wheat inside the Vortex chamber of RFB-SG dryer and riser of BFB dryer are calculated. The average value of overall uncertainty of different instruments data are presented in the Table 1.

Table 1: Uncertainty values of different experimental parameters

Experimental Parameters	Uncertainty Values (%)
Air flow rate	±2
Temperature	±1.5
Air humidity	±3.7
Initial moisture content	±4.5
Final moisture content	±0.6
Inventory	±2.5- ±4.5

Appendix D

Calibration of Screw feeder for paddy feeding system

The screw feeder is used for feeding of the paddy inside the vortex chamber of the RFB-SG. There are different dosing parameters for feeding of paddy gram per second. Fig. A.3 presents the calibration curve of paddy feeding via screw feeder.

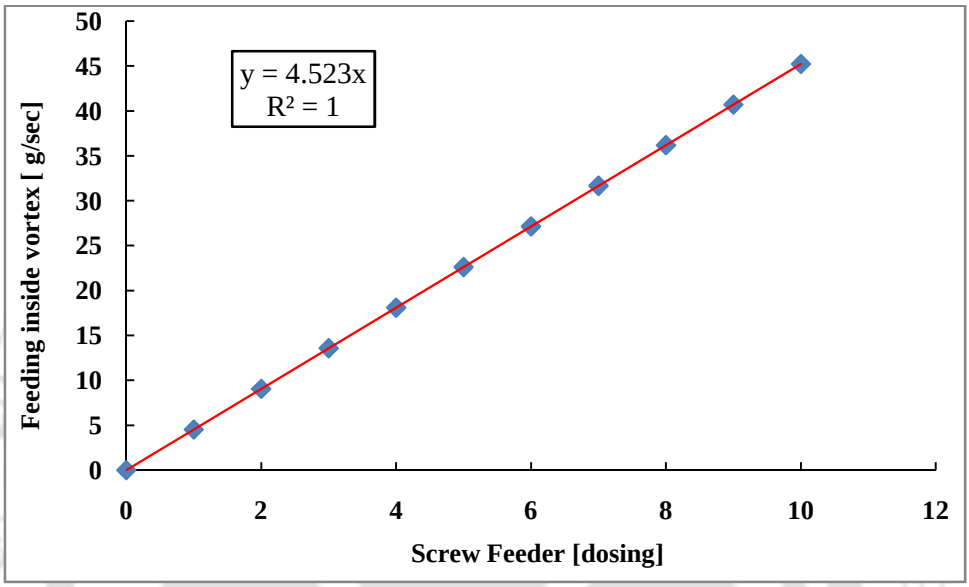

Fig. D.1 Paddy feeding calibration curve

The screw feeder is content 1 - 10 dosing system and different dose send different gram/second paddy inside the drying chamber. For requirement of sample, different time is required for particular measurement of feeding. This time period and dosing are introduced inside the labview program. PID controller and labview program are running to give fixed amount of paddy like 300 – 600g send inside the vortex chamber of RFB-SG with 1.5 bar external pressure. In this case, the feeding is depends 10 dosing with 45.23 g/sec with different time for different inventory.

Calibration of Screw feeder for wheat feeding system

The screw feeder is used for feeding of the wheat inside the vortex chamber of the RFB-SG. There are different dosing parameters for feeding of wheat gram per second. Fig. A4 presents the calibration curve of wheat feeding via screw feeder.

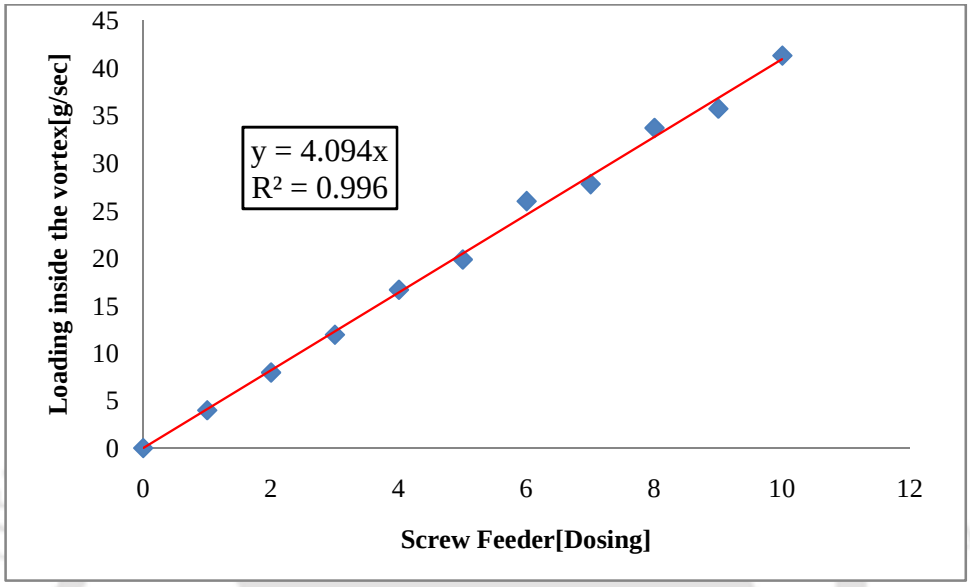

Fig. D.2 Wheat feeding calibration curve

The screw feeder is content 1 - 10 dose and different dose send different gram/second paddy inside the drying chamber. For requirement of sample, different time is required for particular measurement of feeding. This time period and dosing are introduced inside the labview program. PID controller and labview program are running to give fixed amount of paddy like 300 – 600g send inside the vortex chamber of RFB-SG with 1.5 bar pressure. In this case, the feeding is depends 10 dosing with 41.31 g/sec with different time for different inventory

Appendix E

Calibration of PT 100 - type Thermo-sensor

Calibration of thermo-sensor is done using the water circulating bath. The ambient temperature is taking as reference temperature. The water circulating bath temperature is varied and measured by thermo sensor. The water is heated to a temperature upto 100^0C and then cooled back to room temperature. A high precision multi-meter is connected in the circuit to see the emf generation. In every 5^0C, the increase of water temperature the emf (mili volts) generation is recorded during both heating and cooling. Following data has been obtained.

Table E.1 Data are collected in every 5^0C increase temperature

Sl. No.	Voltage in mV (Y_i)	water Temperature,^{0}C	Reference Temperature,^{0}C	Temperature Difference (X_i)
1	0.025	16.82	16	0.82
2	0.05	20	16	4
3	0.07	25	16	9
4	0.14	30	16	14
5	0.33	35	16	19
6	0.56	40	16	24
7	0.85	45	16	29
8	1.05	50	16	34
9	1.2	55	16	39
10	1.39	60	16	44
11	1.57	65	16	49
12	1.74	70	16	54
13	1.92	75	16	59
14	2.05	80	16	64
15	2.27	85	16	69
16	2.45	90	16	74
17	2.48	95	16	79
18	2.59	100	16	84
Total	$\sum Y_i$ = 22.735			$\sum X_i$ = 748.82

Also, $\sum X_i^2 = 43112.67$, $\sum Y_i^2 = 43.04$, $(\sum X_i)^2 = 560731.39$, $(\sum Y_i)^2 = 516.88$, $\sum X_i Y_i = 1357.611$, N = 18 data points

Using regression analysis,

$$A = N \sum X_i Y_i - (\sum X_i \times \sum Y_i) / N \sum X_i^2 - (\sum X_i)^2 = 0.034$$

$$B = \sum Y_i \times \sum X_i^2 - (\sum X_i Y_i \times \sum X_i) / N \sum X_i^2 - (\sum X_i)^2 = -0.168$$

As $Y = a X + b$, $Y = 0.034 X - 0.168$

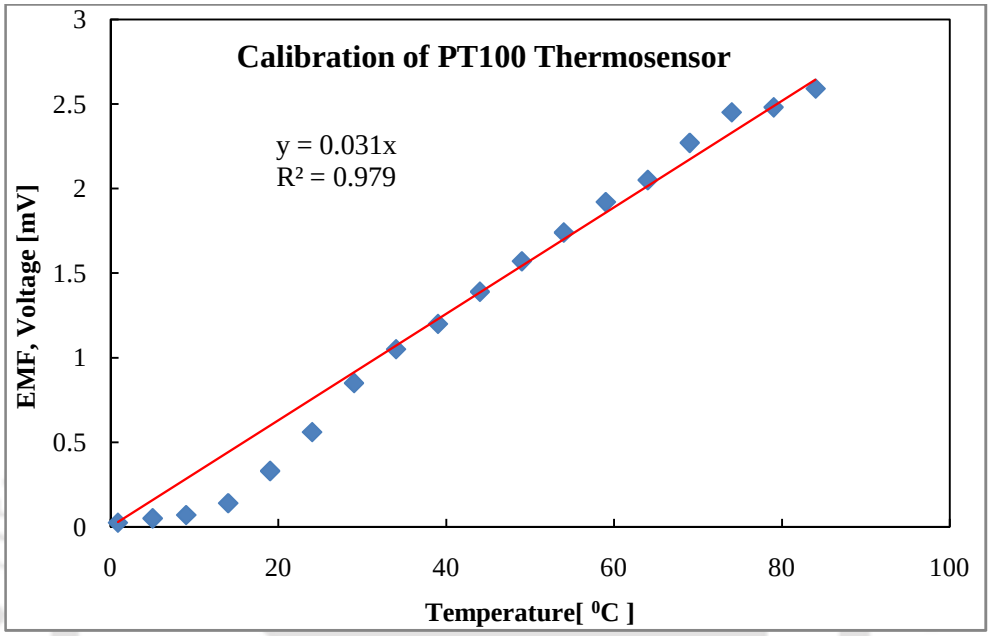

Fig. E.1 Calibration of Thermocouple

Appendix F

Rayleigh's Method to Obtain Non-dimensional Numbers and Developed Correlations

1. Rotating fluidized bed in a Static geometry (RFB-SG)

For RFB-SG dryer, let us take ΔMCp is the difference moisture content of initial and final of the paddy/wheat grains. This is the function of the parameters like density of moist air (ρ_{ma}), volume of the fluidization chamber (ϑ_{fc}), velocity of the fluidizing air(V), drying time(t), temperature of the inlet fluidizing air(T_a),moisture of the ambient air(ϕ_{am}), density of dry air($\rho_{da,}$), density of dry paddy grain(ρ_{dp}), moisture of the wet paddy(ϕ_{wp}) and mass of the wet paddy(m_{wp}).

Now the $\Delta MCp = f(\rho_{ma}, t, V, m_{wp}, \vartheta_{fc})$

Where $\rho_{ma} = f(T_a, \phi_{am}, \rho_{da})$

$\rho_{ma}$is the density of the moist air.

$$\Delta MCp = C\, \rho_{ma}^{a} t^{b} V^{c} m_{wp}^{d} \vartheta_{fc}^{e} \qquad \text{(F.1)}$$

where 'C' is constant.

Expressing the quantities in terms of fundamental dimensions are M, L and T.

$$M^{o}L^{o}T^{o} = (ML^{-3})^{a}(T)^{b}(LT^{-2})^{c}(M)^{d}(L^{3})^{e}$$

For dimensional homogeneity, a, b, c, d, and e terms value should be calculated. These values are putting the equation F.1. According the above equation, there are two π terms are produced.The final correlation is derived as

$$\Delta MCp = C\left[\frac{m_{wp}}{t^{3}\rho_{ma}V^{3}}\right]^{a}\left[\frac{V\,t}{\vartheta_{fc}^{1/3}}\right]^{b} \qquad \text{(F.2)}$$

In the similar way Rayleigh method has been used to obtain the non-dimensional numbers used in the correlation for RFB-SG (Ref. chapter 5, eq. 5.3) and also for correlations on BFB dryer for paddy and wheat grain drying.

2. Use of Findfit Function of Mathematica Version 5.2 to Obtain the Exponents of Non-dimensional Numbers

2.1 Correlation for RFB-SG (Paddy)

Steps to follow

In Mathematica 5.2, using following information, data.

Table F.1

ΔMC_P	V	m_{wp}	t	ϑ_{fc}	ρ_{ma}
35.51	36.41	0.3	65	0.00226	1.00924007
40	37.03	0.3	55	0.00226	1.01193027
39.28	37.65	0.3	45	0.00226	1.00911274
39.35	38.27	0.3	40	0.00226	1.00894864
39.61	36.41	0.4	70	0.00226	1.01235884
38.84	37.03	0.4	60	0.00226	1.00938816
39.61	37.65	0.4	50	0.00226	1.01130613
37.88	38.27	0.4	45	0.00226	1.01121285
Table F.1 Cont….					
38.24	36.41	0.5	75	0.00226	1.00880762
33.81	37.03	0.5	65	0.00226	1.00960074
35.18	37.65	0.5	55	0.00226	1.00921752
35.93	38.27	0.5	48	0.00226	1.00853525
34.79	36.41	0.6	80	0.00226	1.00913201
35.18	37.03	0.6	70	0.00226	1.00928181
33.46	37.65	0.6	60	0.00226	1.00921752
35.5	38.27	0.6	50	0.00226	1.00946463
34.66	45.52	0.3	60	0.00226	1.00956404
35.83	46.29	0.3	50	0.00226	1.00960074
38.82	47.06	0.3	35	0.00226	1.00869328
40.23	47.83	0.3	30	0.00226	1.00863865
37.73	45.52	0.4	65	0.00226	1.00956404
38.06	46.29	0.4	55	0.00226	1.00949447
35.59	47.06	0.4	40	0.00226	1.00900792
33.59	47.83	0.4	35	0.00226	1.00884534
33.01	45.52	0.5	70	0.00226	1.00945608
33.1	46.29	0.5	60	0.00226	1.00896257
35.82	47.06	0.5	45	0.00226	1.00848335
38	47.83	0.5	38	0.00226	1.00997979
36.75	45.52	0.6	75	0.00226	1.01042645
36.9	46.29	0.6	65	0.00226	1.01066164
35.72	47.06	0.6	50	0.00226	1.01047229

38.68	47.83	0.6	40	0.00226	1.01069965
33.91	54.62	0.3	45	0.00226	1.00913201
33.68	55.55	0.3	38	0.00226	1.00928181
36.98	56.48	0.3	28	0.00226	1.01109787
40.29	57.4	0.3	22	0.00226	1.00977382
38.56	54.62	0.4	50	0.00226	1.00945608
35.65	55.55	0.4	40	0.00226	1.00917543
34.67	56.48	0.4	30	0.00226	1.00953166
36.97	57.4	0.4	26	0.00226	1.01039133
32.63	54.62	0.5	55	0.00226	1.00967196
39.01	55.55	0.5	50	0.00226	1.0105557
36.16	56.48	0.5	35	0.00226	1.01015904
36.58	57.4	0.5	28	0.00226	1.00997979
33.21	54.62	0.6	60	0.00226	1.00848293
35.63	55.55	0.6	55	0.00226	1.01076755
40.05	56.48	0.6	40	0.00226	1.01088947
37.79	57.4	0.6	32	0.00226	1.01090502

After using these values, two π terms values are derived and putting the values in Mathematica 5.2 software.

data={{131.5280348,18034.24184,35.51},{131.17837,15519.59041,40},{131.544631,12910.44904,39.28},{131.5660264,11664.93457,39.35},{174.8304484,19421.49121,39.61},{175.3449845,16930.46226,38.84},{175.0124367,14344.94338,39.61},{175.0285819,13123.05139,37.88},{219.3073616,20808.74058,38.24},{219.1350787,18341.33412,33.81},{219.2182892,15779.43772,35.18},{219.3665896,13997.92149,35.93},{263.0842382,22195.98995,34.79},{263.0451899,19752.20597,35.18},{263.061947,17213.93206,33.46},{262.9975523,14581.16821,35.5},{131.4858272,20812.16965,34.66},{131.4810472,17636.85071,35.83},{131.599333,12551.1587,38.82},{131.6064613,10934.16163,40.23},{175.3144363,22546.51712,37.73},{175.3265188,19400.53578,38.06},{175.4110609,14344.18137,35.59},{175.4393302,12756.5219,33.59},{219.1664815,24280.86459,33.01},{219.2736814,21164.22085,33.1},{219.377879,16137.20404,35.81},{219.0528362,13849.93806,38},{262.7472056,26015.21206,36.75},{262.6860609,22927.90592,36.9},{262.7352867,17930.22671,35.72},{262.6761833,14578.88217,38.68},{131.5421191,18729.58106,33.91},{131.522595,16085.38698,33.68},{131.2863639,12050.81926,36.98},{131.4585105,9622.732804,40.29},{175.3331852,20810.64562,35.56},{175.3819452,16931.98629,

35.65},{175.3200589,12911.59207,34.67},{175.1708911,11372.32059,36.97},{219.1196216,22891.71018,32.67},{218.9279988,21164.98287,39.01},{219.0139655,15063.52408,36.16},{219.0528362,12247.11448,36.58},{263.2535653,24972.77474,33.21},{262.6585377,23281.48115,35.63},{262.6268572,17215.45609,40.05},{262.6228174,13996.70226,37.79}}

expr=C*X^a*Y^b

X^aY^bC

pars={C,a,b}

{C,a,b}

vars={X,Y}

{X,Y}

fit=FindFit[data,expr,pars,vars,MaxIterations→1000]

{C→104.509, a→-0.0227354,b→-0.0959066}

exprfitted = expr/.fit

$$\frac{104.509}{X^{0.0227354}\,Y^{0.0959066}}$$

replacerule[dat_]:=Table[vars[[i]]→data[[dat,i]],{i,Length[vars]}]

Table[{Last[data[[i]]],exprfitted/.replacerule[i],Last[data[[i]]]-exprfitted/.replacerule[i]},{i,Length[data]}]

After running this programming, experimental ΔMC and theoretical ΔMC will producethe results.

The results are given below.

{35.51,36.5418,1.03177},{40,37.0741,2.92589},{39.28,37.732,1.548},{39.35,38.1008,1.24923},{39.61,36.049,3.56103},{38.84,36.5242,2.31576},{39.61,37.111,2.49903},{37.88,37.4291,0.450889},{38.24,35.6272,2.61284},{33.81,36.0617,2.25169},{35.18,36.5855,1.40548},{35.93,37.0077,1.07768},{34.79,35.2611,0.47111},{35.18,35.6579,-0.477917},{33.46,36.1314,-2.67136},{35.5,36.7114,-1.21136},{34.66,36.0434,-1.38338},{35.83,36.6202,0.790241},{38.82,37.8339,0.986084},{40.23,38.3376,1.89236},{37.73,35.5346,2.19543},{38.06,36.0504,2.00962},{35.59,37.1092,1.51924},{33.59,37.5289,3.93894},{33.01,35.1043,2.09427},{33.1,35.5694,2.46945},{35.81

,36.5063,0.696294},{38,37.0466,0.953369},{36.75,34.7293,2.02073},{36.9,35.1528,1.74722},{35.72,35.9914,0.271384},{38.68,36.7129,1.96707},{33.91,36.4093,2.49934},{33.68,36.9448,3.2648},{36.98,37.9839,1.00387},{40.29,38.8113,1.47871},{35.56,35.8086,0.24857},{35.65,36.5237,0.873746},{34.67,37.4861,2.81605},{36.97,37.946,0.975957},{32.67,35.3034,2.63335},{39.01,35.5706,3.4394},{36.16,36.7495,0.589541},{36.58,37.4862,0.906205},{33.21,34.8642,1.65422},{35.63,35.1013,0.528697},{40.05,36.1324,3.91758},{37.79,36.8569,0.933126}}

2.2 Correlation for BFB (paddy)

data={{25.116013,1716.346561,32.6},{25.10829919,1513.196137,40.1},{25.11883993,1302.139317,39.63},{25.11131402,1203.529003,38.63},{33.49865347,1830.769665,36.46},{33.49865719,1629.595839,38.96},{33.48835161,1420.515619,40.5},{33.4783742,1323.881903,38.69},{41.83790992,1945.19277,35.63},{41.86895638,1745.995542,35.45},{41.86473322,1538.89192,36.22},{41.8775699,1444.234803,37.83},{25.10539655,1924.767916,34.01},{25.0952589,1676.155721,36.95},{25.10597229,1420.954863,35.5},{25.10371786,1320.36795,36.29},{33.48093595,2062.251339,38.65},{33.47773226,1815.835364,39.91},{33.47120373,1563.050349,40.37},{33.48175203,1467.0755,37.66},{41.86888276,2199.734761,38.07},{41.83846494,1955.515007,38.64},{41.84757188,1705.145835,38.62},{41.85725968,1613.783005,40.32},{25.11867062,2084.213547,36.25},{25.10568839,1794.971266,36.15},{25.10597229,1492.332039,38.08},{25.11131402,1179.150952,38.85},{33.47386207,2244.537666,40.45},{33.47773226,1958.150472,39.8},{33.50210225,1658.14671,38.67},{33.51562711,1347.601088,35.05},{41.83349459,2404.861785,35.75},{41.8908049,2121.329678,34.23},{41.88193051,1823.961381,38.08},{41.89028957,1516.051224,38.67}}

expr = C*X^a*Y^b

X^aY^bC

pars={C,a,b}

{C,a,b}

vars={X,Y}

{X,Y}

fit = FindFit[data,expr,pars,vars,MaxIterations→1000]

{C→57.6895,a→0.0530522,b→-0.0824617}

exprfitted = expr/.fit

$$\frac{57.6895\, X^{0.0530522}}{Y^{0.0824617}}$$

replacerule[dat_]:=Table[vars[[i]]→data[[dat,i]],{i,Length[vars]}]

Table[{Last[data[[i]]],exprfitted/.replacerule[i],Last[data[[i]]]-exprfitted/.replacerule[i]},{i,Length[data]}]

After running this programming, experimental ΔMC and theoretical ΔMC will produced results.

Table F.2

ΔMC_P	V	m_{wp}	t	ϑ_{fc}	ρ_{ma}
32.6	5.21	0.3	75	0.0118	1.01225178
40.1	5.3	0.3	65	0.0118	1.01256276
39.63	5.39	0.3	55	0.0118	1.01213786
38.63	5.48	0.3	50	0.0118	1.0124412
36.46	5.21	0.4	80	0.0118	1.01193038
38.96	5.3	0.4	70	0.0118	1.01193027
40.5	5.39	0.4	60	0.0118	1.01224167
38.69	5.48	0.4	55	0.0118	1.01254335
35.63	5.21	0.5	85	0.0118	1.01278676
35.45	5.3	0.5	75	0.0118	1.01203577
36.22	5.39	0.5	65	0.0118	1.01213786
37.83	5.48	0.5	60	0.0118	1.01182761
34.01	6.26	0.3	70	0.0118	1.01267983
36.95	6.36	0.3	60	0.0118	1.01308892
35.5	6.47	0.3	50	0.0118	1.01265661
36.29	6.68	0.3	45	0.0118	1.01274755
38.65	6.26	0.4	75	0.0118	1.01246587
39.91	6.36	0.4	65	0.0118	1.01256276
40.37	6.47	0.4	55	0.0118	1.01276026
37.66	6.68	0.4	50	0.0118	1.0124412
38.07	6.26	0.5	80	0.0118	1.01203755
38.64	6.36	0.5	70	0.0118	1.01277333
38.62	6.47	0.5	60	0.0118	1.01255293
40.32	6.68	0.5	55	0.0118	1.01231857
36.25	7.3	0.3	65	0.0118	1.01214468
36.15	7.43	0.3	55	0.0118	1.01266806

38.08	7.55	0.3	45	0.0118	1.01265661
Table F.2Cont….					
38.85	7.67	0.3	35	0.0118	1.0124412
40.45	7.3	0.4	70	0.0118	1.01267983
39.8	7.43	0.4	60	0.0118	1.01256276
38.67	7.55	0.4	50	0.0118	1.01182621
35.05	7.67	0.4	40	0.0118	1.0114179
35.75	7.3	0.5	75	0.0118	1.01289366
34.23	7.43	0.5	65	0.0118	1.01150793
38.08	7.55	0.5	55	0.0118	1.01172226
38.67	7.67	0.5	45	0.0118	1.01152037

After running this programming, experimental ΔMC and theoretical ΔMC will produce the results. The results are given below.

{{32.6,37.0371,4.43706},{40.1,37.4232,2.6768},{39.63,37.8905,1.73951},{38.63,38.1367,0.493259},{36.46,37.4077,0.947687},{38.96,37.7685,1.19151},{40.5,38.1979,2.30205},{38.69,38.4199,0.270101},{35.63,37.6627,2.03271},{35.45,38.0012,2.55123},{36.22,38.3988,2.17875},{37.83,38.6009,0.770924},{34.01,36.6879,2.67786},{36.95,37.1079,0.157875},{35.5,37.6176,2.11761},{36.29,37.8459,1.55587},{38.65,37.0412,1.60883},{39.91,37.4317,2.47828},{40.37,37.8969,2.47309},{37.66,38.0961,0.436098},{38.07,37.2842,0.785829},{38.64,37.6463,0.9937},{38.62,38.0745,0.545541},{40.32,38.2482,2.07178},{36.25,36.4489,0.198898},{36.15,36.8997,0.749713},{38.08,37.4659,0.614113},{38.85,38.2011,0.648851},{40.45,36.7829,3.66705},{39.8,37.1995,2.60046},{38.67,37.7146,0.95536},{35.05,38.3659,3.31594},{35.75,37.0094,1.25941},{34.23,37.397,3.16696},{38.08,37.8652,0.214795},{38.67,38.4474,0.222622}}

2.3 Correlation for RFB-SG (Wheat)

data={{131.3876047,19421.4912,58.51},{131.3017675,17776.9854,58.5},{131.4083793,15779.4377,56.19},{131.5525623,14581.1682,56.25},{174.9415455,20808.7406,59.14},{175.1368905,19752.206,58.08},{175.1894363,18074.6287,55.25},{175.1851548,16914.1551,54.68},{219.2603514,22195.99,58.64},{218.9027566,19752.206,56.56},{219.4395928,18648.4264,55.7},{219.1265853,17497.4019,49.97},{262.8032282,24970.4887,59.14},{262.799058,22573.9497,53.53},{263.0155446,21517.4151,57.47},{262.7536629,18955.5187,55.23},{131.3386306,22546.5171,56.48},{131.4630637,21164.2209,57.87},{131.4587088,18647.4358,57.61},{131.3875286,1

7494.6586,56.03},{174.9415455,24280.8646,53.62},{175.5097611,22927.9059,50.52},{175.0484852,20799.063,58.43},{175.2565625,19317.0189,53.06},{218.9256858,26015.2121,57.84},{219.0360175,23986.117,51.42},{219.1500737,22233.4811,56.14},{218.8790252,20045.963,57.9},{262.6185797,29483.907,53.09},{262.6860609,26455.2761,53.78},{262.4619398,23309.2947,52.17},{262.4099094,21868.3233,60.86},{131.4016141,24972.7747,59.83},{131.3774662,23281.4812,59.5},{131.1514651,21519.3201,50.87},{131.3127422,19682.8626,58.64},{175.1330889,28302.478,51.78},{175.1975327,25397.9794,56.23},{175.138772,22810.4793,50.98},{174.9860048,20995.0534,56.44},{219.0073615,29967.3297,50.13},{219.1581485,27514.4777,53.68},{218.7768066,23671.2521,58.98},{218.8168039,21869.8473,53.79},{262.9238789,31215.9684,55.66},{262.6585377,29630.976,59.52},{262.3567768,25823.1841,59.62},{262.3462099,24056.832,56.08}}

expr = C*X^a*Y^b

X^aY^bC

pars={C,a,b}

{C,a,b}

vars={X,Y}

{X,Y}

fit = FindFit[data,expr,pars,vars,MaxIterations→1000]

{C→76.3605, a→ -0.017526, b→ -0.0220619}

exprfitted = expr/.fit

$$\frac{76.3605}{X^{0.017526}\,Y^{0.0220619}}$$

replacerule[dat_]:=Table[vars[[i]]→data[[dat,i]],{i,Length[vars]}]

Table[{Last[data[[i]]],exprfitted/.replacerule[i],Last[data[[i]]]-exprfitted/.replacerule[i]},{i,Length[data]}]

After running this programming, experimental ΔMC and theoretical ΔMC will produce results.

Table F.3

ΔMC_P	V	m_{wp}	t	ϑ_{fc}	ρ_{ma}
56.38	36.41	0.3	70	0.00226	1.010319
56.49	37.03	0.3	63	0.00226	1.010979
56.63	37.65	0.3	55	0.00226	1.010159
56.73	38.27	0.3	50	0.00226	1.009052
56.01	36.41	0.4	75	0.00226	1.011716
56.07	37.03	0.4	70	0.00226	1.010587
56.18	37.65	0.4	63	0.00226	1.010284
56.28	38.27	0.4	58	0.00226	1.010309
55.71	36.41	0.5	80	0.00226	1.009024
55.85	37.03	0.5	70	0.00226	1.010672
55.92	37.65	0.5	65	0.00226	1.0082
56	38.27	0.5	60	0.00226	1.00964
55.39	36.41	0.6	90	0.00226	1.010211
55.51	37.03	0.6	80	0.00226	1.010227
Table F.3Cont….					
55.57	37.65	0.6	75	0.00226	1.009396
55.73	38.27	0.6	65	0.00226	1.010402
56.19	45.52	0.3	65	0.00226	1.010695
56.27	46.29	0.3	60	0.00226	1.009739
56.43	47.06	0.3	52	0.00226	1.009772
56.51	47.83	0.3	48	0.00226	1.010319
55.82	45.52	0.4	70	0.00226	1.011716
55.89	46.29	0.4	65	0.00226	1.00844
56.01	47.06	0.4	58	0.00226	1.011098
56.1	47.83	0.4	53	0.00226	1.009897
55.51	45.52	0.5	75	0.00226	1.010566
55.61	46.29	0.5	68	0.00226	1.010057
55.71	47.06	0.5	62	0.00226	1.009532
55.83	47.83	0.5	55	0.00226	1.010782
55.19	45.52	0.6	85	0.00226	1.010921
55.32	46.29	0.6	75	0.00226	1.010662
55.47	47.06	0.6	65	0.00226	1.011525
55.55	47.83	0.6	60	0.00226	1.011725
56.06	54.62	0.3	60	0.00226	1.010211
56.15	55.55	0.3	55	0.00226	1.010397
56.25	56.48	0.3	50	0.00226	1.012138
56.36	57.4	0.3	45	0.00226	1.010895
55.63	54.62	0.4	68	0.00226	1.010609
55.76	55.55	0.4	60	0.00226	1.010238

55.89	56.48	0.4	53	0.00226	1.010577
56	57.4	0.4	48	0.00226	1.011459
55.34	54.62	0.5	72	0.00226	1.01019
55.44	55.55	0.5	65	0.00226	1.009494
55.63	56.48	0.5	55	0.00226	1.011254
55.73	57.4	0.5	50	0.00226	1.011069
55.11	54.62	0.6	75	0.00226	1.009747
55.18	55.55	0.6	70	0.00226	1.010768
55.35	56.48	0.6	60	0.00226	1.01193
55.43	57.4	0.6	55	0.00226	1.011971

After running this programming, experimental ΔMC and theoretical ΔMC will produce the results. The results are given below.

{58.51,56.3809,2.12914},{58.5,56.4917,2.00833},{56.19,56.6396,0.449615},{56.25,56.7373,0.487299},{59.14,56.0133,3.12665},{58.08,56.0767,2.00332},{55.25,56.1863,0.936296},{54.68,56.2686,1.58864},{58.64,55.7127,2.92727},{56.56,55.8579,0.702116},{55.7,55.9264,0.226391},{49.97,56.0065,6.03645},{59.14,55.392,3.74799},{53.53,55.5155,1.98547},{57.47,55.5734,1.8966},{55.23,55.73,0.500017},{56.48,56.1959,0.284051}{57.87,56.2735,1.59649},{57.61,56.4309,1.17906},{56.03,56.511,0.480978},{53.62,55.823,2.20297},{50.52,55.8905,5.37045},{58.43,56.0133,2.41668},{53.06,56.1036,3.04358},{57.84,55.5194,2.32059},{51.42,55.6185,4.19847},{56.14,55.7111,0.428855},{57.9,55.8398,2.0602},{53.09,55.19,2.10002},{53.78,55.3219,1.5419},{52.17,55.4775,3.30747},{60.86,55.5558,5.30418},{59.83,56.0689,3.76109},{59.5,56.1559,3.3441},{50.87,56.2552,5.3852},{58.64,56.3648,2.2752},{51.78,55.6335,3.85348},{56.23,55.7662,0.463825},{50.98,55.8989,4.91886},{56.44,56.0021,0.437918},{50.13,55.3461,5.21609},{53.68,55.4498,1.76979},{58.98,55.6358,3.34416},{53.79,55.7329,1.9429},{55.66,55.1194,0.540568},{59.52,55.1838,4.33619},{59.62,55.3526,4.26736},{56.08,55.4393,0.640727}}

2.4 Correlation for BFB (Wheat)

data ={{25.1426528, 2059.616, 49.83},{25.1344829, 1862.395, 58.94},{25.1446765, 1657.268, 51.99},{25.1367203, 1444.235, 55.52},{33.5342297, 2174.039, 59.01},{33.5336794, 1978.795, 59.42},{33.5227823, 1775.645, 54.01},{33.5122317, 1564.588, 54.69},{41.882192, 2288.462, 57.45},{41.9127111, 2095.195, 56.58},{41.9077941, 1894.021,

54.32},{41.9200463, 1684.941, 57.84},{25.1319799, 2199.735, 58.25},{25.1213738, 1955.515, 53.78},{25.1317413, 1705.146, 54.71},{25.1290845, 1467.075, 59.62},{33.516418, 2337.218, 52.12},{33.5126439, 2095.195, 51.95},{33.5055444, 1847.241, 53.2},{33.5156271, 1613.783, 55.45},{41.9133295, 2474.702, 59.7},{41.8820586, 2234.874, 51.65},{41.8862355, 1989.337, 57.7},{41.89963, 1760.491, 51.57},{25.1453245, 2244.538, 57.21],{ 25.1318584, 1958.15, 57.34},{25.1317413, 1823.961, 58.76},{25.1367203, 1516.051, 51.02},{ 33.5093065, 2404.862, 54.34},{33.5091445, 2121.33, 58.86},{33.5366052, 1989.776, 56.44},{33.5496791, 1684.501, 58.93},{41.8777533, 2565.186, 52.81},{41.9346752, 2284.509, 50.58},{41.9250818, 2155.591,50.82},{41.9328324, 1852.951, 51.45}}

expr = C*X^a*Y^b

X^aY^bC

pars={C,a,b}

{C,a,b}

vars={X,Y}

{X,Y}

fit = FindFit[data,expr,pars,vars,MaxIterations→1000]

{C→60.2464, a→ -0.0425184, b→ 0.00808605}

exprfitted = expr/.fit

$$\frac{60.2464\, Y^{0.00808605}}{X^{0.0425184}}$$

replacerule[dat_]:=Table[vars[[i]]→data[[dat,i]],{i,Length[vars]}]

Table[{Last[data[[i]]],exprfitted/.replacerule[i],Last[data[[i]]]-exprfitted/.replacerule[i]},{i,Length[data]}]

After running this programming, experimental ΔMC and theoretical ΔMC will produce results.

Table F.4

ΔMC_P	V	m_{wp}	t	ϑ_{fc}	ρ_{ma}
55.87	5.21	0.3	90	0.0118	1.011179
55.82	5.3	0.3	80	0.0118	1.011508
55.77	5.39	0.3	70	0.0118	1.011098
55.71	5.48	0.3	60	0.0118	1.011418
55.21	5.21	0.4	95	0.0118	1.010857

55.17	5.3	0.4	85	0.0118	1.010873
55.12	5.39	0.4	75	0.0118	1.011202
55.06	5.48	0.4	65	0.0118	1.01152
54.71	5.21	0.5	100	0.0118	1.011716
54.67	5.3	0.5	90	0.0118	1.010979
54.63	5.39	0.5	80	0.0118	1.011098
54.58	5.48	0.5	70	0.0118	1.010802
55.9	6.26	0.3	80	0.0118	1.011609
55.84	6.36	0.3	70	0.0118	1.012036
55.78	6.47	0.3	60	0.0118	1.011618
55.71	6.68	0.3	50	0.0118	1.011725
55.24	6.26	0.4	85	0.0118	1.011394
55.19	6.36	0.4	75	0.0118	1.011508
55.14	6.47	0.4	65	0.0118	1.011722
55.08	6.68	0.4	55	0.0118	1.011418
54.75	6.26	0.5	90	0.0118	1.010964
54.7	6.36	0.5	80	0.0118	1.011719
54.65	6.47	0.5	70	0.0118	1.011618
54.6	6.68	0.5	60	0.0118	1.011295
55.9	7.3	0.3	70	0.0118	1.011072
55.84	7.43	0.3	60	0.0118	1.011614
55.81	7.55	0.3	55	0.0118	1.011618
55.73	7.67	0.3	45	0.0118	1.011418
55.26	7.3	0.4	75	0.0118	1.011609
55.2	7.43	0.4	65	0.0118	1.011614
55.17	7.55	0.4	60	0.0118	1.010785
55.09	7.67	0.4	50	0.0118	1.010391
54.76	7.3	0.5	80	0.0118	1.011823
54.71	7.43	0.5	70	0.0118	1.01045
54.68	7.55	0.5	65	0.0118	1.010681
54.62	7.67	0.5	55	0.0118	1.010494

After running this programming, experimental ΔMC and theoretical ΔMC will produce the results. The results are given below.

{49.83,55.8706,6.04056},{58.94,55.8259,3.11413},{51.99,55.7723,3.78226},{55.52,55.711,0.190996},{59.01,55.2147,3.79529},{59.42,55.1728,4.24725},{54.01,55.1252,1.11521},{54.69,55.0696,0.379569},{57.45,54.718,2.73201},{56.58,54.6773,1.90273}, {54.32, 54.6329,-0.312933},{57.84,54.5806,3.25939},{58.25,55.9013,2.34869}, {53.78, 55.8491,-2.06914}, {54.71, 55.7863,-1.07633},{59.62,55.7188,3.90122}, {52.12,55.2483,-3.12828},{51.95,55.1997,-3.24973},{53.2,55.144,-1.94404}, {55.45,55.0831,0.366881},{59.7,54.7509,4.94911},{51.65,54.7075,3.05752},{57.7,

54.6558,3.04418},{51.57,54.6011,3.0311},{57.21,55.9092,1.30084}{57.34,55.8488,1.49124},{58.76,55.8167,2.94328},{51.02,55.7329,4.71286},{54.34,55.2615,0.921526},{58.86,55.2055,3.65449},{56.44,55.175,1.26498},{58.93,55.0998,3.83015},{52.81,54.7688,1.95877},{50.58,54.7143,4.13431},{50.82,54.6892,3.86915},{51.45,54.6219,-3.17186}}

Appendix G

Exergy inflow and outflow for RFB-SG

The exergy in flow and out flow are calculated based on below formula.Where E_x is exergy of the system, $\dot{m}_{da}$ is the mass of dry air, C_p specific heat of drying air, T_1 is the temperature of the drying air and T_o is the ambient temperature shown in equation (G.1).

$$E_x = \dot{m}_{da}\, c_p \left[(T_1 - T_o) - T_o \ln \frac{T_1}{T_o} \right] \quad \text{(G.1)}$$

$$\dot{E}_{x\,dci} = \dot{m}_{da}\, c_p \left[(T_{dci} - T_o) - T_o \ln \frac{T_{dci}}{T_o} \right] \quad \text{(G.2)}$$

$$\dot{E}_{x\,dco} = \dot{m}_{da}\, c_p \left[(T_{dco} - T_o) - T_o \ln \frac{T_{dco}}{T_o} \right] \quad \text{(G.3)}$$

Where$T_{dci}=T_1$ and $T_{dco}=T_3$ are the input and output temperature of the drying chamber, respectively.

Now exergy utilized can be calculated as

$$\sum \dot{E}_u = \sum \dot{E}_{Xdci} - \sum \dot{E}_{X\,dco} \quad \text{(G.4)}$$

Table G.1 Exergy inflow (kJ/s) at different air flow rate and inlet air temperature

Air flow rate (Nm^3/h)	Exergy inflow (kJ/s)			
	50^0C	55^0C	60^0C	65^0C
400	0.282	0.376	0.484	0.606
500	0.352	0.470	0.605	0.758
600	0.423	0.563	0.725	0.908

Table G.2 Exergy outflow (kJ/s) at different air flow rate and inlet air temperature

Air flow rate (Nm^3/h)	Exergy outflow (kJ/s)			
	50 ^{0}C	55 ^{0}C	60 ^{0}C	65^{0}C
400	0.252	0.345	0.435	0.531
500	0.278	0.397	0.473	0.610
600	0.357	0.456	0.606	0.687

2. EXERGY INFLOW AND OUTFLOW FOR BFB

Table G.3 Exergy inflow (kJ/s) at different air flow rate and inlet air temperature

Air flow rate (Nm^3/h)	Exergy inflow (kJ/s)			
	50^{0}C	55^{0}C	60^{0}C	65^{0}C
125	0.088	0.115	0.149	0.187
150	0.098	0.140	0.181	0.227
175	0.112	0.164	0.210	0.263

Table G.4 Exergy outflow (kJ/s) at different air flow rate and inlet air temperature

Air flow rate (Nm^3/h)	Exergy outflow (kJ/s)			
	50 ^{0}C	55 ^{0}C	60 ^{0}C	65^{0}C
125	0.052	0.062	0.089	0.103
150	0.058	0.083	0.113	0.134
175	0.066	0.100	0.122	0.141

Appendix H

Economic evaluation of drying of paddy/wheat for dryers

The sample calculations' regarding economic evaluation of the dryers is described.

RFB-SG (Stainless Steel)

Table H.1 Different cost are described for RFB-SG and BFB dryer (paddy)

Calculation parameters	RFB-SG	BFB
Wet Paddy Rate (100kg)	1100/-	1100/-
Dry Paddy Rate (100kg)	1600/-	1600/-
Electricity kWh	@2.25/-	@2.25/-
Unskilled Labour	Rs150 @ Day	Rs150 @ Day
Interest rate	8.5% of investment	8.5% of investment
Repair and Matainance	4% of investment	4% of investment
Dryer Utilization	300 days	300 days
Dryer Cost	30,000/-	10,000/-
Instrumentation	20,000/-	20,000/-
Drying of paddy @ hour	6kg	4kg
Dryer running 20 hours	120kg/day	80kg/day

The blower mass flow rate and electric hater power is calculated (www.agmark.nic.in, www.Botanical.com).

$$CFM = 1.75 \times (watt/Temp.\ Difference) \quad (H.1)$$

According the above formula, the use of total electricity used for one hour is 2.5kW for drying of paddy in RFB-SG dryer.

Total cost of Dryer = Rs30, 000+ Rs20, 000 = Rs 50,000

The total life span of the dryer assumed as 10 years.

The total interest of investment per year @8.5% = Rs 4,250

Now, for one (1) year fixed cost is depend on Rs 5,000 and interest Rs 4,250.

So total fixed cost = Rs5, 000 +Rs4, 250=Rs 9,250

Annual maintenance and repairing are @ 4% of Initial investment = Rs 2000

Table H.2 One day expenditure for drying of paddy for RFB-SG dryer

Fixed Cost per day	Rs 30
Matainance per day	Rs7
Electricity used per day	Rs 112
Unskilled labour per day	Rs 150
Total expenditure per day	Rs299

For one day, total 120kg paddy is dried with the expenditure of Rs299.

The cost of drying per kg of paddy is **Rs 2.49**

Total collected dry paddy is 71kg from 120kg wet paddy. Selling of one kg dry paddy is collected by extra Rs5.

Total collected money is 71kg@Rs5 = Rs355

Profit = Selling price of paddy – Expenditure price for drying of paddy (H.2)

Profit = Rs 355 – Rs299 = Rs 56 per day

One year(300days), it will be Rs56 ×300=Rs16, 800

Payback period or BEP (Break even period)

$$N^{*} = \frac{A}{S} \quad \text{(H.3)}$$

where S is net annual saving (profit), A is capital cost (investment) and N^{*} is the payback period (year).

N = (Rs50, 000/Rs16, 800) = **2.9** year.

The cost of one kg wet paddy and payback period for RFB-SG dryer is Rs 2.49 and 2.9 year, respectively.

For validation of the RFB-SG dryer, net present value method (NPV) is used.

Cash flows (savings) streams at different time periods differ in values and can be compared only when they are expressed in terms of a common denominator i.e., present value.

$$\text{Present value} = \frac{CF_1}{(1+i)} + \frac{CF_2}{(1+i)^2} + \frac{CF_3}{(1+i)^3} + \ldots\ldots\ldots + \frac{CF_N}{(1+i)^N} \quad \text{(H.4)}$$

Where CF, i are cash flow and interest.

Net present value (NPV) = present value of cash inflow – present value of cash out flow

Table H.3NPV calculation for RFB-SG dryer

Year	CF (Rs)	Present value at 8.5%	Total present value (Rs)
1	16,800.00	0.921	15,487.00
2	16,800.00	0.849	14,270.00
3	16,800.00	0.782	13,152.00
4	16,800.00	0.721	12,122.00
5	16,800.00	0.665	11,172.00
6	16,800.00	0.612	10,281.00
		Total	76,484.00

NPV = Rs 76,484.00 – Rs 50, 000.00 = Rs 26, 484.00

Hence, the RFB-SG dryer for paddy drying is viable.

Similarly, for drying of paddy in BFB (Plexi glass) dryer is calculated.

Total cost of the BFB dryer is Rs 30,000 and the life span of the dryer is 10 years. The interest coat of the dryer per year is @8.5% i.e. Rs 2,550. The fixed cost for one year is Rs 5,550. Applying the formula of (Eq.H.1)

The total consumption of electricity for one hour is 1kW @ Rs 2.25.

Annual maintenance and repairing @ 4% of Initial investment = 1200/-

Table H.4One day expenditure for drying of paddy for BFB dryer

Fixed Cost per day	Rs 18
Matainance per day	Rs4
Electricity used per day	Rs45
Unskilled labour per day	Rs 150
Total expenditure per day	Rs217

For one day, total 80kg paddy dried with the expenditure Rs217.

The cost of drying per kg of paddy is **Rs 2.71**

Total collected dry paddy is 48 kg from 80 kg wet paddy. Selling of one kg dry paddy is collected by extra Rs5.

Total collected money is 48 kg@Rs5 = Rs240

Profit = Rs 240 – Rs217 = Rs 23 per day

One year (300days), it will be Rs23 ×300=Rs6, 900

Payback period or BEP (Break even period)

Where S is net annual saving, A is capital cost and N is the payback period (year).

N = (Rs30,000/Rs6,900) = **4.4 year**.

The cost of one kg wet paddy and payback period for RFB-SG dryer is Rs 2.71 and 4.4 year, respectively.

For validation of the BFB dryer, net present value method (NPV) is used by using H.4 equation.

Table H.5NPV calculation for BFB dryer

Year	CF (Rs)	Present value at 8.5%	Total present value (Rs)
1	6,900.00	0.921	6,359.00
2	6,900.00	0.849	5,861.00
3	6,900.00	0.782	5,402.00
4	6,900.00	0.721	4,978.00
5	6,900.00	0.665	4,588.00
6	6,900.00	0.612	4,229.00
		Total	31,419.00

NPV = Rs 31,419.00 – Rs 30, 000.00 = Rs 1,419.00

Hence, the BFB dryer for paddy drying is viable.

Table H.6 Different cost are described for RFB-SG and BFB dryer (wheat)

RFB-SG (Stainless Steel)

Calculation parameters	RFB-SG	BFB
Wet Wheat Rate (100kg)	1200/-	1200/-
Dry Wheat Rate (100kg)	2000/-	2000/-
Electricity kWh	@2.25/-	@2.25/-
Unskilled Labour	Rs150 @ Day	Rs150 @ Day
Interest rate	8.5% of investment	8.5% of investment
Repair and Matainance	4% of investment	4% of investment
Dryer Utilization	300 days	300 days

Dryer Cost	30,000/-	10,000/-
Instrumentation	20,000/-	20,000/-
Drying time	38 minute	55minutes
Drying of paddy @ hour	5kg	3kg
Dryer running 20 hours	100kg/day	60kg/day

All calculation is based on the previous RFB-SG dryer for paddy drying.

Table H.7 One day expenditure for drying of wheat for RFB-SG dryer

Fixed Cost per day	Rs 30
Matainance per day	Rs7
Electricity used per day	Rs 112
Unskilled labour per day	Rs 150
Total expenditure per day	Rs299

For one day, total 100kg paddy dried with the expenditure Rs299.

The cost of drying per kg of wheat is **Rs 2.99**

Total collected dry wheat is 43 kg from 100 kg wet wheat. Selling of one kg dry wheat is collected by extra Rs 8.

Total collected money is 43 kg@Rs8 = Rs344

Profit = Rs344 – Rs299 = Rs 45 per day

One year (300days), it will be Rs 45 ×300 = Rs13, 500

Payback period or BEP (Break even period)

Where S is net annual saving, A is capital cost and N is the payback period (year).

N = (Rs50,000/Rs13,500) = **3.7 year**.

The cost of one kg wet wheat and payback period for RFB-SG dryer is Rs 2.99 and 3.7 year, respectively.

For validation of the RFB-SG dryer, net present value method (NPV) is used by using H.4 equation.

Table H.8NPV calculation for RFB-SG dryer

Year	CF (Rs)	Present value at 8.5%	Total present value (Rs)
1	13,500.00	0.921	12,442.00
2	13,500.00	0.849	11,467.00
3	13,500.00	0.782	10,569.00
4	13,500.00	0.721	9,741.00
5	13,500.00	0.665	8,978.00
6	13,500.00	0.612	8,262.00
		Total	61,459.00

NPV = Rs 61,459.00 – Rs 50, 000.00 = Rs 11,459.00

Hence, the RFB-SG dryer for wheat drying is viable.

Table H.9One day expenditure for drying of wheat for BFB dryer

Fixed Cost per day	Rs 18
Matainance per day	Rs4
Electricity used per day	Rs45
Unskilled labour per day	Rs 150
Total expenditure per day	Rs217

For one day, total 60kg paddy dried with the expenditure Rs217.

The cost of drying per kg of wheat is **Rs3.60**

Total collected dry wheat is 29 kg from 60 kg wet wheat. Selling of one kg dry wheat is collected by extra Rs 8.

Total collected money is 29 kg@Rs8 = Rs 232

Profit = Rs232 – Rs 217 = Rs 15 per day

One year (300days), it will be Rs 45 ×300 = Rs 4, 500

Payback period or BEP (Break even period)

Where S is net annual saving, A is capital cost and N is the payback period (year).

N = (Rs30, 000/Rs4, 500) = **6.5 year**.

The cost of one kg wet wheat and payback period for BFB dryer is Rs 3.60 and 6.5 year, respectively.

For validation of the BFB dryer, net present value method (NPV) is used by using H.4 equation.

Table H.10NPV calculation for BFB dryer

Year	CF (Rs)	Present value at 8.5%	Total present value (Rs)
1	4,500.00	0.921	4,147.00
2	4,500.00	0.849	3,820.00
3	4,500.00	0.782	3,523.00
4	4,500.00	0.721	3,246.00
5	4,500.00	0.665	2,992.00
6	4,500.00	0.612	2,758.00
7	4,500.00	0.564	2,542.00
8	4,500.00	0.520	2,343.00
9	4,500.00	0.479	2,159.00
10	4,500.00	0.442	1,990.00
		Total	29,520.00

NPV = Rs 29,520.00 – Rs 30, 000.00 = -Rs 480.00

In this case, the NPV value is negative. So the BFB dryer is not viable for wheat drying.

Appendix I

CERTIFICATE FOR QUALITY DRYING

Wallonie

cra-w

Centre wallon de Recherches agronomiques
Département Valorisation des productions
Unité Technologies de la Transformation des Produits

Annex to the trial report RE14086_2_1_UCL-IMAP

1. Samples

Paddy rice and wheat samples were delivered to the laboratory for the analysis of dry matter and total protein content (N° DQ/14/0528, 08/07/2014)

		Moisture	Dry Matter	Prot	Prot	Prot	Prot
Numéro interne	Référence client	%	%	N*5.7 %	N*5.7 % DM	N*6.25 %	N*6.25 % DM
DQ/14/0528-01	Paddy original Sample	12.1	87.9			5.9	6.8
DQ/14/0528-02	Paddy Conventional FB	11.6	88.4			5.9	6.7
DQ/14/0528-03	Paddy RFB (aftyer drying)	10.5	89.5			6.1	6.9
DQ/14/0528-04	Wheat original sample	12.2	87.8	9.5	10.8	10.4	11.8
DQ/14/0528-05	Wheat Conventional FB	11.3	88.7	10.0	11.3	11.0	12.4
DQ/14/0528-06	Wheat RFB (After drying)	10.9	89.1	10.2	11.4	11.1	12.5

PROCEDURE FOR QUALITY MEASUREMENTS

The drying paddy and wheat sample are collected and send to centre wallon de researches agronomiques, Belgium. After grounding in a Foss-Cyclotech mill with a 1.0 mmgrid, the moisture/ dry matter content of the different paddy and wheat sample of before and after drying was determined using a near-infrared reflectance spectrometer (Foss NIRS ystems 5000). According to the Dumas principle, the nitrogen content is determined by total content is obtained with a conventional coefficient of 6.25. The protein content will not be affected by the heat treatment.

UCL Université catholique de Louvain

École polytechnique de Louvain (EPL)

epl

RESEARCH CERTIFICATE

We undersigned, Professor Michel Verleysen, Dean of Louvain Engineering School and Professor Juray De Wilde, academic responsible, certify, following the training agreement signed by Professor Juray De Wilde and Professor P. Mahanta

Mr Jnyana Ranjan PATI

Born at Sergarh Orissa (India) on 3rd June 1973

has made, during the academic year 2013-2014, a scientific training in the Institute of Mechanics, Materials and Civil Engineering (iMMC) / Materials and process engineering (IMAP), of the Université Catholique de Louvain on the following subject

Experimental study of intensified biomass drying and spray drying in vortex chambers.

Ottignies-Louvain-la-Neuve, 9th September 2014

Dean of the Louvain Engineering School,

Academic responsible,

Juray De Wilde

Université catholique de Louvain
Institut de mécanique, matériaux et génie civil - iMMC
IMAP - Place Sainte Barbe, 2
B-1348 Louvain-la-Neuve
Tél.: +32 (0)10 47 24 87

UCL Université catholique de Louvain

Institute of Mechanics, Materials and Civil Engineering (IMMC)

iMMC

Louvain-la-Neuve, September 2, 2014

To whom it may concern,

I hereby confirm that Mr. Jnyana Ranjan PATI, born on June 3, 1973 in Sergarh Orissa (India), completed a 13-month research project in the Materials and Process Engineering Division (IMAP) at the Université catholique de Louvain (UCL) in Belgium between August 2013 and September 2014.

The research project was supported by a Marie Curie International Research Staff Exchange Scheme Fellowship within the 7th European Community Framework Programme (Grant Agreement Number: PIRSES-GA-2012-312261; Project: "iComFluid – International Collaboration on Computational Modeling of Fluidized Bed Systems for Clean Energy Technologies").

Mr. PATI carried out excellent experimental research on the use of vortex chambers and conventional chambers for paddy and wheat drying and for spray drying.

Université catholique de Louvain
Institut de mécanique, matériaux et génie civil - iMMC
IMAP - Place Sainte Barbe, 2
B-1348 Louvain-la-Neuve
Tel.: +32 (0)10 47 24 87

Prof. Dr. ir. Juray De Wilde

Thank you for the interesting collaboration.
It was a pleasure working with you and I wish you all the best with the finalization of your Ph.D.
Juray De Wilde

UCL Université catholique de Louvain

Institute of Mechanics, Materials and Civil Engineering (IMMC)

iMMC

Louvain-la-Neuve, September 2, 2014

To whom it may concern,

I hereby confirm that Mr. Jnyana Ranjan PATI completed the course LMAPR2330, Reactor Analysis and Design, at the Université catholique de Louvain on January 15, 2014 and obtained the following grade: 17/20.

Université catholique de Louvain
Institut de mécanique, matériaux et génie civil - iMMC
IMAP - Place Sainte Barbe, 2
B-1348 Louvain-la-Neuve
Tél.: +32 (0)10 47 24 87

UCL Université catholique de Louvain

Ecole Polytechnique
1, rue Archimède
1348 Louvain-la-Neuve (Belgique)

Prof. Dr. ir. Juray De Wilde

Publications from Present work

LIST OF PUBLICATIONS

International Journals

1. **Pati, Jnyana R**. Dutta, Subhajit. Eliaers, Philippe. Mahanta, Pinakeswar. Chatterjee, Pradip K. De Wilde, Juray. (2016) "Experimental study of paddy drying in a vortex chamber" Drying Technology, Vol. 34, No. 9, PP. 1073 - 1084
2. Eliaers, Philippe. **Pati, Jnyana R**. Dutta ,Subhajit., De Wilde, Juray. (2015) "Modeling and simulation of biomass drying in vortex chambers" Chemical Engineering Science, vol. 123, pp. 648-664
3. **Pati , Jnyana R**., Hotta, Santosh K., Mahanta, P. (2015) "Effect of Waste Heat Recovery on Drying characteristics of Sliced Ginger in a Natural Convection Dryer" procedia engineering, Vol. 105, pp. 145-152

International/National Conferences

4. Mahanta P., Hotta Santosh k., **PatiJnyana R**.,(2013) "Studies on heat transfer and drying characteristics of ginger in a natural convection dryer" 22nd National and 11th ISHMT-ASME Heat and Mass Transfer Conference, Dec 28-31, 2013, Paper ID- 123, IIT Kharagpur, India
5. **Pati, Jnyana R**., Hotta, Santosh K., Mahanta, P. (2014) "Effect of Waste Heat Recovery on Drying characteristics of Sliced Ginger in a Natural Convection Dryer" 6th BSME International Conference on Thermal Engineering (ICTE 2014), 19-21 December, 2014, Paper-ID 137,Dhaka, Bangladesh.
6. Eliaers, Philippe., Dutta, Subhajit,**Pati, Jnyana R**., De Wilde, Juray., "Modeling, Simulation and Scale-up Study of Biomass Drying in a Vortex Chamber", American Institute of Chemical Engineers (AIChE) 2014 Annual Meeting, Atlanta, USA, Paper-ID 387608, November 16-21, 2014
7. **Pati , J. R** ., Mahanta, P., Dutta S. " Experimental Study and Comparison of Paddy Drying in Natural Convection and Rotating Fluidized Bed in a Static Geometry dryer (RFB-SG)" ICAER-2015, IIT Bombay, India, 15th -17th December, 2015, Paper-ID 281.

8. **Pati, Jnyana.R**, Mahanta. P., De Wilde, J. (2016), "Experimental and Compare Study of Wheat Drying in Rotating Fluidized Bed in a Static Geometry (RFB-SG) and Conventional Bubbling Fluidized Bed (BFB) Dryer. ETAE, 27-30 December, IIT, Kharagpur, Paper ID-1306.